P. Zhao, D. Astruc, and N. Li

DOI: 10.1002/anie.201300441

Nanoparticles

Anisotropic Gold Nanoparticles: Synthesis, Properties, Applications, and Toxicity

Na Li, Pengxiang Zhao, and Didier Astruc**

Keywords:
anisotropy · gold nanoparticles · nanocatalysis · nanomedicine · plasmon

Dedicated to Professor Henri Bouas-Laurent on the occasion of his 80th birthday

Angewandte International Edition Chemie

Anisotropic gold nanoparticles (AuNPs) have attracted the interest of scientists for over a century, but research in this field has considerably accelerated since 2000 with the synthesis of numerous 1D, 2D, and 3D shapes as well as hollow AuNP structures. The anisotropy of these nonspherical, hollow, and nanoshell AuNP structures is the source of the plasmon absorption in the visible region as well as in the near-infrared (NIR) region. This NIR absorption is especially sensitive to the AuNP shape and medium and can be shifted towards the part of the NIR region in which living tissue shows minimum absorption. This has led to crucial applications in medical diagnostics and therapy ("theranostics"), especially with Au nanoshells, nanorods, hollow nanospheres, and nanocubes. In addition, Au nanowires (AuNWs) can be synthesized with longitudinal dimensions of several tens of micrometers and can serve as plasmon waveguides for sophisticated optical devices. The application of anisotropic AuNPs has rapidly spread to optical, biomedical, and catalytic areas. In this Review, a brief historical survey is given, followed by a summary of the synthetic modes, variety of shapes, applications, and toxicity issues of this fast-growing class of nanomaterials.

From the Contents

1. Introduction

Although nanogold represents one of the most remarkable areas of modern nanoscience and nanotechnology, spherical gold nanoparticles (AuNPs) have been known for millenia. Illustratory examples from history are the Lycurgus cup[1] and the Faraday publication.[2] Modern milestones from the second half of the 20th century are the Turkevitch[3] and Schiffrin–Brust synthetic methods,[4] Schmid's magic number of gold atoms in stable colloids,[5] and Haruta's discovery of the efficient oxidation of CO by O_2 at low temperatures by small (<5 nm) AuNPs.[6] The outstanding properties of AuNPs are related to their easy stabilization and handling through thiolate ligands (Giersig and Mulvaney)[7] and the quantum size effect that is involved when the de Broglie wavelength of the valence electrons is on the same order as the size of the particle itself.[8] The free mobile electrons are trapped in a quantum box (the particle) and show the collective oscillation frequency of the plasman resonance, thus giving rise to the well-known plasmon absorption near 530 nm for 5–20 nm spherical AuNPs that causes the deep-red color and provides a variety of optical applications.[9–11] The resulting single-electron transitions result in the observed Coulomb blockade and, for example, the generation of up to 15 high-resolution quantized double-layer chargings in hexanethiol-Au_{38} particles.[12] This Coulomb blockade can lead to applications as transistors, switches, electrometers, oscillators, and sensors. Finally, the large surface/volume ratio of AuNPs results in the AuNPs having an extraordinary reactivity that provides a large variety of catalytic applications.[13–16]

Scientists already noticed the existence of anisotropic AuNPs at the beginning of the 20th century. In his book that was published in 1909, Zsimondy noted that gold particles "*are not necessarily spherical when their size is 40 nm (μm) or below*". He also discovered different colored anisotropic gold particles. Zsimondy invented the ultramicroscope, which allowed him to visualize the shapes of gold particles, and he received the 1925 Nobel Prize for "his demonstration of the heterogeneous nature of colloidal solutions and for the methods he used". He observed that gold often crystallized in a leaflike form with six sides.[17] In a well-known seminal article in 1908, Mie theoretically described the absorption and scattering to explain the colors (surface plasmon band) of gold particles. Although his theory applied only to spherical AuNPs, Mie attributed the deviations in some cases to nonspherical gold particles.[8] In 1912 Gans extended Mie's theory and showed that aspherical particles absorb at a longer wavelength than spherical particles of comparable size.[18] Some years later, Svedberg, who discovered that particles could be separated with an ultracentrifuge, described experiments in which X-ray scattering was used to determine size- and shape-dependent properties of gold particles,[19] and he was awarded the 1926 Nobel Prize for "his work on disperse systems". Following Einstein's description of Brownian motion as a diffusion process and development of a viscosity relationship in 1905 for dilute solutions of spherical particles,[20] in 1922 Jefferey extended the hydrodynamic calcu-

[*] N. Li, Dr. P. Zhao, Prof. D. Astruc
ISM, UMR CNRS 5255, Univ. Bordeaux
33405 Talence Cedex (France)
E-mail: d.astruc@ism.u-bordeaux1.fr
Dr. P. Zhao
Science and Technology on Surface Physics and Chemistry Laboratory
P.O. Box 718-35, Mianyang 621907, Sichuan (China)
E-mail: zhaopengxiang831015@126.com

lations of the viscosity increase to solutions containing ellipsoidal particles.[21]

The investigations of anisotropic shapes and morphologies of AuNPs in particular have increased during the last decade, most often relying on the development of seed-mediated synthetic methods. In this respect, AuNPs are probably the class of nanoparticles that has provided the largest variety of shapes and has been studied the most. Such syntheses of anisotropic AuNPs have attracted interest because the structural, optical, electronic, magnetic, and catalytic properties are different from, and most often superior to, those of spherical AuNPs and have potential applications. In particular, compared to spherical (nonhollow) AuNPs, the main attractive feature of most anisotropic and hollow AuNPs is probably the appearance of a plasmon band in the near-infrared (NIR) region, where absorption by tissues is low. Therefore, the "water window" between 800 nm and 1300 nm can be used for medicinal diagnostics and photothermal therapy ("theranostics").[22–25] Other noteworthy properties of nonspherical AuNPs are the enhancement of the SERS effect[26] and the catalytic properties of small AuNPs (< 5 nm) on textured surfaces.[12–21] In this Review, we highlight the synthesis, properties, and applications of the various shapes of AuNPs, with an emphasis on nonspherical and hollow AuNPs.

2. Pioneering Syntheses of Anisotropic AuNPs

AuNPs with hexagonal (icosahedral) and pentagonal (decahedral) profiles were synthesized by vapor deposition methods in 1979[27] and 1981.[28] In 1989, Wiesner and Wokaun reported the first example of rod-shaped AuNPs by adding Au seeds to solutions of $HAuCl_4$.[29] The Au seeds were formed by reduction of $HAuCl_4$ with phosphorus (as in Faraday's synthesis),[2] and then gold nanorods (AuNRs) were grown by reduction of Au^{III} with H_2O_2. Modern concepts of seed-mediated synthesis were established by the Murphy research group at the beginning of the 2000s. They reported the synthesis of AuNRs by the addition of citrate-capped AuNPs to an Au^{I} growth solution generated by the reduction of Au^{III} with ascorbic acid in the presence of cetyltrimethylammonium bromide (CTAB) and Ag^+ (Figure 1).[30] The seed-growth method has become established as the most efficient and popular one to synthesize specific shapes in high yields.[30,31] Bulk-solution methods have been reported to produce nanocrystals with multiple shapes, but with a low yield of a specific shape.[32]

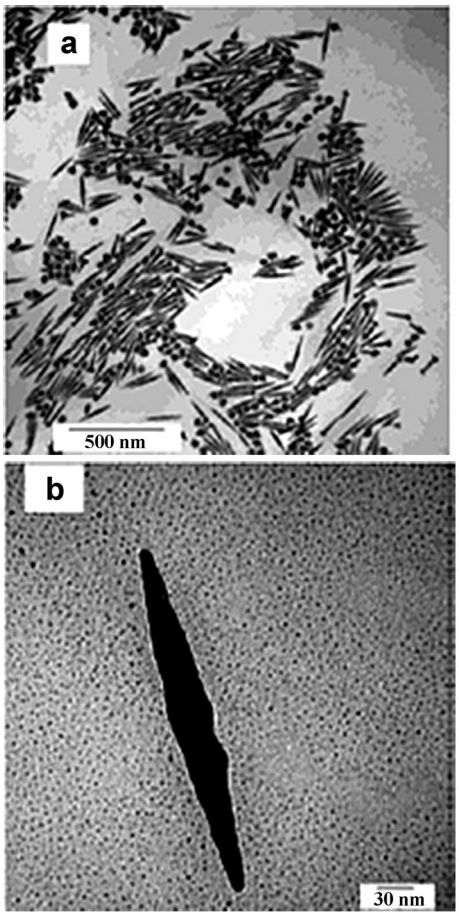

Figure 1. Seed-mediated synthesis of AuNRs by Murphy and co-workers. From Ref. [30]. Copyright 2001 Wiley-VCH.

The first physical synthetic method used to make AuNRs was the photochemical reduction of auric acid reported in 1995 by Esumi et al.[33] In this method, Au^{III} ions bound to rodlike cationic micelle surfactants to form ion pairs and when excited by UV light are reduced to Au^0. A two-step process was proposed, involving the aggregation of metal nuclei to form primary particles followed by aggregation of

Li Na was born in Ningxia province, China. She studied chemical engineering with Prof. Shiqiang Yan at Lanzhou University in Lanzhou, China. She then joined the research group of Prof. Didier Astruc at the University of Bordeaux, France, in 2011, for PhD study. Her research interests are the functionalization and engineering of gold nanoparticles for applications in nanomedicine.

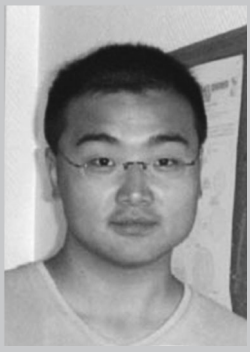

Pengxiang Zhao was born near Chengdu, China. He studied chemistry and engineering with Prof. Wuyong Chen at Sichuan University in Chengdu. He completed his PhD in 2012 in the group of Prof. Didier Astruc at the University of Bordeaux on the application of gold nanoparticles for docetaxel delivery. He is currently an independent researcher position at the Science and Technology on Surface Physics and Chemistry Laboratory at Mianyang, Sichuan, China. His research interests concern gold nanoparticles.

these particles to form rod-shaped particles resulting from the stabilization of a specific crystal face by surfactant micelles.[34]

Another early method to form AuNRs was the electrochemical reduction method, which was developed by the Wang research group in the late 1990s.[35,36] It was later shown that CTAB was crucial in this method for the high-yielding formation of AuNRs. In 2001 the El-Sayed research group already noted that CTAB induced the formation of a bilayer structure on the longitudinal surface of AuNRs, with the trimethylammonium head groups of the primary layer facing the AuNR surface.[37]

3. Methods and Techniques for the Synthesis of Anisotropic AuNPs

A large variety of bottom-up methods and techniques involving templates or capping agents have been used during the last decade to synthesize many types of anisotropic or hollow AuNPs. However, the versatile and more-complex seed-mediated method has become dominant, especially for the synthesis of AuNRs. Two or several of these methods are often combined (in particular, a template method with another method) for the synthesis of anisotropic AuNPs. Supramolecular chemistry also provides a means of assembling AuNPs. Top-down routes (mostly lithography) are much rarer, but are sometimes combined with a bottom-up technique.

3.1. Simple Chemical Reduction of Au^{III}

Cetyltrimethylammonium bromide (CTAB) is a frequently used surfactant for the structuration of nonspherical AuNPs, and the role of its purity and mechanism of action have been debated.[22–24] Forms of silver, either as $AgNO_3$ or Ag nanoplates,[38,39] are also often used because of the key role silver plays in anisotropic growth.[40] For example, the addition of ascorbic acid to a mixture of CTAB, silver plates, and $HAuCl_4$ reduced orange Au^{III} to almost colorless Au^{I}. The rapid addition of NaOH then induced the formation of anisotropic AuNPs, whose color changed from pale blue to dark red within one day. The TEM images showed the formation of various shapes, including spheres (40%), tadpole-like monopods (25%), L-shaped, I-shaped, and V-shaped bipods (23%), T-shaped, Y-shaped, and regular triangular tripods (9%), and cross-like tetrapods (3%; fcc structures, no incorporation of silver; Figure 2). NaOH plays a role in the branching of the NPs, as the use of $NaBH_4$ instead only yields spherical and rod-shaped AuNPs. The function of the silver plates is only to improve the yield, while the presence of Ag^+ is detrimental.[40] This example clearly shows the use of structuring agents for the formation of anisotropic AuNPs, but also the need for sophistication to improve the yields.[41]

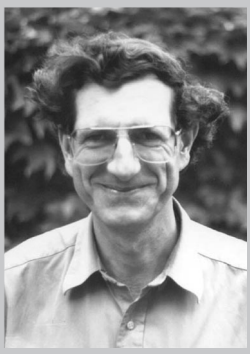

Didier Astruc was born in Versailles and studied in Rennes, where he completed his PhD with Prof. R. Dabard. After postdoctoral research at MIT in Cambridge with Prof. R. R. Schrock he took sabbatical leave at the University of California, Berkeley with Prof. K. P. C. Vollhardt. He is a full Professor at the University of Bordeaux and a Member of the Institut Universitaire de France. His research interests are inorganic chemistry and nanomaterials, including catalysis, sensors, molecular electronics, and nanomedicine.

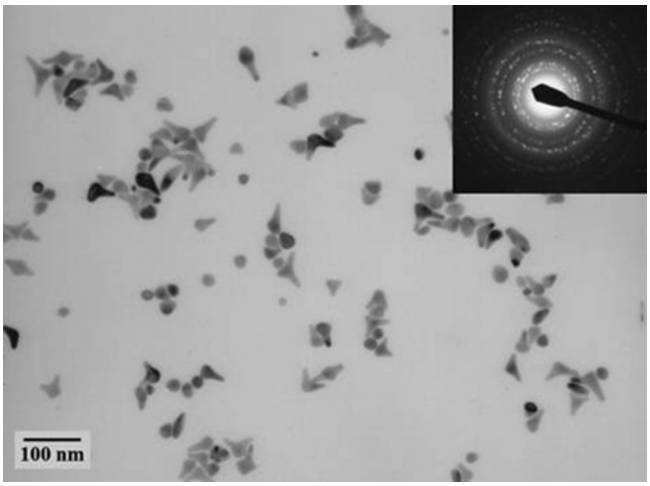

Figure 2. TEM image of branched gold nanocrystals and the corresponding electron diffraction pattern. From Ref. [40]. Copyright 2003 American Chemical Society.

3.2. The Seed-Mediated Method

Compared with the in situ synthesis, the seed-growth method enlarges the particles step by step, so that it becomes easier to control the sizes and shapes of the AuNPs. Thus, this procedure is widely used in the most recent size- and shape-controlled AuNPs syntheses.

The seed growth usually takes place over two steps. In the first step, small AuNP seeds are prepared. In the second step, the seeds are added to a "growth" solution containing $HAuCl_4$ and the stabilizing (capping) and reducing agents, and the newly reduced Au^0 then grows on the seed surface to form large AuNPs. The reducing agents used in the second step are always mild ones that reduce Au^{III} to Au^0 only in the presence of Au seeds as catalysts (in the absence of the Au^0 catalyst, ascorbic acid only reduces Au^{III} to Au^{I} in acidic medium). Thus, the newly reduced Au^0 can only assemble on the surface of the Au seeds, and no nucleation of new particles occurs in solution. Moreover, as a consequence of the use of a mild reducing agent, the second step is much slower than the first one, and it can be repeated to continue the growth process.

In the course of the seed-growth synthesis of AuNPs, the size, shape, and surface properties are controlled by the amount and nature of the reducing agent and stabilizer, as well as their ratio to the Au precursor.

A two-step method was devised by Zsigmondy, who combined his technique with Faraday's method, which had

remained ignored for 40 years before Zsimondy took notice. Zsimondy's two-phase method was published in his book in 1909,[42] and it is this two-step method that was much later renamed as the seed-growth method.

In the seminal procedure by the Murphy research group for the formation of AuNRs, $HAuCl_4$ is reduced to $HAuCl_2$ by ascorbic acid in the presence of CTAB and $AgNO_3$, then citrate-capped spherical AuNPs are added to this $HAuCl_2$ solution.[30] These spherical AuNPs catalyze the reduction of Au^I to Au^0 by ascorbic acid. A three-step procedure in the absence of $AgNO_3$ allows longer AuNRs with aspect ratios (length/width) of up to 25 to be prepared. The AuNRs formed in the first stage serve as seeds for a second growth, and the latter are in turn used as seeds for the third growth (Figure 3).[41–45] The yield and monodispersity are improved by addition of nitric acid to the third seeding growth solution.[46]

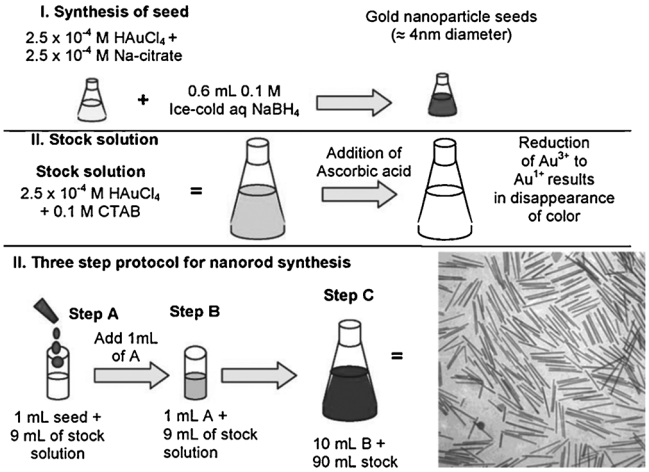

Figure 3. Three-step seed-mediated growth approach for making gold and silver nanorods with a controlled aspect ratio. From Ref. [45]. Copyright 2005 American Chemical Society.

Other modifications from the El-Sayed research group, which improved the yield and polydispersity of the AuNRs, were the replacement of sodium citrate by the stronger CTAB stabilizer during the formation of the seeds and the use of $AgNO_3$ to control the aspect ratio of the AuNRs (Figure 4).[47] In this approach, the seeds are formed upon reduction of $HAuCl_4$ with $NaBH_4$ at 0 °C in the presence of CTAB followed by the addition of $AgNO_3$; this seed solution is then added to $HAuCl_2$ previously formed in the presence of CTAB. The AuNRs are obtained in 99% yield with aspect ratios between 1.5 and 4.5 by using this method. Higher aspect ratios up to 10 or 20 are obtained upon addition of a cosurfactant (benzylhexadecylammonium chloride (BDAC)[47] or Pluronic F-127[48]) to the original growth solution and changing the $AgNO_3$ concentration. Even higher aspect ratios of up to 70 have been obtained by a fourth addition of growth solution.[42] Optimization studies have clearly shown that many parameters play a role in influencing the yield, shape, and dispersity.[41–55] In particular, impurities in the various commercial CTAB sources greatly affect the yield, dispersity, and

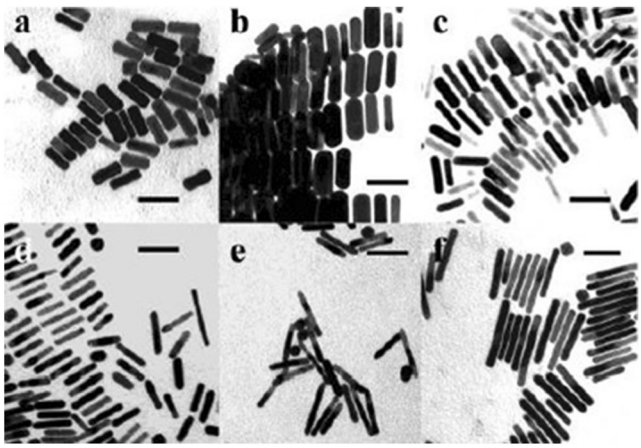

Figure 4. TEM images of gold NRs with different positions of the plasmon bands. Scale bar = 50 nm. From Ref. [47]. Copyright 2003 American Chemical Society.

aspect ratio. Traces of iodide, in particular, have a significant affect, because it binds selectively to the Au(111) facet, thus leading to the AuNRs.[54,55]

Two AuNR growth mechanisms have been proposed[45,56,57] and discussed[22,56–59] (Scheme 1). They involve a growth that is governed either by preferential binding of the head group of a cationic surfactant to the {100} face of the AuNP seed (rather than the less-favored rod end)[45,56] or by the electric field of the double layer between the positively charged seed and negatively charged $AuCl_2^-$ on the CTAB micelle (Scheme 1a,b).[57] Studies of the role of Ag^+ have shown that single-crystalline CTAB-capped seeds lead to single-crystalline AuNRs with {110} faces on the side and {100} faces on the end, whereas multiply twinned crystalline citrate-capped seeds grow into multiply twinned structures. (The role of Ag^+ and the effect of an under deposition potential (UPD) are discussed in Section 3.8.) Ag deposition on the {110} side of the rod is faster than on the {100} ends, and consequently seeds grow into rods.[50,60] Murphy and coworkers have also proposed a hybrid mechanism involving diffusion of $AuCl_2^-$ on the CTAB micelles to CTAB-capped seed spheres resulting from electric-field interactions. Subsequently, silver ions preferentially deposit onto the {110} facets, on which CTAB is preferentially bound, thereby resulting in particle growth into AuNRs along the [110] direction (Scheme 1c).[60] The critical role of the bromide counterion of CTAB or NaBr in the formation of AuNRs has been illustrated by the observation that there is a critical $[Br^-]/[Au^{3+}]$ ratio around 200 that leads to the maximum aspect ratio of the AuNRs, beyond which Br^- is a poison.[61]

3.3. Photochemistry

Photochemistry is also a convenient method to generate anisotropic AuNPs. UV light can reduce $HAuCl_4$ to form AuNRs when a cationic micelle with a rod shape is bound to $HAuCl_4$. The photoreduction to Au^0 atoms is followed in this case by controlled aggregation.[33,34] The micelle surfactant

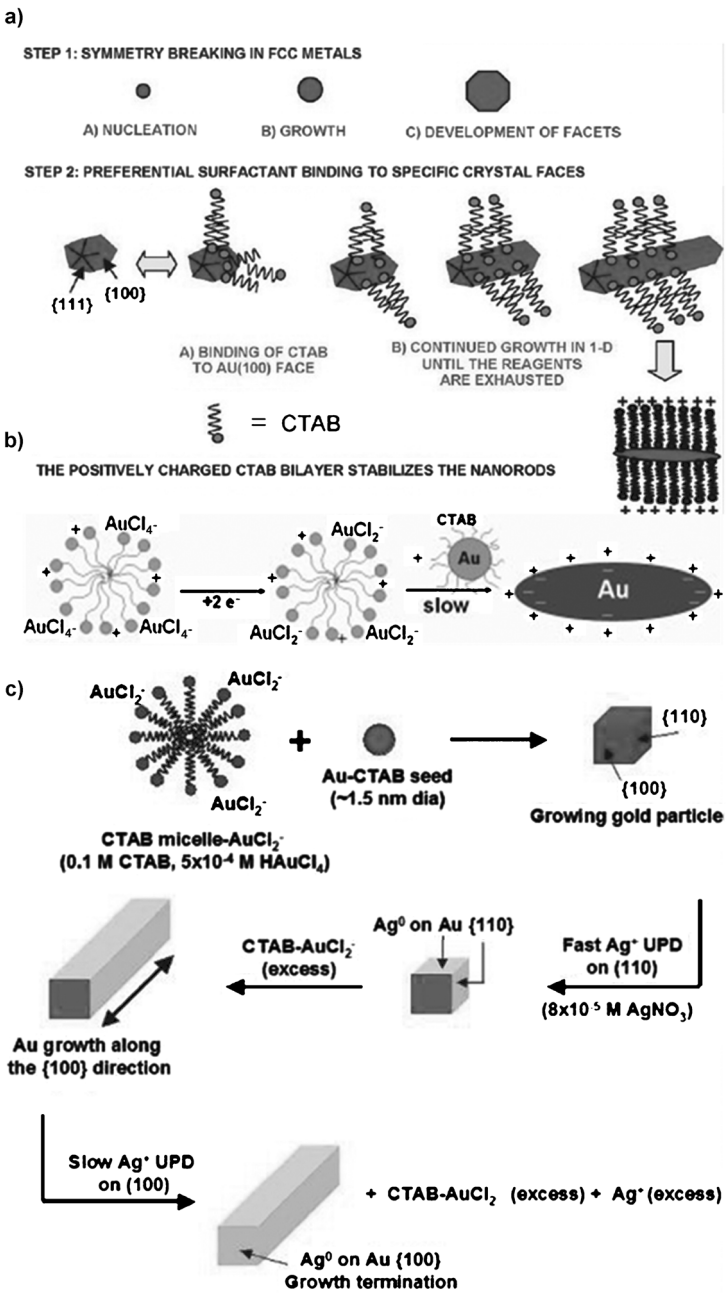

Scheme 1. Mechanisms for the formation of AuNRs. a,c) Reproduced from Refs. [45] and [60] with permission. Copyright 2005 American Chemical Society and 2006 American Chemical Society, respectively. b) Reproduced from Ref. [57] with permission. Copyright 2004 Wiley-VCH.

stabilizes a specific crystal face, as in the seed-growth procedure, thereby leading to AuNRs.[34,62–64] The presence of NaCl increases the AuNR aspect ratio and yield.[34] As in the seed-growth process, Ag^+ also improves the aspect ratio and yield.[63] UV light with a wavelength of 300 nm is optimal for these properties.[64] The method largely benefits from the improvement observed in the seed-growth method, namely the use of sodium borate, $AgNO_3$, ascorbic acid, and CTAB; the advantage here is that the AuNRs are obtained in high yield in a single step,[65,66] unlike in the seed-growth method itself. The amount of sodium borate[65] and the temperature[66] can alter the aspect ratio. The photochemical route has also been performed in the presence of poly(vinylpyrrolidone) (PVP) and ethylene glycol,[67] or TiO_2 colloids.[68–70] For example, the Zhang research group synthesized platelet-like AuNRs with an asymmetric five-twinned structure as well as, in combination with seed growth, six-star AuNPs. TiO_2 serves both as a photocatalyst and a stabilizer of the AuNPs (Scheme 2).[70] Graphene oxide was also used to assemble Au nanodots to patterned chains.[71] Although the photochemical method requires a long reaction time on the order of 30 h,[62,63] this period can be reduced to 30 min if $HAuCl_4$ is first reduced by ascorbic acid, and then exposed to UV irradiation in the presence of $AgNO_3$.[72–74] The use of ketyl radicals with a short triplet lifespan (generated from 4-(2-hydroxyethyloxy)phenyl(2-hydroxy-2-propyl)ketone, known as Irgacure-2959 (I-2959)) results in an especially efficient reaction, and causes the rapid reduction of Au^{III} to Au^0 and formation of AuNRs upon irradiation at 300 nm.[75–77]

3.4. Electrochemistry

The electrochemical method to produce AuNPs was first reported by Svedberg in 1921.[78] In the modern electrochemical technique developed by Wang and co-workers, an Au plate anode and a Pt plate cathode were immersed in an electrolyte containing CTAB and tetradodecylammonium bromide (TOAB) as a cosurfactant. Electrolytic oxidation of the Au anode then formed $Au^{III}Br_4^-$ bound to the CTAB micelle, which then underwent migration to the cathode and cathodic reduction to Au^0. AuNRs were formed with aspect ratios that were controlled by the presence of Ag^+ cations produced by the redox reaction between Au^{III} and an Ag plate. The latter was gradually inserted into the solution. The AuNRs were separated from the cathode by ultrasonification.[35,36] This method produces AuNRs with aspect ratios of 3–7 that are single crystals without stacking faults, twins, or dislocations, as shown by HRTEM and diffraction studies (Figure 5).[79] Gold nanorods have also been electrochemically deposited inside porous membranes.[80–82] Although the electrochemical method is one of the pioneering methods for the synthesis of AuNPs, including anisotropic AuNPs, it remains actively investigated because of its simplicity, efficiency, and applicability.[83,84]

3.5. Sonochemistry

Ultrasound has become a useful tool for the synthesis of very small nanoparticles, because the effects derived from acoustic cavitation drives chemical reactions under extreme conditions. This method, however, yields nanoparticles with multiple shapes and a wide size distribution.[85] This problem

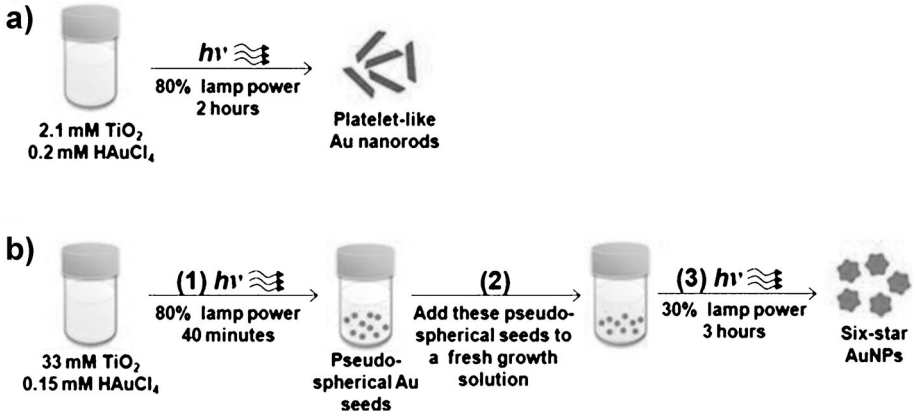

Scheme 2. TiO_2-catalyzed photochemical synthesis of a) Au platelet-like nanorods and b) six-star AuNPs. Reprinted from Ref. [70] with permission. Copyright 2010 American Chemical Society.

Han and co-workers have synthesized single-crystalline flexible Au nanobelts with a width of 30–50 nm and a length of several micrometers with this method (Figure 6).[90]

3.6. Templates

The synthesis of nonspherical AuNPs is often driven by the use of templates that have a complementary morphology to the AuNPs.[24] The templates are solid substrates, such as porous membranes,[91,92]

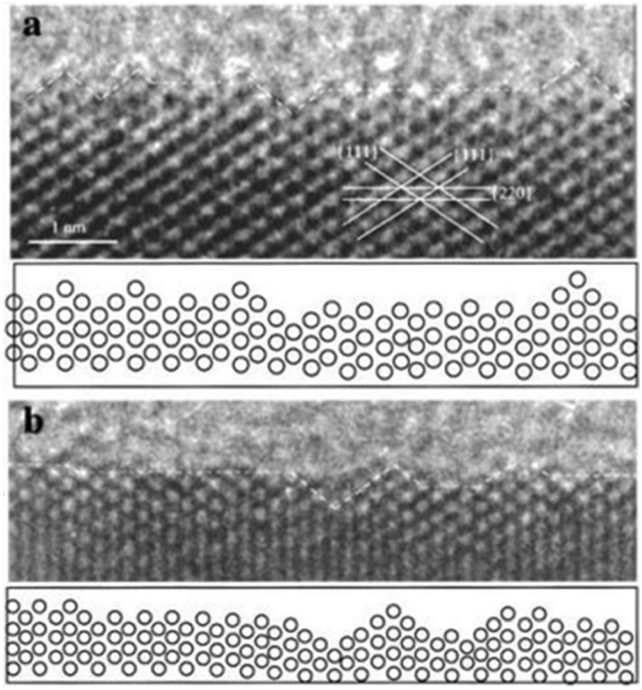

Figure 5. HRTEM images recorded from a [110]-oriented Au nanorod and the corresponding positions of the projected atom rows. From Ref. [79]. Copyright 2000 American Chemical Society.

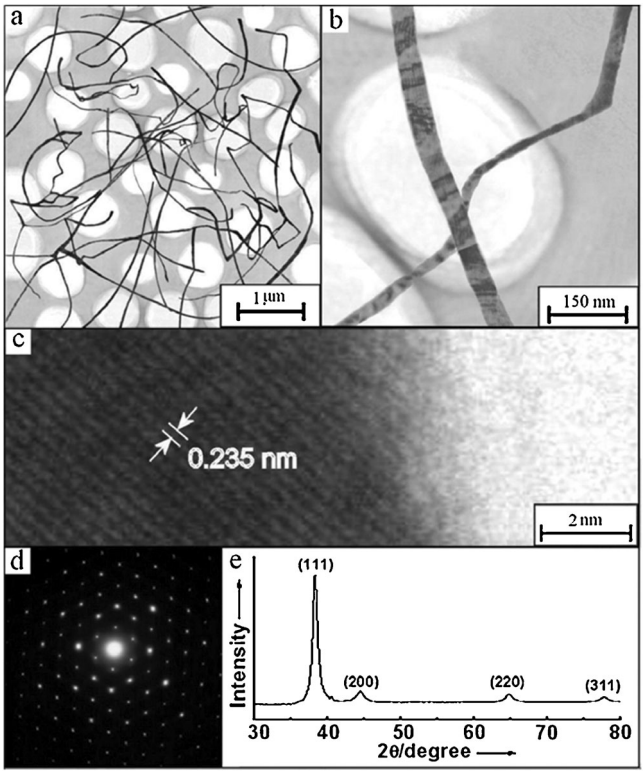

Figure 6. a,b) TEM images, c) HRTEM image, d) SAED pattern, and e) XRD pattern of gold nanobelts synthesized by a sonochemical method. From Ref. [90]. Copyright 2006 Wiley-VCH.

is circumvented by the use of surfactants, as in other methods, and added alcohols also serve to control the particle shape and size.[86,87] For example, in the presence of α-D-glucose, the major reactions in the sonolysis process of aqueous $HAuCl_4$ follow Equations (1)–(4).[88,89]

$$H_2O \rightarrow H^{\cdot} + OH^{\cdot} \quad (1)$$

$$\text{sugar} \rightarrow \text{pyrolysis radicals} \quad (2)$$

$$Au^{III} + \text{reducing radicals} \rightarrow Au^0 \quad (3)$$

$$n\,Au^0 \rightarrow AuNP \quad (4)$$

mesoporous silica,[93] Si(100) wafers,[91] pyrolytic graphite,[94] polymers[92,95] (including block copolymers),[96] nanoparticles,[97,92] carbon nanotubes,[98] inorganic clusters such as $LiMo_3Se_3$,[99] surfactants organized in micelles,[35,42,43,100] or Langmuir–Blodgett films,[101] as well as biomolecules such as plant extracts,[102,103] microorganisms,[104] polypeptides, and DNA.[105]

The essential role of the surfactant for the growth of anisotropic AuNPs (AuNRs) was already detailed in Section 3.2. Mulvaney proposed the electric-field model, according to which the rods grow because of a higher rate of mass

transfer of gold cations to the tips as a result of the asymmetric double layer around the rod. The CTAB bilayer confers a positive charge onto the Au rods, and the CTAB also binds Au^{I} ions (produced by reduction of Au^{III} by ascorbic acid), which retards its transfer to the Au rods. The surface potential decays more rapidly at the tips because of their curvature, thereby explaining why the rod tips grow faster than the lateral facets.[106] Other models have been proposed[57,106,107] and discussed,[58] in particular in terms of steric and chemical factors to direct preferential interactions between the cationic head group of CTAB and the growth sites.[107]

Templates are frequently also used in combination with photochemistry, electrochemistry, and sonochemistry for the synthesis of anisotropic AuNPs. The template structure directs anisotropic growth by selective adsorption on specific crystallographic sites of the metal. This has been used in combination with surfactants, for example, with poly(vinylpyrolidone) (PVP). PVP also serves as a reductant, for example, for the synthesis of Au plates.[108,109] The reducing ability of PVP is due to its hydroxy termini and is dramatically enhanced in the presence of water bound to the PVP. Thus, kinetic control of the AuNP growth depends on the solvent and nature of the reductant and yields various morphologies that can sometimes be made selectively.[110]

One of the most successful nanomaterials for the synthesis of AuNPs is silica nanospheres, which serve as templating cores around which Au layers can be coated. This powerful strategy was reported by Halas and co-workers, and allows the size of the Au nanoshell and the thickness of the nanogold layer to be controlled at will by changing the reaction time and the concentration of the plating solution (Figure 7).[111–114]

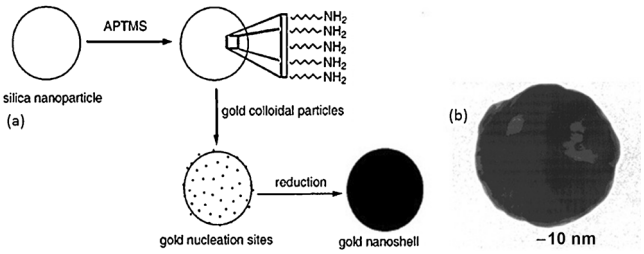

Figure 7. a) Formation of a nanoshell around a silica nanoparticle core, and b) the TEM image of an Au nanoshell. From Ref. [111]. Copyright 2002 American Chemical Society.

3.7. Galvanic Replacement

Galvanic replacement is a very simple approach in which gold cations in the plating bath are spontaneously (i.e. in a thermodynamically and kinetically favorable reaction) reduced by a metal without external current sources.[115–130] The driving force is the difference in the redox potential between the reducing metal and the Au^{3+}/Au system. This method was proposed and exploited by Crooks and co-workers to prepare AuNPs encapsulated in dendrimers by metal exchange between dendrimer-encapsulated CuNPs and Au^{III} from $HAuCl_4$.[115,122,129] Au@Pt dendrimer-encapsulated nanoparticles have also recently been fabricated in this way.[129] The driving force for exchange is the lower redox potential of Cu^{II}/Cu^{0} ($E° = 0.340$ V versus NHE) compared to $AuCl_4^-/Au^0$ ($E° = 0.99$ V versus NHE).

The reducing Ag metal ($E°_{Ag/Ag+} = 0.80$ V versus NHE; $E°_{Ag/AgCl} = 0.22$ V versus NHE) in the form of an Ag nanostructure has been used extensively as a sacrificial template, in particular by the Xia research group[116,118,121,123,124,125] to fabricate hollow Au nanostructures. Gold nanocages (AuNCs) have been synthesized in this way starting from Ag nanocubes and an aqueous $HAuCl_4$ solution. These reactions proceed in two steps: 1) formation of seamless hollow structures with the walls made of Au-Ag alloys by galvanic replacement of Ag and Au^{III} by Ag-Au alloying and 2) formation of hollow structures with porous walls by dealloying.[123]

Aluminum foil is also often used as the metal source, because it is inexpensive and has a very low oxidation potential [$E°(Al^{3+}/Al = -1.67$ V versus SHE] and can thus reduce many transition-metal cations through an exergonic reaction [Eq. (5)]:

$$Al + Au^{III} \rightarrow Al^{III} + Au^{0} \quad (5)$$

This reaction is marred, however, by the thin layer of alumina Al_2O_3 on the aluminum metal surface. The use of the metal chloride ($AuCl_3$ or $HAuCl_4$) in a high concentration[131] together with prior removal of the aluminum oxide with NaOH[132] can circumvent this difficulty. In the presence of chloride anions, oxidized aluminum cations form soluble tetrachloroaluminate salts that do not prevent the deposition of AuNPs. Fluoride forms stronger bonds than chloride, and NaF and NH_4F have also been used to dissolve the alumina layer to allow the galvanic displacement through Al^{III} dissolution [Eq. (6)].

$$Al_2O_3 + 6\,H^+ + 12\,F^- \rightarrow 2\,AlF_6^{3-} + 3\,H_2O^{[133]} \quad (6)$$

This galvanic technique does not require the presence of template, surfactant, or stabilizer and is conducted at room temperature. The use of Al foil, NaF, and $HAuCl_4$ for the galvanic replacement of Al by Au^{III} results in Au dendrites.[133]

3.8. The Effect of Ag^+ Salts and Underpotential Deposition

A crucial finding by Murphy and co-workers was the favorable role of $AgNO_3$ in the controlled formation of long AuNRs.[41] By varying the parameters and using the seed-growth procedure it was possible to direct the aspect ratio, optimize the yield (up to 50%), and obtain long AuNRs (Figure 8).[60,134,135] Nikoobahkt and El-Sayed further improved the yield of the AuNRs up to 99% by using CTAB[31] instead of the citrate-capped seeds used by Murphy and co-workers. The seed-mediated growth was much slower in the presence of CTAB. However, along with AuNR formation, the longitudinal surface plasmon band (SPB) is red-shifted in the absence of $AgNO_3$ (increase in the aspect ratio, that is, AuNR growth at the tips), whereas in the

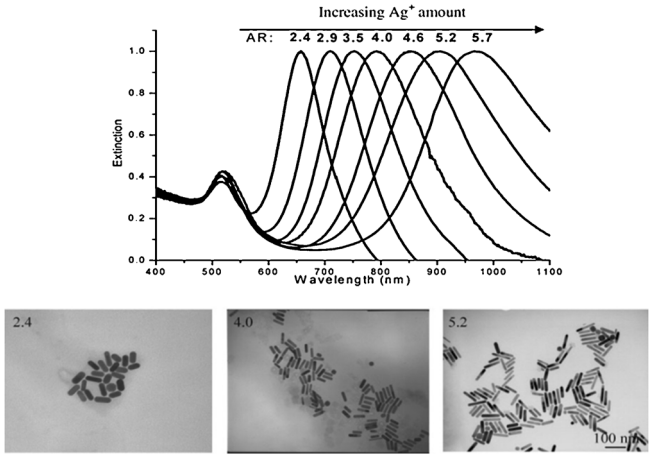

Figure 8. Increasing the amount of silver ions leads to gold nanorods of higher aspect ratios, which is consistent with the red-shifting LSPR. From Ref. [59]. Copyright 2009 Wiley-VCH.

presence of $AgNO_3$ it is blue-shifted after 2 minutes. Thus, the length and aspect ratio quickly increases during this short time, then slowly decreases.[135] $AgNO_3$ immediately forms AgBr in the presence of CTAB. It was proposed that Ag^+ is not reduced at acidic pH values, (typically pH 3) because the ascorbic acid reductant is too weak, as confirmed by the lack of the AgNP SPB at 400 nm (AgNPs only form at a basic pH value, typically pH 8). Consequently, Ag^+ forms ion pairs [AgBr] that decrease the charge density on the Br^- ion and the repulsion between head groups on the AuNR surface, thus inducing CTAB elongation.[31] It was alternatively argued that the adsorption of [AgBr] on the Au nanocrystal facets slows down the reduction of the gold ion and induces the growth of single-crystalline AuNR.[56]

An underpotential deposition of Ag onto the AuNR has been invoked to explain the dramatic role of $AgNO_3$ on the growth of the AuNRs.[50] Underpotential deposition is the deposition of a metal adlayer onto a metal surface (Au) below the Nerst reduction potential (up to 0.5 to 0.9 V) of the metal ions ($AgNO_3$/Ag), as a result of strong bonding interactions between the two metals in the adsorbed layer.[10,139] It appears that Ag^+ is essentially not reduced, although CIP analysis has shown the presence of Ag at up to 4.5 %.[60] However, it is the Ag^+ adsorption on AuNR (in the form of AgBr) that considerably slows down the growth of AuNRs. This rate decrease is selective and less efficient on the tips because of poorer coverage, which results in the formation of AuNRs.

The role of Ag^+ is not only crucial for the formation of AuNRs, but also for other shapes of AuNPs, as recently shown by several research groups. High-index concave cubic Au nanocrystals with {720} surfaces have indeed been synthesized by Mirkin and co-workers by the reduction of $HAuCl_4$ with ascorbic acid in the presence of a chloride-containing surfactant and small amounts of $AgNO_3$.[137] Ag^+ has also been used for the synthesis of {730}-faceted bipyramids[50,138] and high-index AuNRs.[31,139–142]

3.9. Supramolecular Arrangements

Supramolecular chemistry[143,144] is another general method for assembling spherical[16] or nonspherical AuNPs (in particular AuNRs[59]) into new nonspherical AuNPs in the form of liquid crystals, supracrystals, or supported ordered arrays.[145–148]

Various examples will be described in the following. Large aligned structures of AuNRs were obtained upon drying a drop of AuNR solution on a copper TEM grid in air with the grid immersed halfway.[149] AuNRs pack together upon drying a rod–sphere mixture on a silicon wafer in a water vapor atmosphere.[150] AuNRs linearly align in a head-to-tail fashion after centrifugation, but a 2D parallel assembly is obtained after three rounds of centrifugation.[151] Liquid-crystalline structures of aligned AuNRs spontaneously form in a side-on arrangement with high aspect ratios in concentrated solutions.[152]

Pileni has examined the ordering of transition-metal nanoparticles over long distances in 3D superlattices called supracrystals.[145,153–157] In particular, it has been shown that this ordering of alkanethiolate-AuNPs into supracrystals depends on the solvent[153] and on the addition of water,[154] with their final morphology determined through either a layer-by-layer growth or a process of nucleation in solution.[153] Gold supracrystals can also grow from suspensions of gold nanocrystals, with the building process taking place in solution and at the air–liquid interface. These growth processes determine the crystallinity and mechanical properties of the supracrystals.[157]

Anisotropic AuNP arrangements can also be formed by using bridging thiolate ligands. Feldheim and co-workers used phenylacetylene oligomers to synthesize 2D and 3D crystalline arrangements of AuNPs (e.g. dimers and trimers). The oligomers play the role of "molecular wires" between the AuNPs. In this way, well-defined, rigid arrays with a variety of geometries could be produced.[158]

Examples of end-to-end AuNR assemblies include the use of biotin disulfide (in combination with streptavidin; Figure 9),[159] thioalkyl carboxylic acids (hydrogen bonding),[160,161] alkanedithiols (thiolate coordination),[162] thiolated DNA (hybridization),[163] thiolated alkynes and azides (click reaction),[164] and polymers such as polystyrene.[165,166]

Mann and co-workers showed that DNA hybridization could also be used to assemble AuNRs side-by-side by first substituting CTAB with thiolated oligonucleotides.[167] Other research groups also described such arrangements (Figure 10).[168–171] Another way to achieve the side-by-side assembly of AuNRs is by appropriate choice of the thiolate ligands (e.g. 1,2-dipalmitoyl-*sn*-glycero-3-phophothioethanol)[172] or mercaptopropylsilane[173]) followed by solvent evaporation.

Polymer engineering (see also Section 3.6)[108–114,165,166,174–179] is a well-developed strategy to assemble AuNPs. Besides the previously discussed use of PVP, other polymers such as poly(*N*-isopropylacrylamide) and its acrylic acid derivative,[174,175] poly(viny alcohol),[176–178] and poly(styrene-*b*-methylacrylate) allow fabrication of anisotropic arrangements of AuNPs.[179]

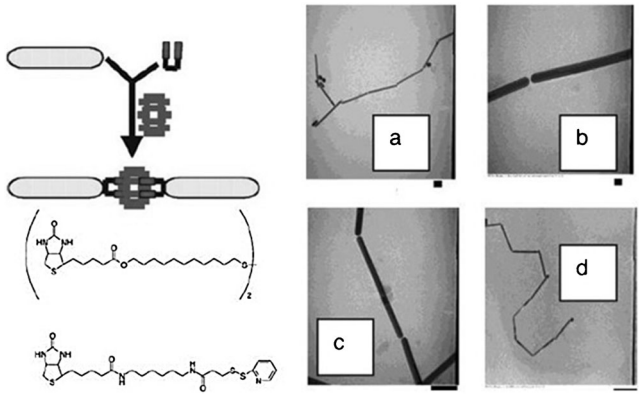

Figure 9. Principle of the formation of gold nanorods by surface functionalization with biotin disulfide as well as the corresponding TEM images. Scale bars: a) 100 nm, b) 20 nm, c) 100 nm, and d) 500 nm. From Ref. [159]. Copyright 2003 American Chemical Society.

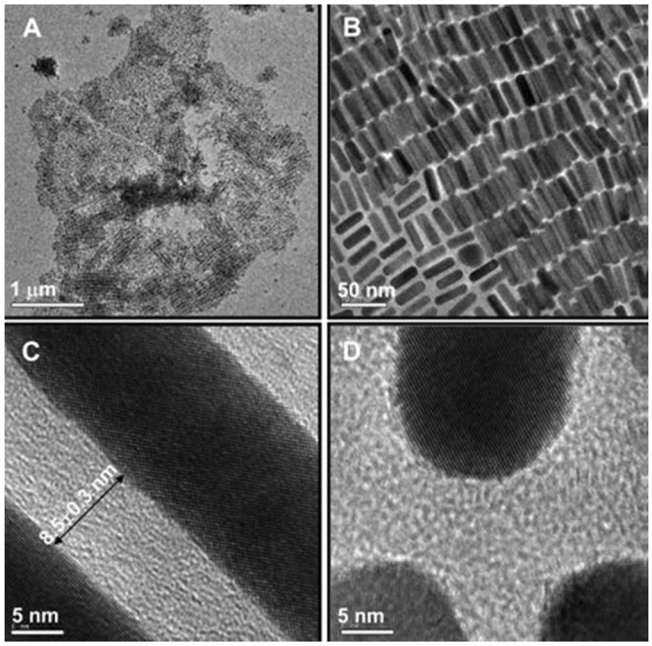

Figure 10. TEM images of the aligned Au nanorods. From Ref. [171]. Copyright American Chemical Society.

3.10. Top-Down Syntheses: Lithography Methods

The most common lithography technique used to produce AuNPs is electron-beam lithography (EBL).[180,181] First, a substrate is coated with an electron-sensitive resist. The electron beam dissociates this coated substrate into fragments, which are removed with a developing agent. The nanoscale structure remaining is suitable for the deposition of AuNPs. Another lithography technique is focused ion beam (FIB) lithography.[180–182] A gallium ion beam sputters parts of a film to form the desired nanostructure shape. These lithography techniques have produced AuNRs[180–183] and Au nanodisks,[184] although a drawback is that AuNPs smaller than 10 nm as well as larger particles are usually not accessible. Ebbesen and co-workers have combined ion-beam and electron-beam techniques[185–187] to synthesize arrays of Au microholes,[185] grooves, and nanowire circuits.[186] Colloidal masks commonly used in lithography[169] have led to the production of, for example, hexagonal arrays of Au triangles[189] and Au nanorings.[190] A modern lithography method, on-wire lithography (OWL), has been reported by the Mirkin research group.[191,192] OWL is a template-based electrochemical process for forming gapped cyclindrical structures on a solid support. The size of the gaps and segment length can be controlled on a length scale of under 100 nm (Figure 11). This method allows the composition and

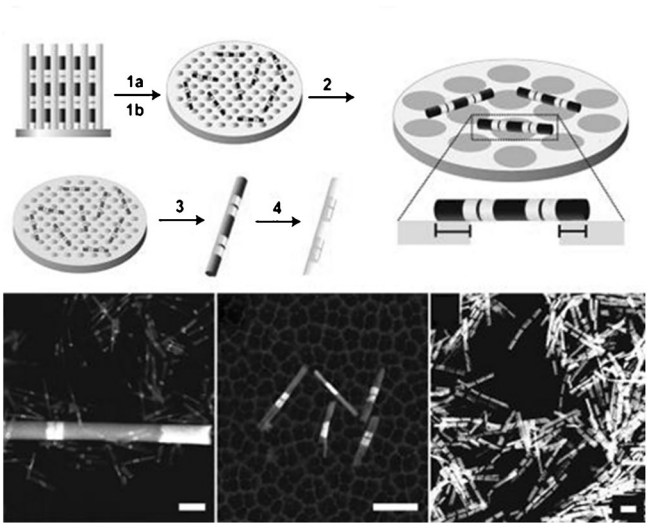

Figure 11. Synthetic strategy for preparing nanostructure arrays with OWL. From Ref. [196]. Copyright 2011 American Chemical Society.

distances between adjacent particles to be tailored down to 2 nm.[193–195] 1D arrays of Au nanostructures as small as 35 nm in diameter, which allow control of the segment length and spacing down to about 6 and 1 nm, respectively, were synthesized in this way.[196] Such nanostructures can be combined with organic and biological molecules to create systems with emergent and highly functional properties.[194]

4. The Morphology of AuNPs

4.1. Platonic AuNPs[123,178,179]

AuNPs with the morphology of the five platonic solids—the tetrahedron (four triangles),[197] hexahedron (cube, six squares),[137,198–200] octahedron (eight triangles),[201] dodecahedron (twelve pentagons),[202] and icosahedron (twenty triangles)[203–210]—and their aqueous synthesis is often based on seed growth, as shown by the Murphy research group.[211] They are characterized by low-index facets ({111} for tetrahedron, octahedron, dodecahedron, and icosahedron and {100} for the cube). Yang and co-workers used a modified polyol process with PVP to form AuNPs in high yield with

distinct highly uniform tetrahedra, cube, octahedra, and icosahedra (dubbed platonic nanocrystals) with sizes of 100–300 nm. Solutions of $HAuCl_4$ and PVP in ethylene glycol were injected simultaneously in boiling ethylene glycol, which also served as the reductant. The shape was controlled by the PVP/$HAuCl_4$ ratio (4.3:1 to 8.6:1), with the AuNP shapes being highly sensitive to the concentration of the $HAuCl_4$.[197] Han and co-workers carried out the synthesis of rhombic dodecahedral AuNPs from an aqueous solution of $HAuCl_4$ without the use of any seeds, surfactants, or foreign metal ions but only with DMF added as both the co-solvent and reductant at 90–95 °C for 15 h. Purification was carried out by centrifugation and washing with ethanol. It was suggested that reaction temperatures lower than the boiling point of DMF (156 °C) results in slower, kinetically controlled reductions that are responsible for the observed shapes formed.[201] Rhombic dodecahedral AuNPs (together with gold bipyramids) were also obtained by Mirkin and co-workers[210] by an Ag-assisted, seed-mediated growth process (Figure 12).[204] Dodecahedral

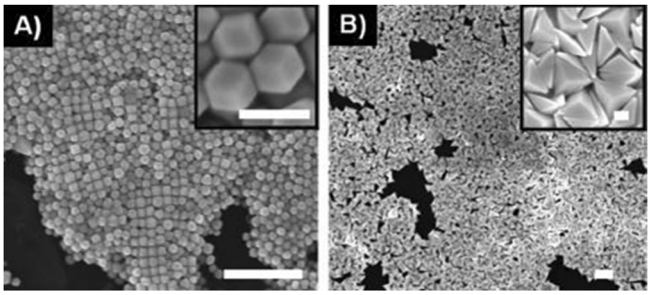

Figure 12. SEM image of AuNPs in the form of A) rhombic dodecahedra and B) bipyramids. Scale bars: 500 nm (main images) and 100 nm (insets). From Ref. [210]. Copyright 2011 American Chemical Society.

AuNPs were transformed into other nonplatonic shapes such as rhombic cuboctahedron and then truncated octahedron in the presence of PVP at a low water content. At high water content, the dodecahedral AuNPs were transformed into rhombic cuboctahedra, then to truncated cubes, then cuboctahedra, and truncated octahedra.[211] Song and co-workers have used the popular polyol process, specifically 1,5-pentanediol at reflux, to successfully and quantitatively produce a variety of shaped AuNPs, including cubes, in the range of about 100 nm by incremental change in the $AgNO_3$ concentration. Smaller cubes and octahedral were also produced by using large amounts of PVP.[199]

4.2. One-Dimensional AuNPs: Nanorods,[212–221] Nanowires,[222–233] Nanotubes,[234–243] and Nanobelts[244–247]

Nanorods are the most extensively investigated one-dimensional anisotropic AuNPs to date. In Section 3, the electrochemical[35] and seed-growth methods leading to the formation of AuNRs were detailed, in particular the seminal studies by the Murphy[45] and El-Sayed[100] research groups, as well as several other synthetic techniques. For example, the seed-mediated growth leads to either single-crystalline or pentahedrally twinned AuNR structures.

Various other remarkable one-dimensional nanogold structures have also been synthesized, including nanowires, nanobelts, and nanotubes. When the aspect ratio of AuNRs increases, these AuNRs are called Au nanowires, thus there is a continuum between these two categories of AuNPs. AuNRs can also be assembled in line (Figures 13 and 14)[176–178,212] or into other hybrid nanostructures such as nanotubes,[213] in particular by using polymer films as hosts.[214] Various aspects of AuNR materials, including their optical properties and

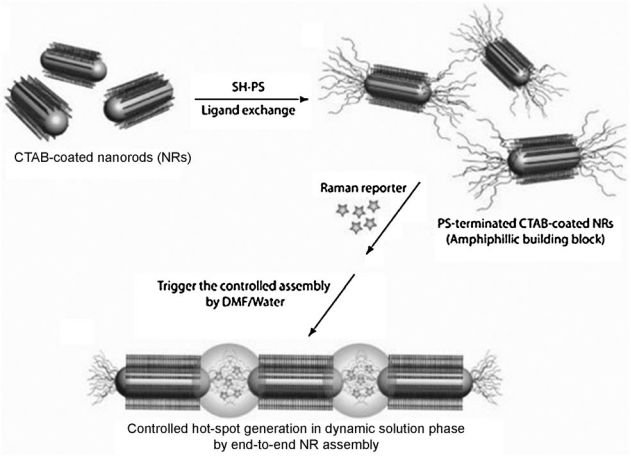

Figure 13. Formation of hot spots by end-to-end self-assembly of gold NRs in chains. From Ref. [212]. Copyright 2011 American Chemical Society.

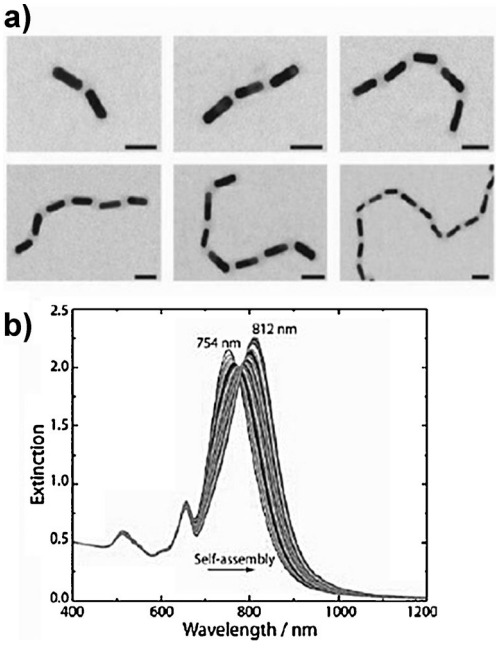

Figure 14. a) STEM images of the self-assembled chains of AuNRs from Figure 13. Scale bar = 40 nm. b) Variation of the extinction properties of NRs during the course of their self-assembly into chains (LSPR shifts from 754 to 812 nm). From Ref. [212]. Copyright 2011 American Chemical Society.

application properties, have been detailed in reviews by the research groups of Murphy,[45,22,215,216] El-Sayed,[59,101] and Liz-Marzan and Mulvaney.[217]

The main interest in AuNRs arises because of their tremendous utility and multifunctionality for the diagnosis and treatment of cancer. They are indeed used as drug-delivery vehicles and as contrast agents for near-IR photothermal tumor ablation (see Section 6).[218–221]

Gold nanowires (AuNWs) are synthesized by the tip-selective growth of AuNRs.[222] AuNRs stabilized by CTAB and pentahedrally twinned are, for example, used for such processess.[223,224] This method produces crystalline AuNWs that are 12–15 μm long with a diameter of (90 ± 10) nm. AuNWs can also be prepared by UV irradiation (> 350 nm), photoreduction, and thermal reduction (at 70 °C) of $HAuCl_4$ in the bulk phase of the block copolymer made from PEG_{20}-PPE_{70}-PEG_{20} (PPO = poly(propylene oxide) and Pluronic P123.[225] AuNWs have potential applications as nanoscale optical waveguides in the visible and near-IR regions.[226–228] AuNWs are indeed an ideal platform to produce surface plasmon waves by direct illumination of one end of the nanostructure. They can thus be used as tools for fundamental studies of subwavelength plasmon-based optics of wave propagation. This strategy was pioneered by Halas and co-workers, who used Ag- and AuNWs with longitudinal dimensions of more than 10 μm. The addition of an adjacent nanowire, substrate, or other symmetry-breaking defect enables direct coupling with the guided waves in a nanowire. Networks of plasmonic AuNWs can serve as the basis for optical devices such as interferometric logic gates, which can lead to nanorouters and multiplexes, light modulators, and a complete set of Boolean logic functions.[228]

Bimetallic AuPtNWs are useful electrochemical sensors for glucose with increased selectivity, sensibility, and repeatability compared to monometallic nanowires.[229] CuAuNWs have been intensively studied because of their widespread applications.[230] Interestingly, the method of fabrication of AuCuNWs can also lead to the formation of AuCu nanotubes (AuCuNTs). Therefore, CuNWs were used as templates, and the AuCuNWs are formed as intermediates that ultimately lead to the AuCuNTs (Scheme 3).[231]

AuNRs and AuNWs have also served as seeds for the fabrication of higher-order AuNRs and AuNWs containing periodic starfruit-like morphologies by Vigderman and Zubarev.[232] Nanowires are required for applications such as ultrasensitive and multiplex DNA detection through SERS and other biomedical SERS-based techniques.[233]

Both AuNWs and Au nanotubes (AuNTs) can be prepared by electroless deposition onto the pore walls of porous polymer membranes, as shown by the seminal study by Wirtz and Martin.[234] In such membranes, the pores act as a template for the nanostructuration. A commercially available example of a support membrane is a polycarbonate filter with cyclindrical nanopores. Long Au deposition times leads to the preparation of AuNWs, while short deposition times give AuNTs. The AuNWs and AuNTs synthesized in this way can be used as nanoelectrodes, molecular filters, and chemical switches.[234] AuNTs are also sensitive refractive index reporters.[235] Finally, AuNTs have also been designed for specific

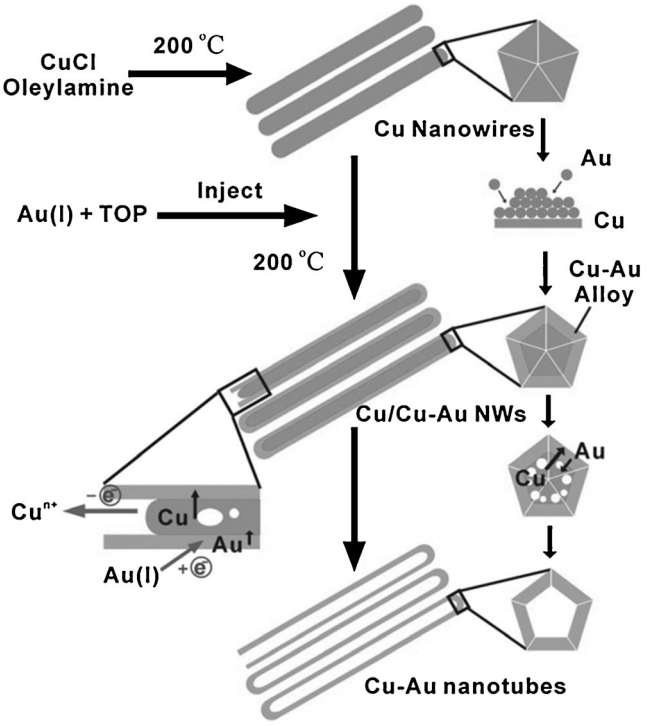

Scheme 3. Mechanism for the formation of Cu-Au alloy nanotubes. Reprinted from Ref. [231] with permission. Copyright 2012 American Chemical Society.

catalytic applications (see Section 6.1). 4-(Dimethylamino)-pyridine is a powerful auxiliary reagent for this electroless deposition method (Figure 15).[236] Indeed, AuNTs are currently synthesized by the galvanic replacement reaction,[235,237] for example, by using an anodized aluminum oxide template[238,239] and a polymer NT as a sacrificial core to produce hollow AuNTs that have exquisite sensitivity to the refractive index.[235] Thiol-functionalized nanoporous films can also act as a scaffold for the development of such highly ordered Au arrays.[240] Conical AuNT/pores can be advantageous to avoid unwanted plugging and are ideally suited to detect protein-type bioanalytes.[241] Inorganic nanostructures that serve as templates for the formation of AuNTs include goethite (FeOOH) rods.[242] Finally, density functional theory can be of tremendous help when designing discrete AuNTs such as Au_{32} units with a zigzag structure.[243]

Among the 1D AuNPs, Au nanobelts (AuNBs; or Au nanoribbons) have attracted interest, because they may represent a good system for examining dimensionally confined transport phenomena and for fabricating functional nanodevices. Han and co-workers synthesized single-crystalline AuNBs by using a combination of ultrasound irradiation and α-D-glucose as a directing agent under ambient conditions (Figure 16). The sugar is pyrolized to provide radicals that reduce Au^{III} to Au^0.[90] Gemini surfactants have also been used as a template in an aqueous phase by using dimethylene bis(tetradecylammonium bromide) (14-2-14) as a capping agent and template. A two-step seed-growth method (to avoid secondary nucleation) was used, whereby the first seed-growth step yielded AuNRs of high aspect ratio; then AuNBs

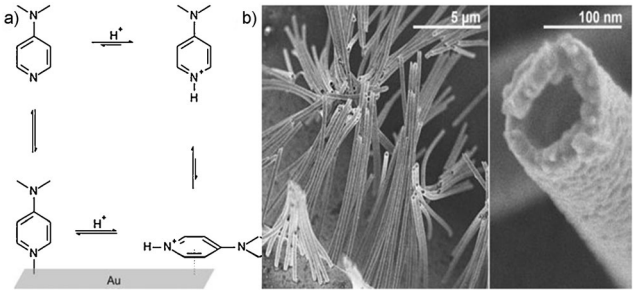

Figure 15. a) Equilibria between DMAP, elemental Au, and protons on Au surfaces. b) SEM images of free-standing NTs. From Ref. [236]. Copyright 2010 American Chemical Society.

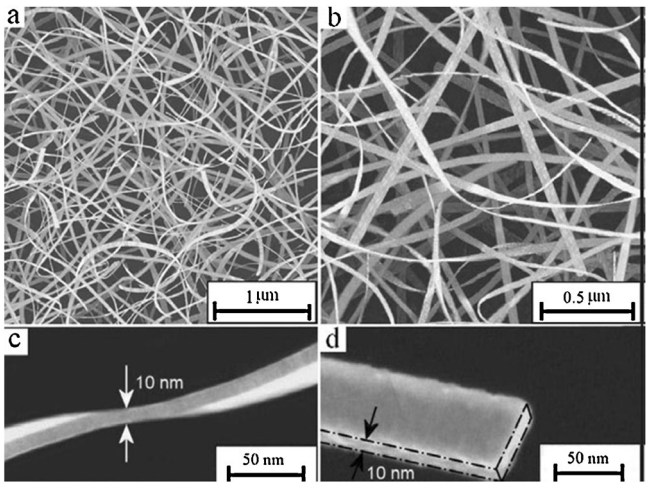

Figure 16. a,b) SEM images and c,d) high-magnification SEM images of gold nanobelts. From Ref. [90]. Copyright 2006 Wiley-VCH.

that were several micrometers long and 5 nm thick were grown in the second step.[244]

Au nanoarrays of single-crystalline AuNBs with long-range identical crystallographic orientation have been synthesized by directional solid-state transformation of an Fe-Au eutectoid followed by a precise electrochemical treatment (Figure 17).[245] Nanostructured reactive precursors have been employed as effective sacrificial templates for the controlled synthesis of 1D inorganic nanostructures with desired compositions. For example, porous AuNBs were fabricated from metal–surfactant complexes of precursor NBs formed by $HAuCl_4$ and a bolaform surfactant containing two quaternary ammonium head groups.[246] Plasmonic effects were studied in nanostructures for the transport of optical information, and tunable plasmon resonance was indeed disclosed in AuNBs with cross-sectional dimensions smaller than 100 nm and narrow transverse plasmon modes.[247]

4.3. Two-Dimensional AuNPs: Gold Nanoplates[248–267]

The synthesis of gold nanoplates with specific shapes (stars, pentagons, squares/rectangles, dimpled nanoplates,[248] hexagons, and truncated triangles) of well-defined particle

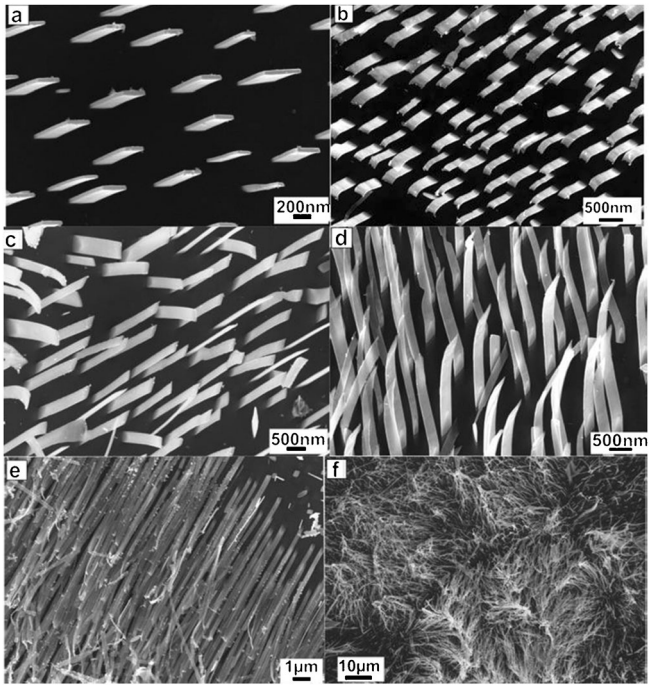

Figure 17. SEM images of Au nanobelts. From Ref. [245]. Copyright 2008 American Chemical Society.

sizes have been extensively exploited for their specific properties and features. One of the simplest and versatile methods to produce gold nanoplates is the polymer template method, whereby the polymers have an extraordinary effect as stabilizers, templates, and reductants. In 2004, Lee and co-workers used bulk polymeric phases of $PEO_{20}PPO_{70}PEO_{20}$ (PEO = poly(ethylene oxide), PPO = poly(propylene oxide)) as both the reductant and stabilizer, with the large (10 μm in width and 100 nm in thickness) gold nanosheets being obtained by reduction of $HAuCl_4$ in THF.[225] In another example, Radhakrishnan and co-workers generated polygonal gold nanoplates in situ in a poly(vinyl alcohol) matrix through thermal treatment.[249] Such a procedure occurs in high yield, does not involve the need for a reducing agent, and has been widely utilized in the synthesis of large single-crystalline gold nanoplates.[250,251] In some cases the polymers acted only as stabilizers, such as in the formation of unprecedented starlike gold nanoplates through the reduction of $HAuCl_4$ by L-ascorbic acid in the presence of poly(*N*-vinyl-2-pyrrolidone) as reported by Nakamoto and co-workers.[252] On the other hand, Hojo and co-workers indicated that the morphology of polyhedral nanoplates was controlled with $HAuCl_4$ and polyvinylpyrrolidone (PVP) through a polyol process when using ethylene glycol as both the solvent and reducing agent.[253]

In addition to the polymer process previously discussed, a wet-chemical route has also been proposed and exploited in the last decade. It was demonstrated that the morphology could be finely adjusted through control of the reactant ratio and the reaction conditions. In 2004, Wang and co-workers also reported a mild large-scale synthesis of micrometer-scale Au nanoplates. In this process, $HAuCl_4$ is reduced by *ortho*-

phenylenediamine in aqueous medium to form hexagonal single-crystalline Au nanoplates with preferential growth along the Au(111) plane. This result suggests that the molar ratio of *ortho*-phenylenediamine to gold is key to producing Au nanoplates.[254] Huang and co-workers carried out the synthesis of trianglular and hexagonal gold nanoplates in aqueous solution by thermal reduction of $HAuCl_4$ with trisodium citrate in the presence of CTAB surfactant in just 5–40 min. The size of the gold nanoplates was varied from as small as 10 nm in width to several hundreds of nanometers. A [CTAB]/[$HAuCl_4$] ratio of 6:1 in the reaction solution was favorable for the formation of gold nanoplates (Figure 18).[255]

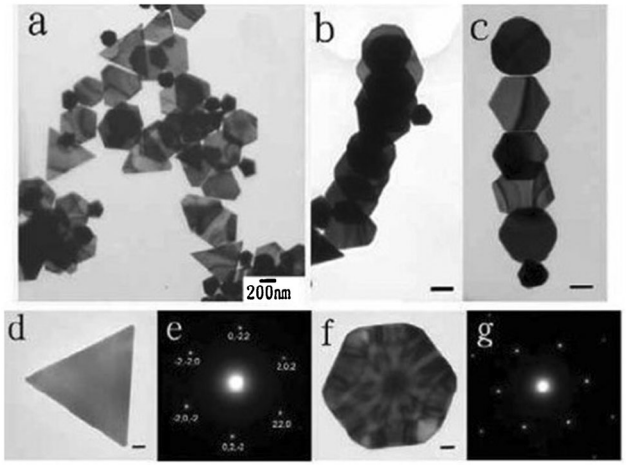

Figure 18. a) TEM image of gold nanoplates. b,c) TEM images of gold nanoplates arranged into chainlike structures. Scale bar = 200 nm. d) TEM image of a single triangular gold nanoplate and e) the corresponding electron diffraction pattern. Scale bar = 50 nm. f) TEM image of a single quasihexagonal gold nanoplate and g) the corresponding electron diffraction pattern. Scale bar = 50 nm. From Ref. [255]. Copyright 2006 American Chemical Society.

A shape transformation from triangular to hexagonal nanoplates was evident on selective etching of Au triangular nanoplates, growing of Au nanodisks, then ripening of hexagonal nanoplates, which corresponded to the change of the medium upon alternate addition of $HAuCl_4$ and ascorbic acid.[256]

Dong and co-workers introduced a mild and relatively "green" one-pot biomimetic method for the fabrication of gold nanoplates. The reactions were carried out at 25 °C in aqueous solution containing $HAuCl_4$ and aspartate as the reductant for 12 h. The hexagonal and truncated triangular nanoplates with a thickness of less than 30 nm were obtained after evaporation of the solvent.[257] This use of a biological reductant was investigated extensively over the last decade. For example, the use of brown seaweed *Sargassum*,[258] tannic acid,[259] or serum albumin protein led to the formation of single-crystalline gold nanoplates,[260] whereas glycine was used in the facile synthesis of concave gold nanoplates.[261] The advantage of this method is that it is environmentally friendly, and it has been applied to the synthesis of other shaped AuNPs.

Gold nanoplates exhibit a wide range of unique electrical and optical properties, for example, a significant surface enhanced Roman scattering (SERS),[262] tip-enhanced Raman scattering (TERS),[263] and a shape- and size-dependent surface plasmon absorbance in the visible to infrared region. These properties result in potential applications as sensors and probes.[263,264]

A particular interesting morphology is triangular nanoprisms that exhibit three congruent edge lengths in the range of 40 nm to 1 μm and a defined thickness ranging from 5 to 50 nm. These triangular nanoprisms have plasmonic features in the visible and IR regions, can be prepared in high yield, and can be readily functionalized with a variety of sulfur-containing adsorbates as well as other functional materials.[265–267]

4.4. 3-Dimensional AuNPs

4.4.1. Gold Nanotadpoles[268–271]

Gold nanotadpoles are a class of anisotropic 3D gold nanostructures with tadpole-like appearance. These interesting nanostructures with special optical and electrical properties have unique potential applications in second-order nonlinear optics, nanoelectronics, and other fields. The successful synthesis of gold nanotadpoles was reported by the Tian research group in 2004. They used a simple chemical procedure in which the tadpole-shaped gold nanoparticles were synthesized in aqueous solution by the reduction of chloroauric acid with trisodium citrate in the presence of sodium dodecylsulfonate as a capping agent. These three-dimensional and crystallized structures were characterized by TEM, AFM, and HRTEM methods (Figure 19).[268] Soon afterwards, tadpole-shaped AuNPs were synthesized in high

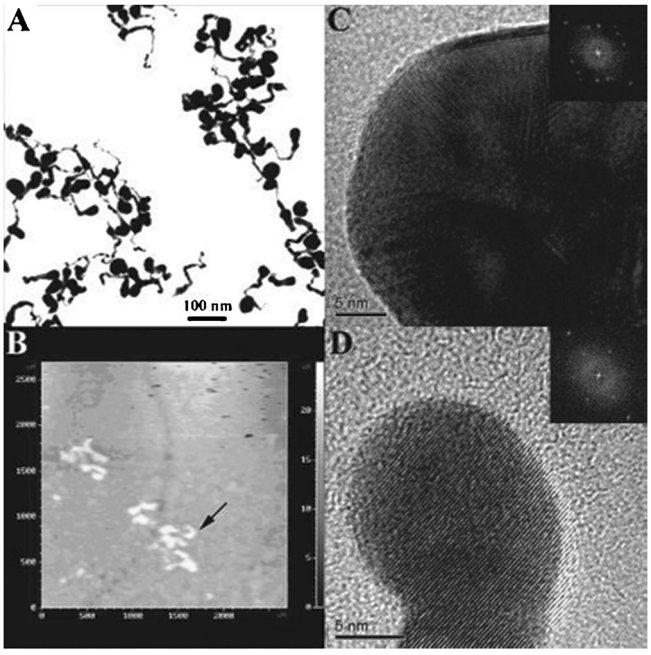

Figure 19. A) TEM and B) AFM images of tadpole-shaped AuNPs. C,D) HRTEM images of the C) head and D) tail of a gold nanotadpole. Insets: the corresponding Fourier transform patterns. From Ref. [268]. Copyright 2004 American Chemical Society.

yield by a temperature-reducing seeding approach, without any additional capping agent or surfactant.[269] An aggregation-based growth process was proposed as the formation mechanism. Very recently, Au nanotadpoles were synthesized through the normal seed-mediated process in the presence of Ag^+ ions and CTAB at room temperature.[270] A hybrid nanostructure consisting of Au heads and Pd tails and the mechanism of formation of this morphology were demonstrated by Xia and co-workers.[271] It was expected that these Pd-Au tadpoles would combine the properties of both the Pd nanorods and AuNPs.

4.4.2. Gold Nanodumbbells (AuNDs)[272–277]

The seed-mediated growth of gold nanodumbbells (AuNDs) was described and particularly well investigated by the Liz-Marzán research group.[272,273] It was reported that the presence of tiny amounts of iodide modified the growth of gold nanorods in such a way that tip growth was greatly enhanced, thereby resulting in the formation of well-defined dumbbell morphologies (Figure 20).

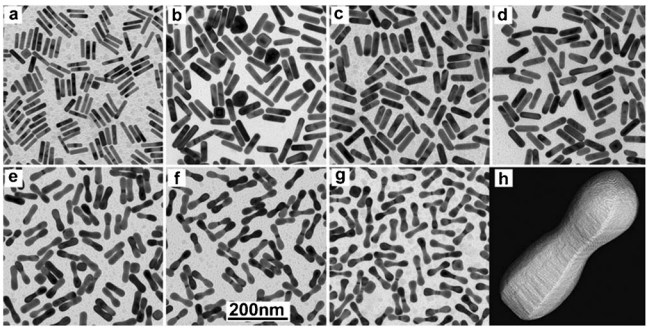

Figure 20. TEM micrographs of Au nanorods: a) initial AuNRs, b) grown in the absence of KI, c–g) grown in the presence of KI and with the amount of KI decreasing from (c) to (g). h) Electron tomography 3D reconstruction of a single Au dumbbell from the sample shown in (g). From Ref. [273]. Copyright 2008 Wiley-VCH.

Gold-containing hybrid nanodumbbells are of a great interest because of their ability to carry multiple functions that can be simultaneously utilized. The Au/Ag core/shell nanodumbbells have recently been synthesized either through the deposition of silver onto the surface of the AuNDs,[274] or by galvanic replacement and reagent reduction.[275] Another hybrid morphology is that of gold-tipped metal nanorods (nanodumbbells), such as CdSe-Au nanodumbbells,[276] The nucleation and growth mechanism of the formation of $CoPt_3$/Au, FePt/Au, and Pt/Au nanodumbbells were systemically studied by Prakapenka and co-workers. The authors were able to propose a general strategy for the synthesis of dumbbells with precise control over the size distribution and yield.[277]

4.4.3. Branched AuNPs: Nanopods and Nanostars[278–291]

Branched gold nanostructures, including monopods, bipods, tripods, tetrapods, hexapods,[278] and multipods such as nanoflowers, nanostars, and urchins[279] are highly desired because of their sharp edges and the correspondingly high localization of any surface plasmon modes. There are great expectations for such branched AuNPs as potential candidates in nanocircuits and nanodevices, and for in vivo application as a result of their high tissue penetration in that spectral range. So far, branched AuNPs have indeed been utilized in biosensing,[280] imaging,[281] targeting,[282] and photothermal therapy.[283]

The synthesis of branched gold nanocrystals in aqueous solution was first reported by Carroll and co-workers in 2003.[40] They demonstrated the use of triangular Ag platelets as seeds for the synthesis of Au monopods, bipods, tripods, and tratrapods through the reduction of Au^{III} with ascorbic acid in the presence of CTAB. Sau and Murphy introduced a seed-mediated synthesis whereby the dimension and number of branches were varied under various combinations of the [seed]/[Au^{3+}] ratio.[211] Subsequently, Hao et al. reported the synthesis of new "branched" gold nanocrystals in high yield (over 90%) by a wet-chemical route during which $HAuCl_4$ was reduced by sodium citrate in a solution of bis-(*p*-sulfonatophenyl)phenylphosphine dipotassium dihydrate (BSPP) and H_2O_2 at room temperature.[284] Many other routes were subsequently used to synthesize branched AuNPs.[279,285–291]

The branched AuNPs are generally not as highly monodisperse as other shapes. It was expected that the branched nanoparticles would have complicated localized surface plasmon resonance (LSPR) spectral features that would be lost in ensemble measurements. To test this hypothesis, scattering spectra were measured on single Au nanostars, and the result showed that the spectra consisted of multiple sharp peaks in the visible and NIR region.[289] The LSPR spectra of highly branched AuNPs have been explored by simulating the simpler structural subunits. The finite-difference time-domain (FDTD) method was used to calculate the near- and far-field properties of a gold nanostar, whereby the nanostar was modeled as a solid core with protruding prolate tips. This study showed that the resulting LSPR energies can be thought of as a hybridization of the core and tip plasmons (Figure 21).[290] This hybridization greatly increases the overall excitation cross-section and field enhancement of the nanostar tips. This antenna effect of the nanostar core may be responsible for the relatively bright and narrow scattering spectra of nanostars in the single particle measurements.[291]

4.4.4. Gold Nanodendrites[292–295]

The Au dendrites possess a hierarchical tree-type architecture with trunks, branches, and leaf components. Gold nanodendrites with hyperbranched architectures have attracted much attention because of their importance in understanding the fascinating fractal growth phenomena and their potential applications in functional devices, plasmonics, biosensing, and catalysis.[292–295] The most important synthetic method for the preparation of Au dendrites is electrochemical deposition because of its ease of control and simple operation, and because it generates highly pure and uniform deposits. Hung and co-workers, obtained hyperbranched Au dendrites

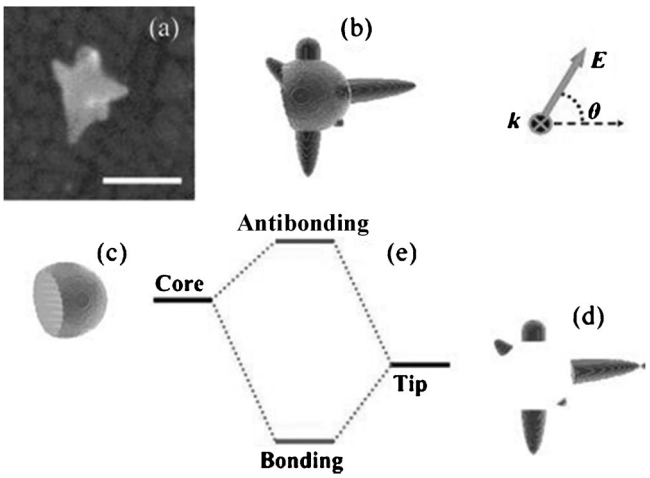

Figure 21. Principle of the plasmon hybridization of the LSPR of a gold nanostar. From Ref. [290]. Copyright 2007 American Chemical Society.

on a glassy carbon electrode by electrodeposition with a square-wave potential from a solution of $HAuCl_4$ containing cysteine as the blocking molecule.[292]

Huang et al. reported the first shape-controlled synthesis of Au nanostructures in the presence of supramolecular complexes formed from dodecyltrimethylammonium bromide (DTAB) and β-cyclodextrin (β-CD). Well-defined planar Au nanodendrites were formed by the reduction of chloroauric acid in aqueous DTAB/β-CD solutions (Figure 22).[293] Another example of surfactant/reductant

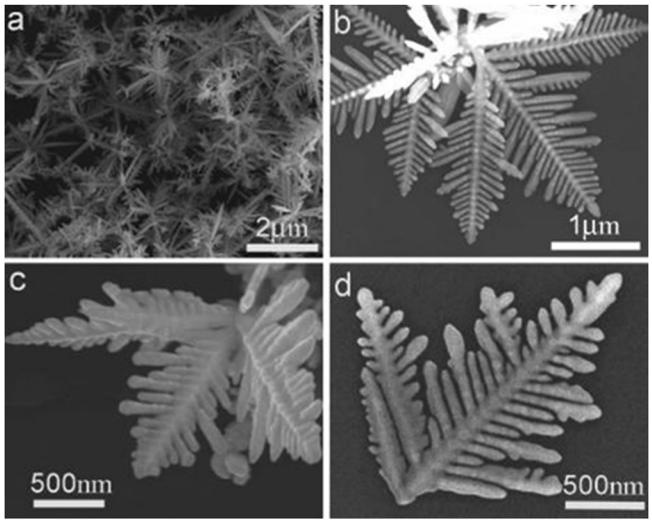

Figure 22. SEM images of Au nanodendrites grown in mixed DTAB/β-CD solution. From Ref. [293]. Copyright 2009 American Chemical Society.

combination has been reported for which the three-dimensional dendritic gold nanostructures were prepared by an ultrafast one-step homogeneous solution method by reducing $HAuCl_4$ in the presence of decane-1,10-bis(methylpyrrolidinium bromide) ([mpy-C_{10}-mpy]Br_2) as the capping agent and L-ascorbic acid (AA) as the reducing agent.[294] Dendritic AuNPs exhibited significant catalytic activities, and the good SERS sensitivity for the detection of biomolecules also indicated their potential applications in biosensing and nanodevices.

4.5. Au Nanoshells[296–308]

Core/shell nanomaterials containing a supporting core material and a thin Au nanoshell in the form of dielectric SiO_2@Au particles have been designed by Radloff and Halas. Such Au nanoshells exhibit a strong plasmon resonance, and the SERS effect sensitively depends on the core radius and shell thickness.[297] The authors provided a seminal systematic approach for "nanoengineering" the optical resonance wavelength of metal NPs. This SPB wavelength could indeed be "tuned" across a large region of the visible and infrared spectrum in particular in the crucial near-infrared region between 700–1100 nm, for biomedical applications, by variation of the relative size of the inner and outer shell layer (see Section 6). Gold nanoshells are among the most important AuNPs and find considerable usage in both therapy and diagnostics (concept of theranostic).[298] Other core@shell nanomaterials with a metal or metal oxide core and Au nanoshells are also known.[296] The scattering spectra of single gold nanoshells were also measured by dark-field microscopy combined with high-resolution scanning electron and atomic force microscopy,[299] and it has been demonstrated that the gold nanoshells show the same fluorescence enhancements as dye molecules.[300–302] The fabrication of supported hemishell structures known as Au nanocups was also reported by the Halas research group.[303] Briefly, a 35 nm thick Au layer was deposited by electron-beam evaporation onto silica NPs (120 nm diameter), thereby forming an Au film on top of the silica NPs. The Au nanocap generates second-harmonic light, whose intensity increases as the angle between the incident fundamental beam and the nanocup symmetry axis is increased (Figure 23). These plasmon structures provide a promising approach for the design and fabrication of stable, synthetic second-order nonlinear optical materials.

SiO_2@Au NPs were also applied to optical imaging,[304] biomedical detection,[305] and photothermal cancer therapeutic ability,[306] and may enable a new class of infrared materials, components, and devices to be developed.

Moreover, Fe_3O_4@Au core/shell NPs modified with antibodies and fluorescent dyes have been reported to act as contrast probes for the multimodal imaging of tumors. This finding illustrates the great potential of Fe_3O_4@Au NPs to improve the accuracy of tumor diagnosis.[307] Very recently, magnetic Co@Au core/shell NPs with a pure Co core, an intermediate Au shell, and a compact outer cobalt oxide shell were reported.[308]

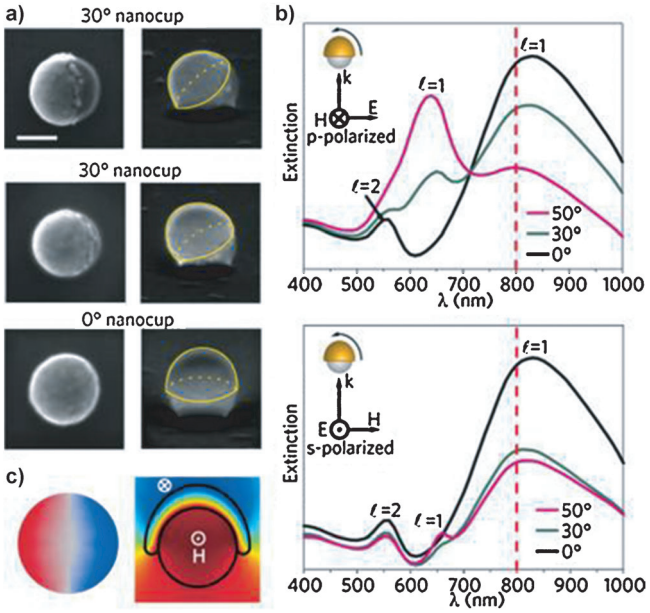

Figure 23. Images and spectra of nanocups. a) SEM images from above (left) and tilted (right). The yellow curves highlight the geometries of the nanocups. Scale bar = 100 nm. b) Theoretical extinction spectra of these nanocups. The dashed red line indicates the wavelength of the incident light in SHG experiments. c) Surface-charge distribution on a nanocup (0°) and the magnetic field on its symmetry plane one-quarter cycle later showing the magnetic dipole mode. From Ref. [303]. Copyright 2011 American Chemical Society.

4.6. Hollow AuNPs

4.6.1. Hollow Gold Nanospheres (HAuNSs)[309–319]

The investigation of HAuNSs was pioneered in 1997 by the Halas research group.[309] They described the properties of Au-coated dielectric nanoparticles, or gold nanoshells, in which the configuration of a dielectric core coated with a metal nanoshell occurs naturally during the growth of Au/Au_2S nanoparticles. It was found that gold nanoshells possess quite remarkable optical properties that differ dramatically from those of solid AuNPs. During the growth of the core/shell cluster, the plasmon-related absorption peak undergoes very large shifts in its wavelength, from 650 to 900 nm. Such structures potentially exhibit tremendous importance for optical applications related to the absorbance of IR light. The plasmon resonant optical properties[310,311] and SERS effects[312] of nanoparticles consisting of core/shell structures were analyzed, and it was shown that they have a tunable plasmon resonance that depends on the ratio of the core radius to the total radius.

One of the most versatile approaches for the preparation of coated and hollow spheres is the layer-by-layer (LbL) assembly method.[111,313] Polyelectrolyte-modified polystyrene (PS) nanospheres were widely introduced as templates for the construction of HAuNS morphologies by the size-controllable LbL technique. The PS core was subsequently treated by either calcination, causing the removal of the core, or dissolution of the core into a specific solvent (such as, THF).[314,315] Wan and co-workers reported a facile and effective approach to fabricate HAuNSs with tunable cavity sizes.[316] These HAuNSs were fabricated by using Co nanoparticles (CoNPs) as sacrificial templates and varying the stoichiometric ratio between the $HAuCl_4$ starting material and the reductants. The formation of these hollow nanostructures is attributed to two subsequent reduction reactions: the initial reduction of $HAuCl_4$ by CoNPs, followed by reduction with $NaBH_4$. This strategy allows the convenient one-pot synthesis of homogeneous HAuNSs.

Recently, biomacromolecules have been investigated as precursor materials for the synthesis of nanoparticles. Rosi and co-workers first reported that, in the presence of inorganic salts and reducing agents, properly designed peptide conjugates can orchestrate a one-pot reaction in which the synthesis and assembly of nanoparticles into complex superstructures occurs simultaneously. Hexanoic acid-AAAYSSGAPPMPPF (C_6-AA-PEP_{Au}) conjugates direct the formation of well-defined HAuNS superstructures (diameter = 136.5 ± 2.6 nm) upon incubation in water for 24 h (Figure 24).[317] Remarkably, the C_{12}-PEP_{Au} conjugate, which has a slightly different composition, directs the dramatic formation of double-helical nanoparticle superstructures.[318] The impact of further modification of the peptide sequence on the resultant nanoparticle assembly was explored with the peptide sequence BP-A_x-PEP Au ($C_{12}H_9CO$-A_x-AYSSGAPPMPPF; x = 0–3; BP = biphenyl). The studies showed

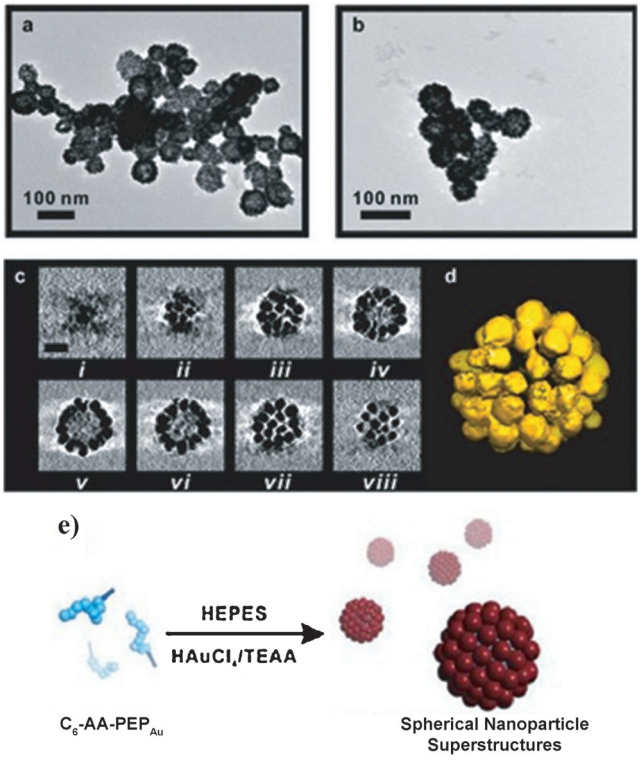

Figure 24. a–c) TEM images, *X-Y* computational slices, *X-Y* computational slices assembly (i–viii), and d) the 3D surface rendering of the hollow spherical gold nanoparticle superstructures. e) Synthesis of the AuNP superstructures. From Ref. [317]. Copyright 2010 American Chemical Society.

that the small modifications to the peptide sequence, in this case the addition of a single alanine residue, can have a significant impact on the diameter of the resulting spherical superstructure (29.4–270 nm). These investigations revealed the versatility of this bio-based method and the rich structural diversity that occurs when this method is employed.[319]

4.6.2. Gold Nanocages and Nanoframes[320–328]

Au nanocages (AuNCs), a novel class of remarkable nanostructures possessing hollow interiors and porous walls, were pioneered by the Xia research group.[320] AuNCs are attractive for colorimetric sensing and biomedical applications. Galvanic replacement is a facile and general synthesis method for the preparation of hollow metal structures. The typical synthesis of gold nanocages can be described as follows: The controlled addition of $HAuCl_4$ solution to a boiling suspension of Ag nanocubes (as both template and reducing agent) leads to galvanic replacement because of the electrochemical potential difference between Au and Ag (the reduction potential of $AuCl_4^-$/Au (0.99 V versus the standard hydrogen electrode, SHE) is more positive than that of AgCl/Ag (0.22 V versus SHE)). The redox reaction takes place according to Equation (7), with the consumption of Ag atoms and the deposition of Au^0 confined to the Ag nanocube surface. When more $HAuCl_4$ is added, the formation of the hollow, porous cagelike Au nanostructure is observed. The morphology was confirmed by Xia and co-workers by SEM and TEM.[123,320]

$$3\,Ag_{(s)} + HAuCl_4 \rightarrow Au_{(s)} + 3\,AgCl_{(s)} + HCl_{(aq)} \quad (7)$$

The controlled selective removal (or dealloying) of Ag from the Au/Ag alloy nanoboxes was achieved with a wet aqueous etchant $Fe(NO_3)_3$. Ag was selectively dissolved from Au/Ag-alloyed nanoboxes or nanocages by galvanic replacement [Eq. (8)], without the deposition of solid Fe.

$$Ag_{(s)} + Fe(NO_3)_3 \rightarrow AgNO_{3(aq)} + Fe(NO_3)_{2(aq)} \quad (8)$$

Nanoboxes derived from 50 nm Ag nanocubes were converted into nanocages and then cubic nanoframes by increasing the amount of the etchant $Fe(NO_3)_3$ in the dealloying process (Figure 25). The structural change was accompanied by the SPR peaks continuously shifting from the visible region to 1200 nm.[321] These nanoframes have sensitivity factors that are several times higher than those of gold nanospheres, gold nanocubes, and gold nanorods, as well as those of comparable-sized AuNCs.[322]

AuNCs and Au nanoframes were investigated in catalysis[323] and biosensing in view of their controllable LSPR properties that depend on the size and, most importantly, the thickness of the walls.[324–328]

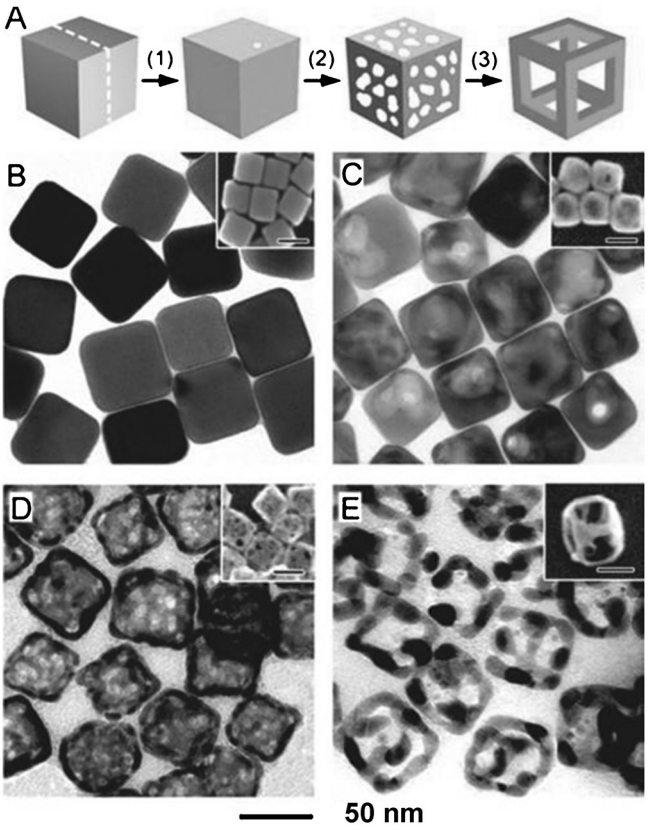

Figure 25. A) Principle of the formation of an AuNC from an Ag nanocube, and then an Au nanoframe. 1) Formation of Au/Ag alloy nanocage, 2) selective removal of the Ag atoms from the nanobox with an aqueous etchant, 3) complete removal of Ag from the nanocage as more etchant is added. B–E) Corresponding TEM and SEM images (insets) of the Ag nanocube, Au nanobox, Au nanocage, and Au nanoframes, respectively. From Ref. [321]. Copyright 2007 American Chemical Society.

5. Optical Plasmonic Properties of Anisotropic AuNPs: SPR and SERS

5.1. SPR Properties of Anisotropic AuNPs

The rates of absorption and scattering, as well as the position of the plasmon band (SPR peak), of AuNPs were found to depend on their shape, size, and structures.[322] Some anisotropic AuNPs have unique SPR properties that are different from those of spherical AuNPs. For example, the AuNRs (also the AuNDs and AuNTs) exhibit two plasmon bands: a strong longitudinal band in the near-infrared region and a weak transverse band, similar to that of spherical AuNPs, in the visible region. The band in the IR region, where tissue absorption is minimal, is very useful for potential in vivo applications in nanomedicine.[235,329] Moreover, the location and intensity of the SPR peaks of AuNRs are remarkably more sensitive to the local refractive index in the vicinity of the nanorods and can be altered by the binding of biomolecular targets to the surface of the AuNR, which forms the basis of their utility as attractive biosensors. Additionally, the nanorods have an inherently higher sensitivity to the local dielectric environment than similarly sized spherical nano-

particles, thus making AuNRs excellent colorimetric probes.[330] The plasmon bands of other intricate-shape AuNPs have recently been explored, and the well-defined plasmon band in the ensemble spectra is observed in every case.[247,278,284,291,288,320] For example, gold nanostars typically show a plasmon band of the core and multiple plasmon bands corresponding to the tips and core–tip interactions.[284] The hollow AuNPs (AuNCs and other Au nanoframes) have the highest sensitivity factors, and their plasmon bands are tunable throughout the visible and into the near-infrared regions. The relative intensity of the scattering and absorption cross-sections of the hollow-structured AuNPs can be tuned by varying their size, and this feature makes them attractive for colorimetric sensing and biomedical applications.[320] Although silica@Au nanoshells are spherical and present a single broad plasmon absorption, the fine-tuning at will of the position of this SPB differentiates them from standard spherical AuNPs and allows their efficient use in vivo for cancer therapy and imaging (see Section 6).[22,114]

5.2. SERS Properties of Anisotropic AuNPs

The SERS effect originates from the dramatic amplification of electromagnetic fields in the NP ensembles. Considerable enhancement occurs at the AuNP surface, because the intensity of the Raman signals depends on the fourth power of the local electric field, which is very high at the AuNP surface because of the plasmon resonance. This enhancement also originates from electromagnetic coupling between adsorbed molecules and the AuNP surface as a result of charge transfer between the adsorbed molecules and the AuNP surface. Amplified electromagnetic fields at AuNP junctions contribute to SERS, because the selective enhancement of SERS is controlled by polarization-dependent resonance bands. In addition to the elastically scattered light by the AuNPs themselves, which can be imaged using a dark-field optical microscope, the AuNP surface provokes an inelastic SERS effect as a result of adsorbed molecules generating a Raman spectrum, which enables their identification. The two main strategies for SERS detection are direct identification of Raman-active adsorbed molecules and indirect detection of molecules that are incorporated into a biolabel.[330,331]

The Raman scattering signal of molecules located on nonspherical AuNPs is distinctly enhanced by contributions from the strong absorptions in the near IR regime and the extremely high electric field intensities at their tips or hollow structure.[332–335] Thus, controlling the size, shape, and structure of anisotropic AuNPs is critical to enhance the sensitivity for effective molecular detection.[238,336] For example, El-Sayed and co-workers showed that oral cancer cells can align AuNRs that have been conjugated with anti-epidermal growth factor receptor antibodies on the cell surface, thereby leading to a SERS fingerprint specific to the cancer cell.[337] The Halas research group has discriminated between acidic cancer cells and healthy cells by monitoring changes in the Raman spectrum induced by pH changes of carboxy groups in a mercaptobenzoic acid layer on HAuNSs that were active in the NIR region.[338]

5.3. Fluorescence Enhancement

The interaction between AuNPs and a fluorophore results from a change in the electromagnetic field and the intensity of the photonic mode near the fluorophore. For AuNP–fluorophore distances less than 4 nm, the fluorescence is strongly quenched. At larger distances, the fluorescence intensity is increased, including by coupling with far-field scattering. For example, the quantum yield of indocyanine green (ICG), a near-infrared fluorophore, was increased by up to 80% near the surface of an Au nanoshell. Such conjugates have been used for enhancing sensitivities in fluorescence imaging in vitro and in vivo.[114,301,302]

6. Applications of Anisotropic AuNPs

6.1. Catalytic Applications of Anisotropic AuNPs

The catalytic activity and selectivity of metal NPs (MNPs) is dependent primarily on the size and shape; therefore, nanoengineering is crucial in tailoring NP catalysts. As a consequence of the presence of sharp edges and corners, the number of active surface sites in anisotropic AuNPs is very high compared to spherical AuNPs. The shape of an NP is composed of a particular crystallographic plane, which ultimately determines the number of active surface sites present in that NP. For example, with 5 nm tetrahedral PtNPs, which have only {1,1,1} facets, 35% of the surface atoms are located at corners or edges, whereas this proportion is only 6% for cubes, with {1,0,0} facets. With such PtNPs, the average rate constants were found to increase exponentially as the percentage of surface atoms at the corners and edges increased when surface coordination was involved in the rate-limiting step of the reaction.[344] The {1,1,0} facets found in dodecahedral nanocrystals have the highest energy among the low-index facets. The synthesis of metal nanocrystals with high-energy facets is, thus, challenging in terms of catalytic applications, because these facets endow crystals with high activity.

Catalysis of carbon monoxide oxidation by dioxygen at low temperature by small (<5 nm) AuNPs on titanium oxide was pioneered by Haruta et al. in the late 1980s.[339] This study was a breakthrough in catalysis science that opened up a wide area of AuNP-catalyzed oxidation reactions.[5,13–15,339–343] For example, oxide-supported Au/carbon catalysts were found to have high catalytic activity in the selective oxidation of cyclohexene and cyclooctene.[340] It is widely accepted that CO molecules are preferentially adsorbed at edges and steps on the surface of nonspherical or hemispheical AuNPs, rather than on the facets.[341,342] Very recently, it was shown that the perimeter interfaces around AuNPs are the sites for CO oxidation (Figure 26).[343]

Therefore, investigations in catalysis have recently focused on anisotropic AuNPs such as gold nanotubes, nanodendritic gold, gold nanopyramids, and polygonal gold.[344,345] Gold nanotubes were found to be very efficient catalysts for CO oxidation at room temperature.[346,347] For example, gold nanotubes deposited within the pores of

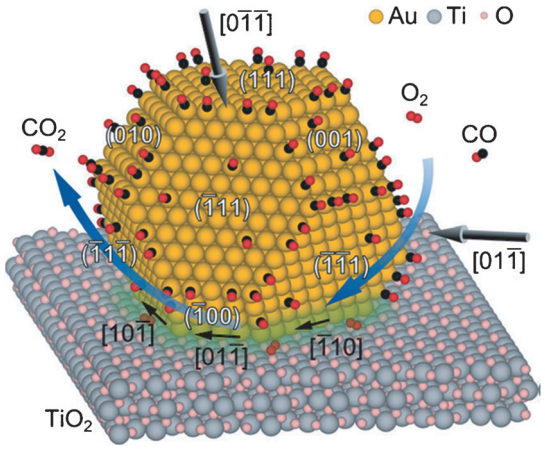

Figure 26. Schematic view of an AuNP under reaction conditions for the oxidation of CO (1 vol% CO in air (100 Pa) at room temperature). An AuNP with {111} and {100} facets has a polygonal interface with the TiO_2 support. Possible catalytically active sites are highlighted in green. From Ref. [343]. Copyright 2012 Wiley-VCH.

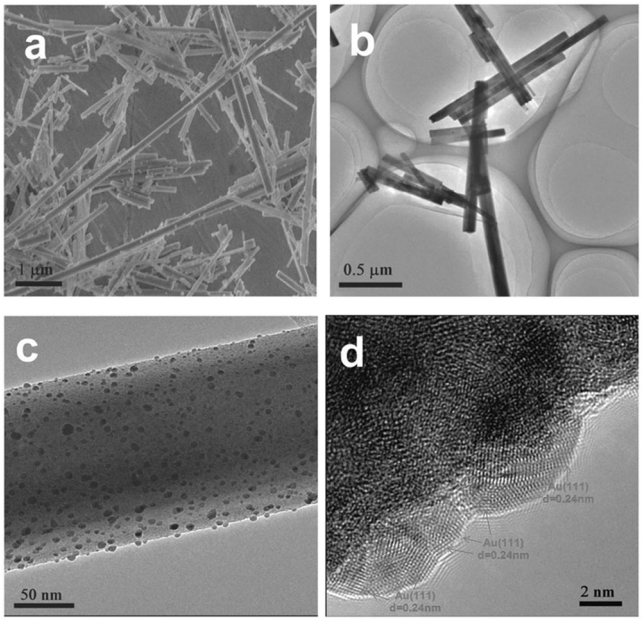

Figure 27. a) SEM image of Au/Ag-Mo nanorods, b) TEM image of Au/Ag-Mo nanorods, c) TEM image of an Au/Ag-Mo nanorod, and d) HRTEM image of an Au/Ag-Mo nanorod. From Ref. [349]. Copyright 2012 Royal Society of Chemistry.

polycarbonate membranes played the role of catalysts and nanoreactors, respectively, for CO oxidation. The catalytic efficiency of these nanotubes was found to be higher than simple supported AuNPs.[346] An et al. reported the oxidation of CO at room temperature by using single-walled helical gold nanotubes as catalysts. The high catalytic activity of the (5,3) nanotube for CO oxidation may be due to the presence of under-coordinated Au sites in the helical geometry. On the microscopic level, the high activity may be attributed to the electronic resonance between the d state of the Au atom at the reaction site and the antibonding $2\pi^*$ state of CO and O_2, and the concomitant partial charge transfer.[347]

Huang et al. reported the synthesis of dendritic AuNPs with the cationic surfactant decane-1,10-bis(methylpyrrolidinium bromide) ([mpy-C_{10}-mpy]Br_2). Widely exposed active surface provided active sites for selective adsorption to allow the efficient reduction of *p*-nitroaniline.[294] Very recently, Losic and co-workers highlighted the catalytic properties of gold nanotubes on porous anodic aluminum oxide. The system showed excellent catalytic activity for the reduction of 4-nitrophenol (4-AP) to 4-aminophenol (4-NP).[239]

Some hybrid bimetallic anisotropic AuNPs also exhibit high activities in various catalytic reactions.[348,349,350] For example, Au-ZnO nanopyramids (hexagonal pyramid-like structure) demonstrated a higher photocatalytic efficiency than pure ZnO nanocrystals in the degradation of rhodamine B.[348] Bimetallic Au-Pt nanowires prepared by the electrodeposition method were used as electrocatalysts for the real-time nonenzymatic impedancimetric detection of glucose.[229] Cui et al. prepared Au/Ag-Mo NRs by deposition of AuNPs onto Ag-Mo NRs (Figure 27). This hybrid catalyst was a very efficient heterogeneous catalyst for the tandem reaction of alcohols and nitrobenzenes to generate *N*-alkyl amines and imines.[349]

6.2. Sensors and Molecular Recognition by Anisotropic AuNPs

6.2.1. Detection of Toxic Ions

It is well known that heavy metal ions are widely distributed in biological systems and the environment, and play important roles in many biological and environmental processes. Thus, the analytical determination of toxic metals is an important issue in both environmental monitoring and clinical research.[330] AuNRs currently are the most widely used nonspherical AuNPs for detecting heavy metal ions. This is due to the extinction coefficient of AuNRs of around $10^{10}\,M^{-1}\,cm^{-1}$, which results in the variation of the longitudinal plasmon absorption (wavelength shift or intensity degradation) that is a highly sensitive probe for sensing applications.[351]

For example, AuNRs with various functionalized ligands on the surface led to a characteristic change in the longitudinal plasmon absorption on coordination to different metal ions. Cysteine (Cys) modified AuNRs have been used as colorimetric probes in the titration of Cu^{2+} ions. The strong coordination of Cu^{2+} ions with cysteine results in a stable Cys-Cu-Cys complex and induces the aggregation of the AuNRs along with a rapid color change from blue-green to dark gray.[330] Dithiothreitol (DTT) modified AuNRs were used as a SPR sensor of Hg^{2+} ions. In this case, the DTT was strongly adsorbed on the surface of the AuNRs through SH groups and induced the aggregation of AuNRs. The induced aggregation of AuNRs was inhibited in the presence of Hg^{2+} ions, with the aggregation level dependent on the concentration of Hg^{2+} ions. The degree of aggregation could be determined by the change in the intensity of the longitudinal plasmon absorption in the UV/Vis spectrum (Figure 28).[351] The detection of some

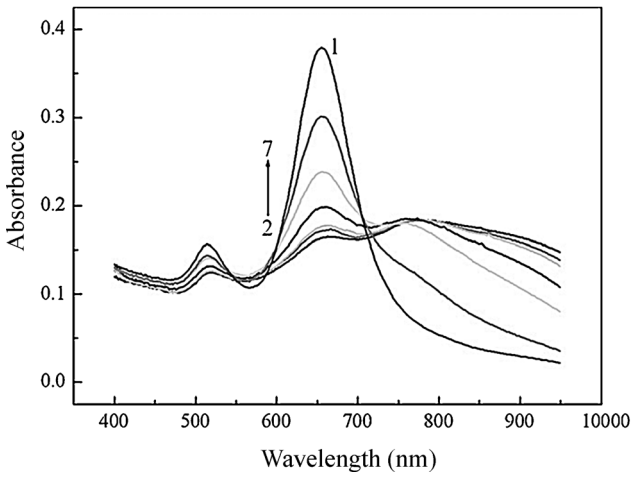

Figure 28. The absorption spectra of AuNRs (1), AuNRs-DTT (2), and the AuNRs-DTT-Hg^{2+} (3–7) system. Hg^{2+} concentrations: 1 (3), 5 (4), 10 (5), 20 (6), and 50×10^{-9} mol L^{-1} (7). From Ref. [351]. Copyright 2012 Elsevier.

other metals such as Cr^{VI} and Pb^{II} was recently reported by using a similar method.[352,353]

Besides the alteration of the longitudinal plasmon absorption, fluorescence is also a very effective method for ion detection. For example, Chen et al. reported a fluorescence method for the detection of Hg^{2+} ions in a homogeneous medium, with AuNRs used as a fluorescence quencher. Under optimum conditions, the method exhibits a dynamic response ranging from 10 pmol L^{-1} to 5 nmol L^{-1}, with a detection limit of 2.4 pmol L^{-1}.[354]

In conclusion, the strong affinity between anisotropic AuNPs and heavy metal cations alters the position of the plasmon band of AuNRs or the fluorescence property of targeted ions. This method allows heavy metal cations to be detected in aqueous solutions with ultrahigh sensitivity and excellent selectivity without sample pretreatment.

6.2.2. *Biosensors and Bioprobes*

The SPR and SERS properties of nonspherical AuNPs have been widely used for biosensing.[355] Up to now, Au nanorods (including bimetallic Au@Ag nanorods), nanopyramids, nanotubes, nanocages, nanowires, and nanostars have been reported as biosensors and bioprobes.[356–358] The typical routes to biosensors are illustrated in Equation (9). The nonspherical AuNPs functionalized with specific molecules (small molecules, DNA, antibodies, and biotin) recognized particular nano-objects (protein, DNA, drugs, and streptavidin), which caused the change in the plasmon absorption or the SERS intensity of the AuNPs.

$$\text{nonspherical AuNP} + \text{special functionalization} \xrightarrow[\text{SPR, SERS, etc.}]{\text{biosensing}} \text{special object} \quad (9)$$

AuNRs also gained the most interest of all the various-shaped nonspherical AuNPs for applications as biosensors and bioprobes. For example, AuNRs modified with double-stranded (DS-) DNA exhibited temperature-dependent assembly and disassembly. Modified AuNRs assembled at low temperature and disassembled at high temperature, with the reversible plasmon band observed during the process.[359] Bimetallic Au/Ag core/shell nanoparticles show a higher SERS activity than monometallic AuNRs, which results in 10 times lower detection limit.[356]

Besides AuNRs, other shaped AuNPs also have advantages for use as biosensors. For example, Yoo et al. presented a SERS sensor based on a patterned Au nanowire (NW) on a film for multiplex detection of pathogen DNA through an exonuclease III assisted recycling reaction of target DNA. Multiple probe DNAs are added to the target DNA solution, and among them, only the complementary probe DNA is selectively digested by exonuclease III, thereby resulting in a decrease in its concentration. The digestion process is repeated by recycling of the target DNAs (Figure 29). The decrease in the complementary probe DNA concentration is detected by SERS, and the detection limit is only 100 fM.[233]

The locally enhanced fields at the sharp ends and tips of Au nanostars were exploited to amplify SERS and allow molecular detection at the zeptomolar level. Dondapati et al. reported Au nanostars functionalized with biotinylated bovine serum albumin (BSA) as a label-free biosensor for streptavidin recognition, and the results showed that the concentrations of streptavidin as low as 100 pM were detected by a plasmon shift of 2.3 nm.[280]

AuNRs and AuNCs were found to act as SPR- and SERS-based probes for the detection of thrombin at concentrations of 10 aM and 1 fM, respectively.[357]

Castellana et al. recently reported a lipid-capped AuNR biosensor for the capture and label-free detection of a membrane-active drug (amphotericin B) by mass spectrometry (MS). In this case, the signal for amphotericin B appeared in the mass spectrum after incubation.[358] This MS method should become a very important technique for biosensors and bioprobes in the future.

Fluorescent enhancement of Au nanoshell/fluorophore conjugates is a powerfull sensing technique that is used in biomedical fluorescence imaging.[144]

6.2.3. *Molecular Recognition*

Based on the same principles of biosensors described above and in Equation (9), anisotropic AuNPs are also used for molecular recognition. The introduction of a thiolate ligand is a key feature for application to molecular recognition.[361,362] For example, functionalized AuNRs and Au nanoplates have been used for toxin recognition and glucose recognition, respectively.[259,363] Mandal and co-workers investigated anisotropic AuNPs for the recognition of organic solvents. Cyclam-stabilized AuNPs (mixture of spherical and triangular) were "dip-coated" onto the wall of a quartz cuvette to form a thin film. The Au thin film showed characteristic changes in the plasmon band in various organic solvents, thus indicating the system to be an excellent refractive index sensor.[364]

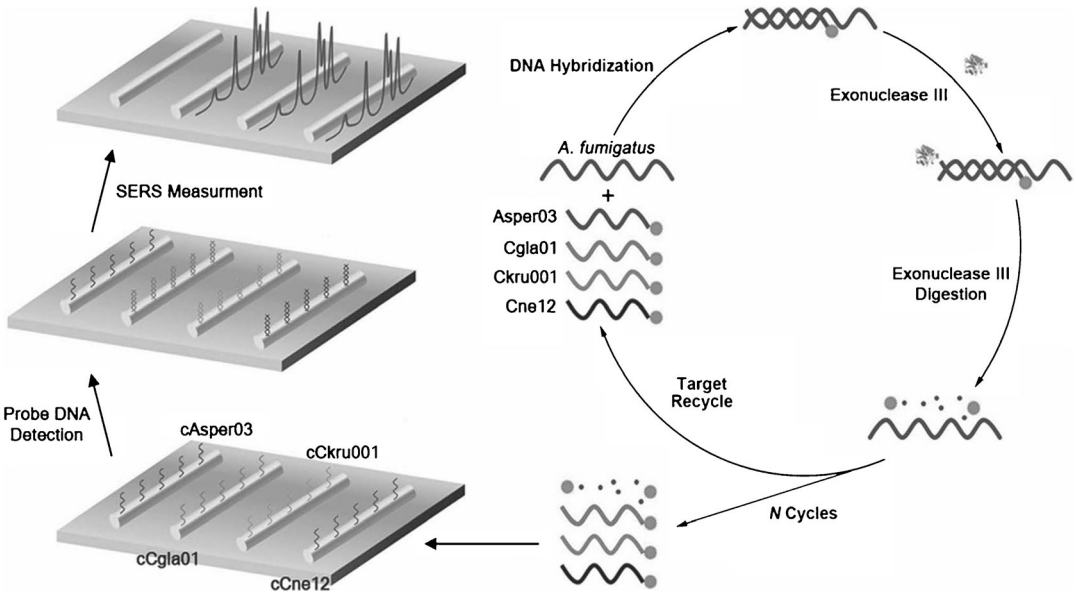

Figure 29. Principle of the identification of pathogenic fungal DNAs by a patterned nanowire-on-film SERS sensor coupled with an exonuclease III assisted target recycling reaction. From Ref. [233]. Copyright 2011 Wiley-VCH.

6.2.4. *Nanoelectrodes*

Nonspherical AuNPs have also been used in electrochemistry applications. Very recently, for example, Au nanotubes were investigated as nanoelectrodes. 3D Au nanoelectrodes were prepared by controlled chemical etching of long Au nanotubes. The cyclic voltammogram of 3D Au nanoelectrodes showed they had a much higher sensitivity (more than twice) than the embedded Au nanoelectrodes and could be used in many applications such as molecular detection.[365]

6.3. Biomedical Applications: Diagnostics and Therapy

Spherical Au NPs, AuNRs, HAuNSs, AuNCs, and Au nanostars are the most remarkable AuNPs for biomedical applications because: 1) they have long body circulation times; 2) they selective accumulate at sites of interest through the enhanced permeability and retention (EPR) effect or by surface modification with specific coatings; 3) they have a large absorption in the near-infrared window for photothermal therapy; 4) their simple functionalization (e.g. with PEG) and structural features allows their use as nanocarriers for drugs, DNA, or RNA.[320,366–385,386] The concept of "theranostic" AuNP nanocomposites has emerged for AuNPs that combine functionalities of both contrast agent and therapeutic actuators within a single nanoparticle. Au nanoshells were the first Au NPs to be used as efficient theranostic agents that combine imaging and phototherapy functions.[114]

6.3.1. *Contrast Agents in Diagnostics*

The development of new techniques to diagnose cancer early is contributing to an increase in cancer survival rates. For example, the resolution of conventional imaging techniques have been improved and new imaging modalities have been developed.[320] AuNPs are photoresistant and stable, thus offering long-time operation for optical imaging. Plasmonic nanoparticles, such as spherical Au nanoshells,[114] AuNPs,[387] AuNRs, Au nanocages, and Au nanostars are efficient contrast agents in optical imaging as a result of their unique interaction process with light particles (i.e., the excitation of the SPR by light). The most important in vivo diagnostic techniques include light scattering imaging, two-photon fluorescence imaging, and photothermal/photoacoustic imaging.[371]

For example, the Au nanoshells developed by Halas and co-workers that scatter light in the NIR physiological "water window" have been used as contrast agents for dark-field scattering,[22,114,304] photoacoustic imaging,[114,325] and optical coherence tomography (OCT).[114,306] With a core radius of 60 nm and a shell thickness of 10–12 nm, Au nanoshells can both absorb and scatter light at 800 nm, and thus serve as both imaging and therapeutic (theranostic) agents.[304] Lee and co-workers compared three different AuNP shapes (cubic cages, rods, and quasispherical), each possessing at least one dimension in the 40–50 nm range. Each NP was covalently functionalized with an antibody (anti-thrombin) and used as part of a sandwich assay in conjunction with an Au SPR chip modified with a DNA–aptamer probe specific to thrombin.

AuNPs strongly scatter light at their plasmon wavelengths. The scattering cross-sections are 10^5–10^6 times stronger than that of the emission from a fluorescent dye molecule. AuNRs that strongly scatter in the near-infrared region are capable of detecting cancer cells under excitation at spectral wavelengths where biological tissues absorb only slightly (Figure 30).[367] Moreover, nucleus targeting and imaging have also been achieved by conjugating the nanorods to the nuclear localization signal (NLS) peptides for potential in vivo imaging.[368] Oldenburg et al. demonstrated that AuNRs less than 50 nm in length are good contrast agents

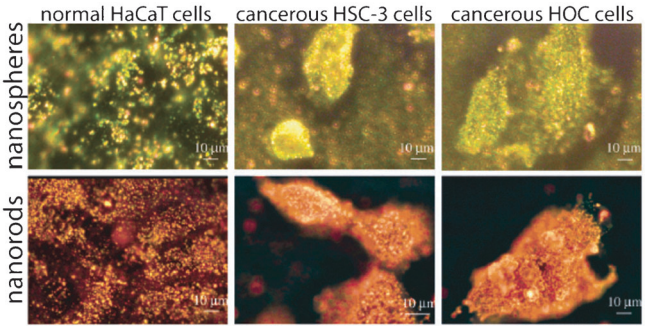

Figure 30. Cancer diagnostics using AuNR-enhanced light scattering. Optical dark-field microscopy of normal HaCaT cells and cancerous HSC and HOC cells incubated with anti-EGFR antibody conjugated gold nanospheres (top panels, left to right). Bottom, as above, but with gold nanorods. Anti-EGFR-conjugated gold nanoparticles specifically bound to cancer cells, thereby resulting in strong scattering under dark-field microscopy and thus enabling detection of malignant cells. From Ref. [367]. Copyright 2006 American Chemical Society

with little back scattering, thus rendering them appropriate for the highly scattering tissue phantom.[369] The sensitivity is comparable to the absorption-based in vivo transmission imaging.[370] Currently, dark-field imaging based on the light-scattering properties of nonspherical AuNPs (shells, spheres, rods, and cages) is widely used for cancer imaging through functionalized nanoparticle–receptor binding to cell-surface biomarkers.[371,372]

Nonspherical AuNPs, especially AuNRs, exhibit enhanced two-photon luminescence (TPL), thereby making them detectable at single-particle levels under femtosecond NIR laser excitation. In comparison to confocal fluorescence microscopy, TPL has the advantages of higher spatial resolution and a reduced background signal. For example, the nanorod-enabled TPL intensity was three times stronger than that of two-photon autofluorescence,[374] and TPL imaging of AuNRs is 100 times stronger than the emission of a single fluorescein isothiocyanate molecule.[375] However, deleterious photothermal effects are induced by plasmon excitation upon continuous scanning with high-intensity pulsed laser light. Despite these problems, TPL has been used recently for cancer imaging in vivo. For example, He et al. reported the detection of circulating tumor cells in vivo by using the TPL technique.[376] In this experiment, CTC-mimetic leukemia cells were injected into the blood stream of live mice, followed by injection of folate-conjugated AuNRs to preferentially label the circulating cancer cells in vivo. TPL imaging with an intravital flow cytometer detected single cancer cells in the vasculature of the mouse ear.

Photothermal (PT) and photoacoustic (PA) imaging are based on the laser-induced heating of materials, with the former relying on the direct detection of heat and the latter on the detection of acoustic waves generated by the thermal expansion of air surrounding the materials. Compared to fluorescence-based approaches, PT imaging has the advantages of a larger detection volume and a high stability of the photothermal signal.[371] The PT imaging technique has usually been employed in photothermal therapy, and thus this technique will also be discussed in the following section. Furthermore, PA imaging is used much more often than PT imaging in biomedicine. This is because the PA technique combines the high contrast of optical imaging with the deep tissue penetration of ultrasound imaging. Numerous applications have been shown in recent years. One of these key areas is in tumor imaging. For example, Agarwal et al. used PT imaging to detect prostate cancer by using AuNRs conjugated with anti-HER2.[377] This technique was also used by Li et al. to perform multiplexed imaging of different cancer cell receptors by using AuNRs of varying aspect ratios and with various target molecules.[378] Another key area is in vivo imaging. For example, Xia and co-workers used PA to image the cerebral cortex of a rat before and after three successive administrations of PEGylated AuNCs. An enhancement of the brain vasculature by up to 81% was observed (Figure 31 A,B). A difference image (Figure 31 C) confirms the

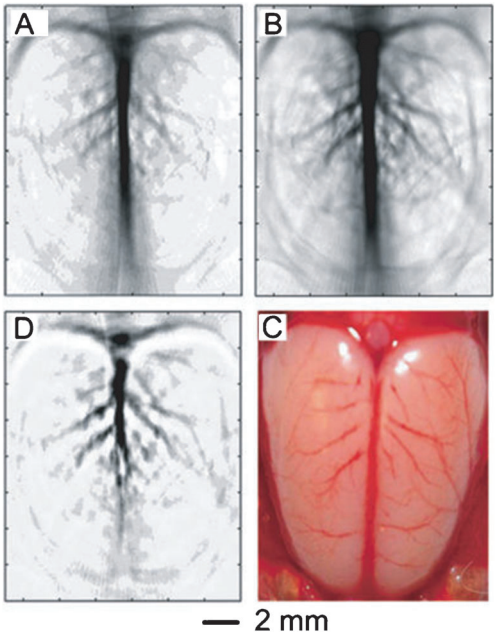

Figure 31. Photoacoustic tomogram (PAT) of a rat's cerebral cortex A) before and B) 2 h after the final injection of PEGylated AuNCs. C) A differential image. D) An open-skull photograph of the rat's cerebral cortex, revealing features of the vasculatur. From Ref. [379]. Copyright 2007 American Chemical Society.

enhancement achieved by administration of the Au nanocage. A photograph of the open skull (Figure 31 D) reveals that the anatomical features of the vasculature match well with those revealed by the PA technique. Moreover, when compared with Au nanoshells, the AuNCs appear to be more effective contrast enhancement agents for PA, which is likely related to their larger absorption cross-section and more compact size.[379]

6.3.2. ***Photothermal Cancer Therapy***

Thermal therapy involves the destruction of cancer tissues by heating. Various energy sources have been applied, including radio frequencies, high-intensity focused ultra-

sound, microwaves, and lasers. The heat energy can be delivered by external or internal means, through interstitial, intraluminal, or intracavitary approaches. However, because of absorption by normal tissues, the amount of energy delivered to the treatment volume is limited, which reduces the potency of the thermal effect. To improve the efficacy and tumor selectivity, light-absorbing materials (known as photothermal contrast agents) are introduced into tumor cells to mediate the photothermal effect. A temperature increase of 30–35 °C provokes cell death. Various Au nanostructures, including nanoshells,[388,389] nanorods, nanocages, and nanostars that absorb NIR light (wavelength 700–850 nm), have been shown to be effective in photothermal therapy.[366]

The first use of anisotropic AuNPs in targeted photothermal therapy was conducted by the Halas research group by using silica@Au nanoshells functionalized with antibodies such as anti-HER2. The antibodies direct the AuNPs toward the cancer cells because they conjugate with surface cell markers that are overexpressed by cancer cells. These antibodies were linked to orthopyridyl disulfide-PEG-*n*-hydrosuccinimide (OPSS-PEG-NHS) that was bound to the Au surface through strong Au–S bonds. The advantage of the PEG linker is that it provides an enhanced permeability and retention (EPR) effect involving the new blood vessels formed at the tumor site. This photothermal therapy was first demonstrated in mice with subcutaneous tumors of 1 cm size. Analysis showed that phothermal treatment resulted in tissue damage over a similar sized area as that exposed to laser irradiation. Magnetic resonance thermal imaging (MRTI) revealed an aveage temperature increase of 37 °C after 5 min irradiation, which is sufficient to induce irreversible tissue damage. Nanoshell-free samples showed an average increase of 9 °C, which was considered to be safe for cell viability.[113] Further experiments determined animal survival times of over 90 days.[22] Theranostic experiments were conducted with the same antibody and Au nanoshells with a core radius of 60 nm and a shell 10 nm thick (plasmon absorption at 800 nm). The cells were imaged with a dark-field microcope, and irradiated with a NIR laser at 820 nm (0.008 $W cm^{-2}$, 7 mn). Only the cancer cells show a distinct enhancement in the dark-field scattering image and a dark circular area of cell death corresponding to the beam spot upon laser irradiation.[304] Au nanoshells have also been used to target tumor hypoxia, regions with reduced blood flow that are resitant to NP accumulation, by combining mild hyperthermia and radiation therapy.[22] Au nanoshells have also been examined in vivo for their ability to enhance optical coherence tomography (OCT) and to induce photothermal cell death.[306] Further use of theranostics by the Halas research group successfully involved multimodal imaging and therapy, that is, with two diagnostic capabilities, MRI and NIR fluorescence, in addition to photothermal therapy. The nanoensembles were prepared by encapsulating Au nanoshells in a silica epilayer doped with 10 nm Fe_3O_4 nanoparticles and indocyanine green (ICG), functionalized with streptavidin, and conjugated with thiolated PEG. These ensembles showed very good results in vitro by targeting breast cancer cells and also in vivo in breast cancer xenografts.[390]

El-Sayed and co-workers pioneered strategies for the application of AuNRs in photothermal therapy. Conjugation of AuNRs to anti-EGFR antibodies enabled selective photothermal therapy as a result of preferential AuNR binding to human oral cancer cells.[367] In more-recent studies, they linked macrolide to PEG-functionalized AuNRs, which preferentially delivered AuNRs into inflamed tumor tissues via tumor-associated macrophage cells (TAMs).[221]

AuNCs with large absorption cross-sections also show a large photothermal effect. The absorbed photons are converted into phonons (lattice vibrations), which in turn produce a localized temperature increase. Xia and co-workers demonstrated the photothermal destruction of breast cancer cells in vitro through the use of immuno-Au nanocages. AuNCs with an edge length of 45 nm were selected because of their predicted large absorption cross-section. SK-BR-3 cells were treated with these immuno-AuNCs, then irradiated with a laser with a wavelength of 810 nm and a power density of 1.5 $W cm^{-2}$ for 5 min. The treated cells were stained with calcein-AM and ethidium homodimer-1 so that live cells fluoresced green and dead cells fluoresced red. This analysis revealed a well-defined zone of cellular death consistent with the size of the laser spot.[380]

Au nanostars were also investigated for phototherapy applications. They were successfully conjugated with anti-HER2 nanobodies and demonstrated specific interaction with HER2t and SKOV3 cells. The FACS data and the dark-field images clearly revealed that the Au nanostars conjugated with anti-HER2 specifically bound to the cells, while almost no binding was observed for the controls. Furthermore, the conjugate resulted in specific photothermal destruction of tumor cells in vitro. Exposing the cells to either only NIR light or nanoparticles did not affect cell viability. Nonspecific NPs conjugated with anti-PSA nanobodies did not result in any cell death upon exposure to laser irradiation, thus demonstrating the high specificity of these anti-HER2-conjugated Au nanostars.[283]

Hybrid nanomaterials composed of two unique components not only retain the beneficial features of both, but also show synergistic properties. Hybrid AuNCs were also investigated in photothermal therapy. Single-wall carbon nanotubes (SWCNTs) were functionalized and attached to AuNCs through a thiol group (Figure 32). The as-prepared AuNC-decorated SWCNTs were then modified with RNA aptamer A9, which is specific to human prostate cancer cells. The photothermal response for the hybrid nanomaterial is much higher than for single nanomaterials.[243]

In conclusion, the in vitro and in vivo studies described have proved remarkably successful, yet tumors that are treated are those that are easily accessible to NIR light and only a few centimeters under the skin surface. It has been suggested that techniques to deliver NIR light into deeper tissues should exploit fiber optic probes, and such a challenge remains crucial.

6.3.3. *Drug and Gene Delivery*

The search for nonviral drug or gene vectors is indispensible because of the risk of cytotoxicity of and immunologic

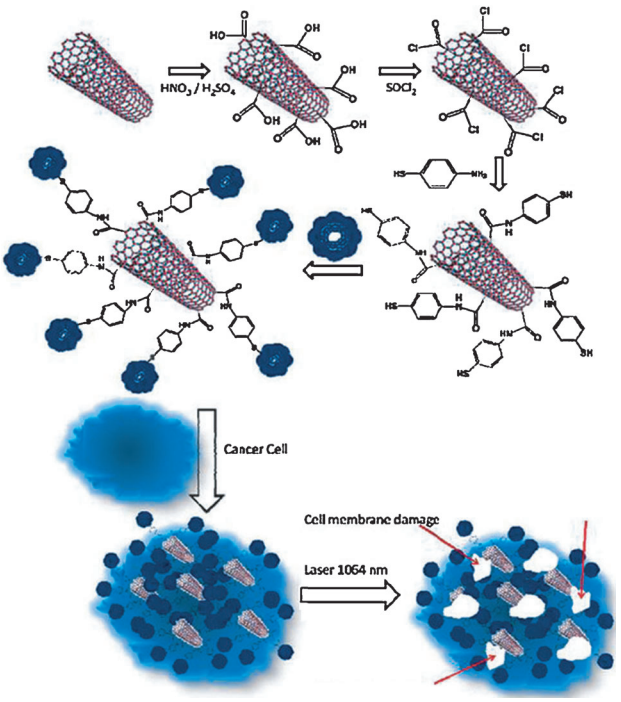

Figure 32. Synthesis protocol for the formation of hybrid nanomaterials and the principle for the imaging and destruction of cancers. From Ref. [366]. Copyright 2012 Royal Society of Chemistry.

responses to conventional virus-mediated drug or gene delivery.[382–384] Nonspherical AuNPs have recently been used as nanocarriers for efficient drug or gene delivery systems.[385,390] Lee et al. reported the use of cationic phospholipid functionalized AuNRs as plasmonic carriers that simultaneously exhibit carrier capabilities, demonstrate improved colloidal stability, maintain plasmonic properties, and show no cytotoxicity under physiological conditions. The in vivo studies demonstrated that these functionalized ANRs are stable under physiological conditions, thus retaining their unique plasmonic properties. Furthermore, the positively charged surface of AuNRs adsorbs cargos such as DNA oligonucleotides, RNA oligonucleotides, and siRNA.[387]

Halas and co-workers described an SiO_2@Au nanoshell that released single-stranded DNA from its surface when illuminated with plasmon-resonant light. This system allowed examination of DNA dehybridization induced by excitation of localized surface plasmons on the NPs (Figure 33).[391] In another study, the light-triggered release of the fluorescent molecule DAPI (4′,6-diamidino-2-phenylindole) inside living cells was investigated from a host–guest complex with DNA bound to SiO_2@Au nanoshells.[392] Diagnostic and therapeutic drug delivery based on SiO_2@Au nanoshells was also investigated recently for the treatment of ovarian cancer[393] and the diagnosis of breast cancer.[394]

With their hollow structures, AuNCs serve as "pockets" that are appropriate for drug release. For example, PEG-coated AuNCs have been used as nanocarriers for doxorubicin and triggered drug release under irradiation with NIR light. This drug delivery system was considered to be a dual-modality cancer therapy that combined both photothermal

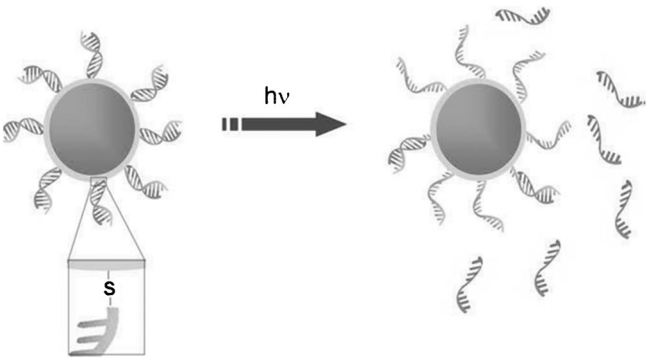

Figure 33. Principle of light-controlled release of ssDNA from Au nanoshells. From Ref. [391]. Copyright 2009 Elsevier.

therapy and chemotherapy. An in vivo study of this delivery system indicated greater antitumor activity than either doxorubicin or AuNCs alone.[366] Moreover, the surface of AuNCs was functionalized with thermally responsive polymers to control the release through NIR laser irradiation or high-intensity focused ultrasound. Another reported controlled-release system used a phase-change material (PCM) loaded in the hollow interiors of AuNCs to achieve the controlled release. An increase in temperature uncaps the pores and releases the guest molecules from the AuNCs. The release is controlled by varying the power or duration of the ultrasound treatment.[395,396] Very recently, Wan and co-workers reported a bioresponsive controlled-release AuNC system. The AuNC was selected as a support and an ATP molecule was used as the target (Figure 34). AuNCs were

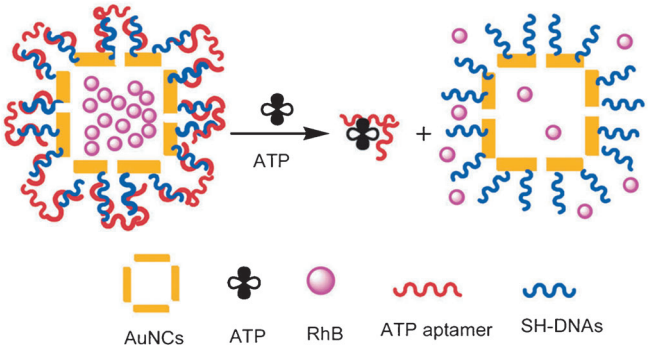

Figure 34. Principle of the aptamer–target interaction for the bioresponsive controlled-release of AuNCs. From Ref. [397]. Copyright 2012 Royal Society of Chemistry.

functionalized with two kinds of thiol-modified single-stranded oligonucleotides (SH-DNAs) by means of Au-thiolate bonding on the surface of the AuNCs. The bases of the two immobilized SH-DNAs were partly complementary to that of the two ends of the ATP aptamer. Mixing the surface-modified AuNCs with the ATP aptamers resulted in hybridization of the ATP aptamers with the two immobilized SH-DNAs. This effected assembly of the ATP aptamers on the surface of the AuNCs, thereby capping the pores. The release of the guest molecule from the aptamer-AuNCs could

be triggered by the addition of ATP molecules, thereby opening the pores and releasing the cargo molecules.[397]

7. Toxicology

A number of in vitro studies have shown that AuNP cores are, in general, nontoxic for cells. These findings are in contrast with other nanoparticles such as carbon nanotubes, asbestos, and metal oxides, which have been shown to cause drastic damage to cells. On the other hand, although it has been extensively demonstrated that anisotropic AuNPs have an enormous potential in theranostics, the in vivo toxicity of these AuNPs nedd to be established before drug administration can be allowed. Therefore, in vitro and in vivo toxicology studies have been undertaken to examine the risk of damage on cells, tissues, and organs of animals. Most of these studies have been conducted on AuNPs that were considered to be spherical[398] and only a few studies have concerned AuNRs that are the prototype of anisotropic AuNPs with biomedical applications. The toxicity of AuNPs has been the subject of excellent reviews.[371,399] Thus, we restrct the discussion to a few general aspects.

The first problem is the distinction between the toxicity of the AuNP core and that of the coating stabilizer, because it is not possible to study the AuNP core without a stabilizer. In vitro studies have shown that the toxicity of AuNRs is due to the CTAB ligands, not the core. Indeed, Murphy, Wyatt, and co-workers have shown that AuNPs that were coated with polyacrylic acid or poly(allylamine) hydrochloride resulted in almost no death of HT29 cells.[400] It is generally considered that AuNP cores larger than 5 nm behave as bulk gold in terms of reactivity, whereas AuNPs smaller than 2 nm are specifically reactive. AuNPs larger than 5 nm are indeed inactive in catalytic reactions, such as CO oxidation by O_2, while oxide-supported AuNPs smaller than 2 nm are highly active.[12–16] This rule of thumb should be considered with caution, especially concerning anisotropic AuNPs, for which the smaller dimension is often much smaller than the largest dimension (AuNRs, AuNTs, HAuNSs, and AuNCs). The "large" AuNPs, that is, with sizes between 5 nm and 100 nm, show a plasmon band that reflects a quantum behavior that probably has an effect on their reactivity. Such particles are more reactive than bulk gold because of the large surface and, more specifically, because of the presence of edges, corners, and numerous structural defects (consider Au dendrites, for example). On the other hand, small AuNPs that are supposed to be highly reactive when they are naked can be well protected, for example, by biocompatible PEGylated thiolate ligands.

The second important problem is that of the oxidation state of gold. We know that AgNPs are very toxic, because of their relative ease of oxidation to Ag^+ salts, which have been generally recognized as intrinsically toxic.[401] Of course, Au^0 is much more difficult to oxidize than Ag^0, but the oxidizability of Au^0 depends on the AuNP size, shape, and surrounding ligands. For example, with the most common citrate and thiolate ligands, the Au–O and Au–S bonds on the AuNP core surface are polarized ($Au^{\delta+}$–$O^{\delta-}$ and $Au^{\delta+}$–$S^{\delta-}$, respectively). Moreover, cationic Au^I and Au^{III} atoms have been generally proposed to be responsible for the activity in the oxidation of substrates in aerobic AuNP-catalyzed oxidation reactions.[12–16,402] Redox reactions are intrinsic to all biological organisms and are facilitated by cytochromes; cytochrome P450, in particular, is a strong oxidation catalyst. Therefore, the potential oxidation of Au atoms to toxic Au^I or Au^{III} ions at the surface of AuNP core that could subsequently be leached should not be underestimated. Again, these potential problems and risks are more acute with anisotropic AuNPs than with isotropic ones because of their highly exposed AuNP surface areas and defects. Although from in vitro studies it appears so far that the AuNP cores of isotropic AuNPs larger than 5 nm are biologically inert,[399,371,402] more studies are needed with anisotropic AuNPs and in vivo studies.

The third problem is the dichotomy between the in vitro and in vivo studies in terms of results and number of studies. A large number of in vitro studies have been carried out using TEM, microscopy techniques, and ICP-MS, and they are interesting from a fundamental point of view and bring mechanistic information (for example, how AuNPs penerate cells as a function of size, coating type, and nature of the cell, as well as how some ionic capping agents such as CTAB or cationic ligands are toxic).[399,371] However, there are very few in vivo studies and there is no correlation with the in vitro results. In vitro studies by Chan and co-workers indicated that the optimum size for cell penetration is 40–50 nm because this is the maximized antibody–receptor interaction for receptor-mediated endocytosis.[403] In vitro studies involve a large variety of parameters that, as underligned by Murphy and co-workers,[399,371] do not provide a precise overall picture of toxicity. Xia and co-workers have distinguished AuNPs that entered cells from others by using a I_2/KI mixture that selectively solvates surface-cell AuNPs that do not induce toxicity.[404] The aspect of AuNP aggregation has also been addressed.[405]

Some in vivo studies have addressed the pharmacokinetics of AuNPs. Toxicity studies of citrate-capped AuNPs in mice by Chen et al. showed that small (3–5 nm) and large AuNPs (30 and 100 nm) were not toxic, whereas medium-sized AuNPs (8, 12, 17, and 37 nm) provoked severe sickness, loss of weight, change in fur color, and shorter life spans. The systemic toxicity was due to injury of the liver, spleen, and lungs.[406] On the other hand, 13 nm, citrate-caped AuNPs were shown by Lasagna-Reeves et al. not to cause any acute side effects.[407] Small 10 nm AuNPs were found by ICP-MS analysis in the liver, spleen, testis, lung, blood, and brain 24 h after intravenous injection, whereas larger AuNPs (up to 250 nm) were found only in the spleen and kidneys.[408] For clearance through the kidneys, the NPs must pass the cross-filtration glomeruli barrier (6–8 nm hydrodynamic diameter) and must, therefore, be smaller than 5.5 nm. Indeed, smaller AuNPs were shown to be excreted in the urine, whereas 18 nm AuNPs accumulated in the liver and spleen.[409,410] Agglomeration of small (2 nm) AuNPs to larger aggregates, however, can also prevent renal clearance.[411] As an example of the coating influence, it was shown that glutathione-coated small (2 nm) AuNPs underwent renal clearance more effi-

ciently (because of low binding to serum proteins) than citrate-coated AuNPs, but larger gluthathione AuNPs (13 nm) did not pass the glomeruli barrier.[411] Studies have also been conducted on the environmental and ecological impact of CTAB-capped AuNRs in model estuarine systems (containing sediments, microbiol films, plants, clams, snails, and fish), and it was found that biofilms were the main route of entry into the food chain.[412]

8. Conclusion and Outlook

A gold rush at the end of the 20th century resulted from the recognition of the excellent catalytic properties of very small AuNPs (<5 nm) and of the potential provided by the quantum dot and optical properties of larger AuNPs (>3 nm). Emphasis was on the size rather than on the shape. Although anisotropic AuNPs have attracted the attention of scientists since the very beginning of the 20th century, increased focus on their investigation only occurred at the beginning of the 21st century with the discovery of myriads of shapes including platonic, 1D, 2D, 3D, and hollow structures. This multiplicity of crystallization modes has questioned the influence of many parameters on the growth mechanisms. Whereas the key role of some stabilizers such as CTAB, Ag^+, and halide ions has been rationalized, the large-scale reproducible production of AuNPs of specific shapes remains a crucial challenge.

The advantage of and great interest in anisotropic AuNPs compared to classic spherical AuNPs are not only their better definition as precise nanocrystals, but also their very important optical and catalytic properties.[344] Whereas the plasmon band is unique in the visible region for homogeneous spherical AuNPs, nonspherical AuNPs show a second plasmon absorption that can be shifted to the near-infrared region between 800 nm and 1300 nm. In this region the absorption by tissues is low, and thus allows phototherapy applications. Important factors for the wide application of anisotropic AuNPs are the scale of production, reproducibility, and toxicity. So far, only the toxic CTAB stabilizer can lead to the generation of such 1D structures. The discovery of alternative, nontoxic stabilizers is another challenging issue. It is remarkable that the preparation of Au nanoshells, AuNCs, and some other anisotropic AuNPs that absorb light in the NIR "water window" and are the subject of clinical anticancer "theranostic" applications do not suffer from the toxicity problem found with CTAB.

The catalytic performance of anisotropic AuNPs is related to the presence of edges, corners, steps, and other defects, which are considerably more numerous than in spherical AuNPs.[413,414] It can be predicted that this field will expand given the well-established role of AuNPs in catalysis. Precise studies at the interface between AuNPs and solid oxide supports should result in a better definition of the oxidation states of surface Au atoms, which are key intermediates in oxidation reactions. This issue is not only important for catalysis, but also for understanding the risk of the oxidation of surface Au atoms in vivo and possible subsequent toxicity. It is, thus, also essential for the future applications of nonspherical and hollow AuNPs as well as SiO_2@Au nanoshells in nanomedicine.[415]

Another aspect is the new bottom-up emergence of Au nanowires that reach longitudinal dimensions of several tens of micrometers for applications as plasmon waveguides and networks for optical devices, such as interferometric logic gates, which are promising for future information processing.[228,416]

Financial support from the University Bordeaux, China Scholarship Council (CSC, PhD grants to L.N. and P.Z.), Science and Technology on Surface Physics and Chemistry Laboratory (Mianyang), CNRS, IUF (D.A.), Nanosolution European consortium, and L'Oréal are gratefully acknowledged.

Received: January 17, 2013
Revised: March 26, 2013
Published online: January 13, 2014

[1] I. Freestone, N. Meeks, M. Sax, C. Higgit, *Gold Bull.* **1976**, *9*, 134 – 139.
[2] M. Faraday, *Philos. Trans. R. Soc. London* **1857**, *147*, 145 – 181.
[3] J. Turkevich, P. C. Stevenon, J. Hillier, *Discuss. Faraday Soc.* **1951**, *11*, 55 – 75.
[4] M. Brust, M. Walker, D. Bethell, D. J. Schiffrin, R. Whyman, *J. Chem. Soc. Chem. Commun.* **1994**, 801 – 802.
[5] G. Schmid, *Chem. Rev.* **1992**, *92*, 1709 – 1727.
[6] M. Haruta, *Nature* **2005**, *437*, 1098 – 1099.
[7] M. Giersig, P. Mulvaney, *Langmuir* **1993**, *9*, 3408 – 3413.
[8] A. P. Alivisatos, *Science* **1996**, *271*, 933 – 937.
[9] G. Mie, *Ann. Phys.* **1908**, *25*, 377 – 445.
[10] U. Kreibig, M. Vollmer, *Optical Properties of Metal Clusters*, Springer, Berlin, **1995**.
[11] P. Mulvaney, *Langmuir* **1996**, *12*, 788 – 800.
[12] B. M. Quinn, P. Liljeroth, V. Ruiz, T. Llaksonen, K. Kontturi, *J. Am. Chem. Soc.* **2003**, *125*, 6644 – 6645.
[13] A. Corma, P. Serna, *Science* **2006**, *313*, 332 – 334.
[14] N. Dimitratos, J. A. Lopez-Sanchez, G. J. Hutchings, *Chem. Sci.* **2012**, *3*, 20 – 44.
[15] *Gold Nanoparticles for Physics, Chemistry, Biology* (Eds.: C. Louis, O. Pluchery), Imperial College, London, **2012**.
[16] M. C. Daniel, D. Astruc, *Chem. Rev.* **2004**, *104*, 293 – 346.
[17] R. Szymondy, *The Chemistry of Colloids*, Wiley, New York, **1917**.
[18] R. Gans, *Ann. Phys.* **1912**, *37*, 881 – 900.
[19] T. Svedberg, *The Formation of Colloids*, Von Nostrand Reinhold, New York, **1921**.
[20] A. Einstein, *Ann. Phys.* **1905**, *17*, 549 – 560.
[21] G. B. Jeffery, *Proc. R. Soc. London Ser. A* **1922**, *102*, 161 – 179.
[22] S. Lal, S. E. Clare, N. J. Halas, *Acc. Chem. Res.* **2008**, *41*, 1842 – 1851.
[23] C. J. Murphy, A. M. Gole, J. W. Stone, P. N. Sisco, A. M. Alkilany, E. C. Goldsmith, S. C. Baxter, *Acc. Chem. Res.* **2008**, *41*, 1721 – 1730.
[24] C. Burda, X. Chen, M. A. El-Sayed, *Chem. Rev.* **2005**, *105*, 1025 – 1102.
[25] Y. Yin, A. P. Alivisatos, *Nature* **2005**, *437*, 664 – 670.
[26] K. L. Kelly, E. Coronado, L. L. Zhao, G. C. Shatz, *J. Phys. Chem. B* **2003**, *107*, 668 – 677.
[27] C. Y. Yang, K. Heinemann, M. J. Yacaman, H. Poppa, *Thin Solid Films* **1979**, *58*, 163 – 168.
[28] A. Renou, M. Gillet, *Surf. Sci.* **1981**, *106*, 27 – 34.
[29] J. Wiesner, A. Wokaun, *Chem. Phys. Lett.* **1989**, *157*, 569 – 582.

[30] N. R. Jana, L. Gearheart, C. J. Murphy, *Adv. Mater.* **2001**, *13*, 1389 – 1393.
[31] B. Nikoobakht, M. A. El-Sayed, *Chem. Mater.* **2003**, *15*, 1957 – 1965.
[32] C. J. Murphy, *Science* **2002**, *298*, 2139 – 2141.
[33] K. Esumi, K. Esumi, K. Matsuhisa, K. Torigoe, *Langmuir* **1995**, *11*, 3285 – 3287.
[34] E. Leontidis, K. Kleitou, T. Kiprianidou-Leodidou, V. Bekiari, P. Lianos, *Langmuir* **2002**, *18*, 3659 – 3668.
[35] Y. Yu, S. S. Chang, C. L. Lee, C. R. C. Wang, *J. Phys. Chem. B* **1997**, *101*, 6661 – 6664.
[36] S. S. Chang, C. W. Shih, C. D. Chen, W. C. Lai, C. R. C. Wang, *Langmuir* **1999**, *15*, 701 – 709.
[37] B. Nikoobakht, M. A. El Sayed, *Langmuir* **2001**, *17*, 6368 – 6374.
[38] S. Chen, D. L. Caroll, *Nano Lett.* **2002**, *2*, 1003 – 1007.
[39] S. Chen, Z. Fan, D. L. Caroll, *J. Phys. Chem.* **2002**, *106*, 10777 – 10781.
[40] S. Chen, Z. L. Wang, J. Ballato, S. H. Foulger, D. L. Caroll, *J. Am. Chem. Soc.* **2003**, *125*, 16186 – 16187.
[41] N. R. Jana, G. L. Gearheart, C. J. Murphy, *J. Phys. Chem. B* **2001**, *105*, 4065 – 4067.
[42] V. Sharma, K. Park, M. Srinivararao, *Mater. Sci. Eng. R* **2009**, *65*, 1 – 38.
[43] B. D. Busbee, S. O. Obare, C. J. Murphy, *Adv. Mater.* **2003**, *15*, 414 – 416.
[44] A. Gole, C. J. Murphy, *Chem. Mater.* **2004**, *16*, 3633 – 3640.
[45] C. J. Murphy, T. K. Sau, A. M. Gole, C. J. Orendorff, J. Gao, L. Gou, S. E. Hunjadi, T. Li, *J. Phys. Chem. B* **2005**, *109*, 13857 – 13870.
[46] H. Y. Wu, H. C. Chu, T. J. Kuo, C. L. Kuo, M. H. Huang, *Chem. Mater.* **2005**, *17*, 6447 – 6451.
[47] B. Nikoobakht, M. A. El-Sayed, *Chem. Mater.* **2003**, *15*, 1957 – 1962.
[48] M. Iqbal, Y. Chung, G. Tae, *J. Mater. Chem.* **2007**, *17*, 335 – 338.
[49] H. M. Chen, H. C. Peng, R. S. Liu, K. Asakura, C. L. Lee, J. F. Lee, S. F. Hu, *J. Phys. Chem. B* **2005**, *109*, 19553 – 19555.
[50] M. Liu, P. Guyot-Sionnest, *J. Phys. Chem. B* **2005**, *109*, 22192 – 22200.
[51] X. C. Jiang, A. Brioude, M. P. Pileni, *Colloids Surf. A* **2006**, *277*, 201 – 206.
[52] X. C. Jiang, M. P. Pileni, *Colloids Surf. A* **2007**, *295*, 228 – 232.
[53] E. Carbó-Argibay, B. Rodriguez-Gonzales, J. Pacifico, I. Pastoriza-Santos, J. Perez-Juste, L. M. Liz-Marzan, *Angew. Chem.* **2007**, *119*, 9141 – 9145; *Angew. Chem. Int. Ed.* **2007**, *46*, 8983 – 8987.
[54] D. K. Smith, B. A. Korgel, *Langmuir* **2008**, *24*, 644 – 649.
[55] J. E. Millstone, W. Ei, M. R. Jones, H. Yoo, C. A. Mirkin, *Nano Lett.* **2008**, *8*, 2526 – 2529.
[56] C. J. Johnson, E. Dujardin, S. A. Davis, C. J. Murphy, S. Mann, *J. Mater. Chem.* **2002**, *12*, 1765 – 1770.
[57] J. Pérez-Juste, L. M. Liz-Marzan, S. Carnie, D. Y. C. Chan, P. Mulvaney, *Adv. Funct. Mater.* **2004**, *14*, 571 – 579.
[58] M. Grzelczak, J. Pérez-Juste, P. Mulvaney, L. M. Liz-Marzan, *Chem. Soc. Rev.* **2008**, *37*, 1783 – 1791.
[59] X. Huang, S. Neretina, M. A. El-Sayed, *Adv. Mater.* **2009**, *21*, 4880 – 4910.
[60] C. J. Orendorff, C. J. Murphy, *J. Phys. Chem. B* **2006**, *110*, 3990 – 3994.
[61] S. Si, C. Leduc, M. H. Delville, B. Lounis, *ChemPhysChem* **2012**, *13*, 193 – 202.
[62] F. Kim, H. Song, P. Yang, *J. Am. Chem. Soc.* **2002**, *124*, 14316 – 14317.
[63] O. R. Miranda, T. S. Ahmadi, *J. Phys. Chem. B* **2005**, *109*, 15724 – 15734.
[64] O. R. Miranda, N. R. Dollahon, T. S. Ahmadi, *Cryst. Growth Des.* **2006**, *6*, 2747 – 2753.
[65] N. R. Jana, *Small* **2005**, *1*, 875 – 882.
[66] P. Zijlstra, C. Bullen, J. W. M. Chon, M. Gu, *J. Phys. Chem. B* **2006**, *110*, 19315 – 19318.
[67] S. Eustis, H. Y. Hsu, M. A. El-Sayed, *J. Phys. Chem. B* **2005**, *109*, 4811 – 4815.
[68] C. Y. Wang, C. Y. Liu, X. Zhang, J. Chen, *J. Colloid Interface Sci.* **1997**, *191*, 464 – 470.
[69] C. Y. Wang, C. Y. Liu, X. Zheng, J. Chen, T. Shen, *Colloids Surf. A* **1998**, *131*, 271 – 280.
[70] X. Huang, X. Qi, Y. Huang, S. Li, C. Xue, C. L. Gan, F. Boey, H. Zhang, *ACS Nano* **2010**, *4*, 6196 – 6202.
[71] X. Huang, X. Z. Zhou, S. X. Wu, Y. Y. Wei, X. Y. Qi, J. Zhang, F. Boey, H. Zhang, *Small* **2010**, *6*, 513 – 516.
[72] K. Nishioka, Y. Niidome, S. Yamada, *Langmuir* **2007**, *23*, 10353 – 10356.
[73] Y. Niidome, K. Nishioka, H. Kawasaki, S. Yamada, *Chem. Commun.* **2003**, 2376 – 2377.
[74] See Ref. [64].
[75] L. K. McGilvray, R. M. Decan, D. Wang, C. J. Scaiano, *J. Am. Chem. Soc.* **2006**, *128*, 15980 – 15981.
[76] L. M. Marin, L. K. McGilvray, C. J. Scaiano, *J. Am. Chem. Soc.* **2008**, *130*, 16572 – 16584.
[77] M. Ahmed, R. Narain, *Langmuir* **2010**, *26*, 18392 – 18399.
[78] T. Svedberg, *The Formation of Colloid*, Von Nostrand Reinhold, New York, **1921**.
[79] Z. L. Wang, R. P. Gao, B. Nikoobakht, M. A. El-Sayed, *J. Phys. Chem. B* **2000**, *104*, 5417 – 5420.
[80] C. R. Martin, *Science* **1994**, *266*, 1961 – 1966.
[81] C. R. Martin, *Acc. Chem. Res.* **1995**, *28*, 61 – 68.
[82] J. C. Hulteen, C. R. Martin, *J. Mater. Chem.* **1997**, *7*, 1075 – 1087.
[83] W. Ye, J. Yan, F. Zhou, *J. Phys. Chem.* **2010**, *114*, 15617 – 15624.
[84] A. Taleb, C. Mangeney, V. Ivanova, *Nanotechnology* **2011**, *22*, 205301.
[85] T. Gao, T. H. Wang, *Chem. Mater.* **2005**, *17*, 887 – 892.
[86] K. Barbour, M. Ashokkumar, F. Grieser, R. A. Caruso, F. Grieser, *J. Phys. Chem. B* **1999**, *103*, 9231 – 9236.
[87] X. F. Qiu, J. J. Zhu, H. Y. Chen, *J. Cryst. Growth* **2003**, *257*, 378 – 383.
[88] K. Okitsu, Y. Mizukoshi, H. Bandow, A. T. Yamamoto, Y. Nagata, Y. Madea, *J. Phys. Chem. B* **1997**, *101*, 5470 – 5472.
[89] J. Belloni, M. Mostafavi, H. Remita, J. L. Marignier, M. O. Delcourt, *New J. Chem.* **1998**, *22*, 1239 – 1255; J. Belloni, M. Mostafavi, H. Remita, J. L. Marignier, M. O. Delcourt, *New J. Chem.* **1998**, *22*, 1257 – 1265.
[90] J. Zhang, J. Du, B. Han, Z. Liu, T. Jiang, Z. Zhang, *Angew. Chem.* **2006**, *118*, 1134 – 1137; *Angew. Chem. Int. Ed.* **2006**, *45*, 1116 – 1119.
[91] J. Henzie, E. S. Kwak, T. W. Odom, *Nano Lett.* **2005**, *5*, 1199 – 1202.
[92] M. Tréguer-Delapierre, J. Majimel, S. Mornet, S. Ravaine, *Gold Bull.* **2008**, *41*, 195 – 207.
[93] G. Lü, R. Zhao, G. Gian, Y. Qi, X. Wang, J. Suo, *Catal. Lett.* **2004**, *97*, 115 – 118.
[94] R. M. Penner, *J. Phys. Chem. B* **2002**, *106*, 3339 – 3353.
[95] V. M. Cepak, C. R. Martin, *J. Phys. Chem. B* **1998**, *102*, 9985 – 9990.
[96] M. Antonietti, A. Thünemann, E. Wenz, *Colloid Polym. Sci.* **1996**, *274*, 795 – 801.
[97] S. E. Skrabalak, J. Chen, L. Au, X. Lu, X. Li, Y. Xia, *Adv. Mater.* **2007**, *19*, 3177 – 3184.
[98] Y. Zhang, H. Dai, *Appl. Phys. Lett.* **2000**, *77*, 3015 – 3017.
[99] J. H. Song, Y. Wu, B. Messer, H. Kind, P. Yang, *J. Am. Chem. Soc.* **2001**, *123*, 10397 – 10398.
[100] M. A. El-Sayed, *Acc. Chem. Res.* **2001**, *34*, 257 – 264.
[101] M. E. Meyre, M. Tréguier-Delapierre, C. Faure, *Langmuir* **2008**, *24*, 4289 – 4294.

[102] J. L. Gardea-Torresdey, J. G. Parsons, E. Gomez, J. Peralta-Videa, H. E. Troiani, P. Santiago, M. J. Yacaman, *Nano Lett.* **2002**, *2*, 397 – 401.
[103] S. P. Chandran, M. Chaudhary, R. Pasricha, A. Ahmad, M. Sastry, *Biotechnol. Prog.* **2006**, *22*, 577 – 583.
[104] S. He, Y. Zhang, Z. Guo, N. Gu, *Biotechnol. Prog.* **2008**, *24*, 476 – 480.
[105] S. Brown, M. Sarikaya, E. Johnson, *J. Mol. Biol.* **2000**, *299*, 725 – 735.
[106] C. Lofton, W. Sigmund, *Adv. Funct. Mater.* **2005**, *15*, 1197 – 1208.
[107] J. Gao, C. M. Bender, C. J. Murphy, *Langmuir* **2003**, *19*, 9065 – 9070.
[108] C. S. Ah, Y. J. Yun, H. J. Park, W. J. Kim, D. H. Ha, W. S. Yun, *Chem. Mater.* **2005**, *17*, 5558 – 5561.
[109] Y. Xiong, I. Washio, J. Chen, H. Cai, Z. Y. Li, Y. Xia, *Langmuir* **2006**, *22*, 8563 – 8570.
[110] J. Zhang, H. Liu, Z. Wang, N. Ming, *Adv. Funct. Mater.* **2007**, *17*, 3295 – 3303.
[111] T. Pham, B. Jackson, N. J. Halas, T. R. Lee, *Langmuir* **2002**, *18*, 4915 – 4920.
[112] J. L. West, N. J. Halas, *Annu. Rev. Biomed. Eng.* **2003**, *5*, 285 – 292.
[113] L. R. Hirsch, R. J. Stafford, J. A. Bankson, S. R. Sershen, B. Rivera, R. E. Price, J. D. Hazle, N. J. Halas, J. L. West, *Proc. Natl. Acad. Sci. USA* **2003**, *100*, 13549 – 13554.
[114] Theranostics applications: R. Bardhan, S. Lal, A. Joshi, N. J. Halas, *Acc. Chem. Res.* **2011**, *44*, 936 – 946.
[115] M. Zhao, R. M. Crooks, *Chem. Mater.* **1999**, *11*, 3379 – 3385.
[116] M. F. Mrozek, Y. Xia, M. J. Waever, *Anal. Chem.* **2001**, *73*, 5953 – 5960.
[117] S. R. Brankovic, J. X. Wang, R. R. Adzic, *Surf. Sci.* **2001**, *474*, L171 – L179.
[118] Y. Sun, B. Mayers, Y. Xia, *Nano Lett.* **2002**, *2*, 481 – 485.
[119] Y. Sun, Y. Xia, *Anal. Chem.* **2002**, *74*, 5297 – 5305.
[120] G. S. Métraux, Y. Cao, R. Jin, C. A. Mirkin, *Nature* **2003**, *425*, 487 – 490.
[121] Y. Sun, B. Mayers, Y. Xia, *Adv. Mater.* **2004**, *16*, 264 – 268.
[122] H. Lang, S. Maldonado, K. J. Stevenson, B. D. Chandler, *J. Am. Chem. Soc.* **2004**, *126*, 12949 – 12956.
[123] Y. Sun, Y. Xia, *J. Am. Chem. Soc.* **2004**, *126*, 3892 – 3910.
[124] J. Chen, B. Wiley, J. McLellan, Y. Xiong, Z. Y. Li, Y. Xia, *Nano Lett.* **2005**, *5*, 2058 – 2062.
[125] L. Au, X. Lu, Y. Xia, *Adv. Mater.* **2008**, *20*, 2517 – 2522.
[126] V. Bansal, A. P. O'Mullane, S. K. Bhargava, *Electrochem. Commun.* **2009**, *11*, 1639 – 1642.
[127] C. M. Cobley, Y. Xia, *Mater. Sci. Eng.* **2010**, *70*, 44 – 62.
[128] Y. S. Shon, G. B. Dawson, M. Porter, M. W. Murray, *Langmuir* **2002**, *18*, 3880 – 3885.
[129] D. F. Yancey, E. V. Carino, R. M. Crooks, *J. Am. Chem. Soc.* **2010**, *132*, 10988 – 10989.
[130] S. Pande, M. G. Weir, B. A. Zaccheo, R. M. Crooks, *New J. Chem.* **2011**, *35*, 2054 – 2060.
[131] Q. Xu, G. Meng, X. Wu, Q. Wei, M. Kong, X. Zhu, Z. Chu, *Chem. Mater.* **2009**, *21*, 2397 – 2402.
[132] C. Zuo, P. W. Jagodzinsski, *J. Phys. Chem. B* **2005**, *109*, 1788 – 1793.
[133] W. Ye, Y. Chen, F. Zhou, C. Wang, Y. Li, *J. Mater. Chem.* **2012**, *22*, 18327 – 18243.
[134] See Ref. [30].
[135] T. K. Sau, C. J. Murphy, *Langmuir* **2004**, *20*, 6414 – 6420.
[136] L. B. Rogers, D. P. Krause, J. C. Griess, D. B. Ehrlinger, *J. Electrochem. Soc.* **1949**, *95*, 33 – 46.
[137] J. Zhang, M. R. Langille, M. L. Personick, K. Zhang, S. Li, C. A. Mirkin, *J. Am. Chem. Soc.* **2010**, *132*, 14012 – 14014.
[138] T. Ming, W. Feng, Q. Tang, F. Wang, L. Sun, J. Wang, C. Yan, *J. Am. Chem. Soc.* **2009**, *131*, 16350 – 16351.
[139] J. Li, L. Wang, L. Liu, L. Guo, X. Han, Z. Zhang, *Chem. Commun.* **2010**, *46*, 5109 – 5111.
[140] X. Kou, W. Ni, C. K. Tsung, K. Chan, H. Q. Lin, G. D. Stucky, *Small* **2007**, *3*, 2103 – 2113.
[141] E. Carbó-Argibay, B. Rodriguez-Gonzalez, S. Gomez-Graa, A. Guerrero-Martinez, I. Pastoriza-Santos, J. Perez-Juste, L. M. Liz-Marzan, *Angew. Chem.* **2010**, *122*, 9587 – 9590; *Angew. Chem. Int. Ed.* **2010**, *49*, 9397 – 9400.
[142] H. Katz-Boon, C. Rossouw, M. Weyland, A. M. Funston, A. M. Mulvaney, J. Etheridge, *Nano Lett.* **2011**, *11*, 273 – 278.
[143] J. M. Lehn, *Supramolecular Chemistry. Concepts and Perspectives*, VCH, Weinheim, **1995**.
[144] L. Isaac, D. N. Chin, N. Bowden, Y. Xia, G. M. Whitesides in *Supramolecular Technology* (Ed.: D. N. Reinhout), Wiley, New York, **1999**, pp. 1 – 46.
[145] M. P. Pileni, *Acc. Chem. Res.* **2007**, *40*, 685 – 693.
[146] D. Nykypanchuk, M. M. Maye, D. van der Lelie, O. Gang, *Nature* **2008**, *451*, 549 – 552.
[147] D. V. Talapin, E. V. Shevchenko, M. I. Bodnarchuk, X. Ye, J. Chen, C. B. Murray, *Nature* **2009**, *461*, 964 – 967.
[148] W. Cheng, M. J. Campolongo, J. J. Cha, S. J. Tan, C. C. Umbach, D. A. Muller, D. Luo, *Nat. Mater.* **2009**, *8*, 519 – 525.
[149] B. Nikoobakht, Z. L. Wang, M. A. El-Sayed, *J. Phys. Chem. B* **2000**, *104*, 8635 – 8640.
[150] Z. C. Xu, C. M. Chen, C. W. Xiao, T. Z. Yang, S. T. Chen, H. L. Li, H. J. Gao, *Chem. Phys. Lett.* **2006**, *432*, 222 – 225.
[151] G. Kawamura, Y. Yang, M. I. Nogamia, *Appl. Phys. Lett.* **2007**, *90*, 261908.
[152] R. Jana, L. A. Gearheart, S. O. Obare, C. J. Johnson, K. J. Edler, S. Mann, C. J. Murphy, *J. Mater. Chem.* **2002**, *12*, 2909 – 2912.
[153] N. Goubet, J. Richardi, P. A. Albouy, M. P. Pileni, *J. Phys. Chem. Lett.* **2011**, *2*, 417 – 422.
[154] C. Salzemann, W. Zhai, N. Goubet, M. P. Pileni, *J. Phys. Chem. Lett.* **2010**, *1*, 149 – 154.
[155] P. Yang, I. Arfaoui, T. Cren, N. Goubet, M. P. Pileni, *Nano Lett.* **2012**, *12*, 2051 – 2055.
[156] P. Yang, I. Arfaoui, T. Cren, N. Goubet, M. P. Pileni, *Phys. Rev. B* **2012**, *86*, 075409.
[157] N. Goubet, H. Portales, C. Yan, I. Arfaoui, P. A. Albouy, A. Mermet, M. P. Pileni, *J. Am. Chem. Soc.* **2012**, *134*, 3714 – 3719.
[158] L. C. Brousseau III, J. P. Novak, S. M. Marinakos, D. L. Feldheim, *Adv. Mater.* **1999**, *11*, 447 – 449.
[159] K. S. Caswell, J. N. Wilson, U. H. F. Bunz, C. J. Murphy, *J. Am. Chem. Soc.* **2003**, *125*, 13914 – 13915.
[160] S. Zhang, X. Kou, Z. Yang, Q. Shi, G. D. Stucky, L. Sun, J. Wang, C. Yan, *Chem. Commun.* **2007**, 1816 – 1818.
[161] N. Varghese, S. R. C. Vivekchand, A. Govindaraj, C. N. R. Rao, *Chem. Phys. Lett.* **2008**, *450*, 340 – 344.
[162] S. T. Shibu Joseph, B. I. Ipe, P. Pramod, K. G. Thomas, *J. Phys. Chem. B* **2006**, *110*, 150 – 157.
[163] B. Pan, L. Ao, F. Gao, H. Tian, R. He, D. Cui, *Nanotechnology* **2005**, *16*, 1776 – 1780.
[164] R. Voggu, P. Suguna, S. Chandrasekaran, C. N. R. Rao, *Chem. Phys. Lett.* **2007**, *443*, 118 – 121.
[165] P. Khanal, E. R. Zubaev, *Angew. Chem.* **2007**, *119*, 2245 – 2248; *Angew. Chem. Int. Ed.* **2007**, *46*, 2195 – 2198.
[166] Z. H. Nie, D. Fava, M. Rubinstein, E. Kumacheva, *J. Am. Chem. Soc.* **2008**, *130*, 3683 – 3689.
[167] E. Dujardin, L. B. Hsin, C. R. C. Wang, S. Mann, *Chem. Commun.* **2001**, 1264 – 1265.
[168] C. J. Orendorff, P. L. Hankins, C. J. Murphy, *Langmuir* **2005**, *21*, 2022 – 2026.
[169] A. Gole, C. J. Murphy, *Langmuir* **2005**, *21*, 10756 – 10762.
[170] B. Pan, C. Cui, C. Ozkan, P. Xu, T. Huang, Q. Li, H. Chen, F. Liu, F. Gao, R. He, *J. Phys. Chem.* **2007**, *111*, 12572 – 12576.

[171] T. S. Sreeprasad, A. K. Samal, T. Pradeep, *Langmuir* **2008**, *24*, 4589 – 4599.
[172] H. Nakashima, K. Furukawa, Y. Kashimura, K. Tirimitsu, *Chem. Commun.* **2007**, 1080 – 1082.
[173] K. Mitamura, T. Imae, N. Saito, O. Takai, *J. Phys. Chem. B* **2007**, *111*, 8891 – 8898.
[174] M. Das, N. Sanson, D. Fava, E. Kumacheva, *Langmuir* **2007**, *23*, 196 – 201.
[175] M. Karg, I. Pastoriza-Santos, J. Perez-Juste, T. Hellweg, L. M. Liz-Marzan, *Small* **2007**, *3*, 1222 – 1229.
[176] C. J. Murphy, C. J. Orendorff, *Adv. Mater.* **2005**, *17*, 2173 – 2177.
[177] J. Pérez-Juste, B. Rodriguez-Gonzáles, P. Mulvaney, L. M. Liz-Marzán, *Adv. Funct. Mater.* **2005**, *15*, 1065 – 1071.
[178] P. Zijlstra, J. W. M. Chon, M. Gu, *Opt. Express* **2007**, *15*, 12151 – 12160.
[179] R. Deshmukh, Y. Liu, R. J. Composto, *Nano Lett.* **2007**, *7*, 3662 – 3668.
[180] L. Billot, M. Lamy de La Chapelle, A. S. Grimault, A. Vial, D. Bachiesi, J. L. Bijeon, P. M. Adam, P. Royer, *Chem. Phys. Lett.* **2006**, *422*, 303 – 307.
[181] E. J. Smythe, E. Cubukcu, F. Capasso, *Opt. Express* **2007**, *15*, 7439 – 7447.
[182] P. Babu Dayala, F. Koyama, *Appl. Phys. Lett.* **2007**, *91*, 111107.
[183] P. K. Jain, W. Huang, M. A. El-Sayed, *Nano Lett.* **2007**, *7*, 2080 – 2088.
[184] A. N. Grigorenko, N. W. Roberts, M. R. Dickinson, Y. Zhang, *Nat. Photonics* **2008**, *2*, 365 – 370.
[185] E. Devaux, T. W. Ebbesen, J. C. Weeber, A. Dereux, *Appl. Phys. Lett.* **2003**, *83*, 4936 – 4938.
[186] W. L. Barnes, A. Dereux, T. W. Ebbesen, *Nature* **2003**, *424*, 824 – 830.
[187] S. I. Bozhevolnyi, V. S. Volkov, E. Devaux, J. Y. Laluet, T. W. Ebbesen, *Nature* **2006**, *440*, 508 – 511.
[188] S. M. Yang, S. G. Yang, D. G. Choi, S. Kim, H. K. Yu, *Small* **2006**, *2*, 458 – 475.
[189] B. J. Y. Tan, C. H. Sow, T. S. Koh, K. C. Chin, A. T. S. Wee, C. K. Hong, *J. Phys. Chem. B* **2005**, *109*, 11100 – 11109.
[190] D. Jia, A. Goonewardene, *Appl. Phys. Lett.* **2006**, *88*, 053105.
[191] L. Qin, S. Park, L. Huang, C. A. Mirkin, *Science* **2005**, *309*, 113 – 115.
[192] L. Qin, S. Zou, C. Xue, A. Atkinson, G. C. Schatz, C. A. Mirkin, *Proc. Natl. Acad. Sci. USA* **2006**, *103*, 13300 – 13303.
[193] M. J. Branholzer, L. D. Qin, C. A. Mirkin, *Small* **2009**, *5*, 2537 – 2540.
[194] A. B. Braunschweig, A. L. Schmucker, W. D. Wei, C. A. Mirkin, *Chem. Phys. Lett.* **2010**, *486*, 89 – 98.
[195] M. J. Banholzer, K. D. Osberg, S. Li, B. F. Mangelson, G. C. Schatz, C. A. Mirkin, *ACS Nano* **2010**, *4*, 5446 – 5452.
[196] K. D. Osberg, A. L. Schmucker, A. J. Senesi, C. A. Mirkin, *Nano Lett.* **2011**, *11*, 820 – 824.
[197] F. Kim, S. Connor, H. Song, T. Kuykendall, P. Yang, *Angew. Chem.* **2004**, *116*, 3759 – 3763; *Angew. Chem. Int. Ed.* **2004**, *43*, 3673 – 3677.
[198] Y. Sun, Y. Xia, *Science* **2002**, *298*, 2176 – 2179.
[199] D. Seo, J. C. Park, H. Song, *J. Am. Chem. Soc.* **2006**, *128*, 14863 – 14870.
[200] E. Boisselier, A. K. Diallo, L. Salmon, C. Ornelas, J. Ruiz, D. Astruc, *J. Am. Chem. Soc.* **2010**, *132*, 2729 – 2742.
[201] C. Li, K. L. Shuford, Q. H. Park, W. Cai, Y. Li, E. J. Lee, S. O. Cho, *Angew. Chem.* **2007**, *119*, 3328 – 3332; *Angew. Chem. Int. Ed.* **2007**, *46*, 3264 – 3268.
[202] J. G. Heong, M. Kim, Y. W. Lee, W. Choi, W. T. Oh, Q. H. Park, S. W. Han, *J. Am. Chem. Soc.* **2009**, *131*, 1672 – 1673.
[203] K. Kwon, K. Y. Lee, Y. W. Lee, M. Kim, J. Heo, S. Ahn, S. W. Han, *J. Phys. Chem. C* **2007**, *111*, 1161 – 1165.
[204] J. F. Parker, C. A. Fields-Zinna, R. W. Murray, *Acc. Chem. Res.* **2010**, *43*, 1289 – 1296.
[205] M. Yavuz, W. Li, Y. Xia, *Chem. Eur. J.* **2009**, *15*, 13181 – 13187.
[206] M. Zhou, S. Chen, S. Zhao, *J. Phys. Chem. Lett.* **2006**, *110*, 4510 – 4513.
[207] O. Guliamov, A. I. Frenkel, L. D. Menard, R. G. Nuzzo, L. Kronik, *J. Am. Chem. Soc.* **2007**, *129*, 10978 – 10979.
[208] Y. Li, H. Cheng, T. Yao, Z. Sun, W. Yan, Y. Jiang, Y. Xie, Y. Sun, Y. Huang, S. Liu, J. Zhang, Y. Xie, T. Hu, L. Yang, Z. Wu, S. Wei, *J. Am. Chem. Soc.* **2012**, *134*, 17997 – 18003.
[209] M. R. Langille, J. Zhang, M. Personick, S. Li, C. A. Mirkin, *Science* **2012**, *337*, 954 – 957.
[210] M. L. Personick, M. R. Langille, J. Zhang, N. Harris, G. C. Schatz, C. A. Mirkin, *J. Am. Chem. Soc.* **2011**, *133*, 6170 – 6173.
[211] T. K. Sau, C. J. Murphy, *J. Am. Chem. Soc.* **2004**, *126*, 8648 – 8649.
[212] B. M. I. van der Zande, L. Pages, R. A. M. Hikmet, A. van Blaaderen, *J. Phys. Chem. B* **1999**, *103*, 5761 – 5767.
[213] M. A. Correa-Duarte, J. Perez-Juste, A. Sanchez-Iglesias, M. Giersig, L. M. Liz-Marzan, *Angew. Chem.* **2005**, *117*, 4449 – 4452; *Angew. Chem. Int. Ed.* **2005**, *44*, 4375 – 4378.
[214] C. J. Murphy, L. B. Thompson, D. J. Chernak, J. A. Yang, S. T. Sivapalan, S. P. Boulos, J. Y. Huang, A. M. Alkimlany, P. N. Sisco, *Curr. Opin. Colloid Interface Sci.* **2011**, *16*, 128 – 134.
[215] J. A. Yang, S. E. Lohse, S. P. Boulos, C. J. Murphy, *J. Cluster Sci.* **2012**, *23*, 799 – 809.
[216] J. Perez-Juste, I. Pastoriza-Santos, L. M. Liz-Marzan, P. Mulvaney, *Coord. Chem. Rev.* **2005**, *249*, 1870 – 1901.
[217] A. Lee, G. F. S. Andrade, A. Ahmed, M. L. Souza, N. Coombs, E. Tumarkin, K. Liu, R. Gordon, A. G. Brolo, E. Kumacheva, *J. Am. Chem. Soc.* **2011**, *133*, 7563 – 7570.
[218] J. V. Jokerst, Z. Miao, C. Zavaleta, Z. Cheng, S. S. Gambhir, *Small* **2011**, *7*, 625 – 633.
[219] B. Y. S. Kim, J. T. Rutka, W. C. W. Chan, *N. Engl. J. Med.* **2010**, *363*, 2434 – 2443.
[220] A. Bajaj, O. R. Mirnda, I. B. Kim, R. L. Phillips, D. J. Jerry, U. H. F. Bunz, V. M. Rotello, *Proc. Natl. Acad. Sci. USA* **2009**, *106*, 10912 – 10916.
[221] E. C. Dreaden, S. C. Mwakwari, L. A. Austin, M. J. Kieffer, A. K. Oyelere, M. A. El-Sayed, *Small* **2012**, *8*, 2819 – 2822.
[222] A. Paul, D. Solis, K. Bao, W. S. Chang, S. Nauert, L. Vidgerman, E. R. Zubarev, P. Nordlander, S. Link, *ACS Nano* **2012**, *6*, 8105 – 8113.
[223] B. P. Khanal, E. R. Zubarev, *J. Am. Chem. Soc.* **2008**, *130*, 12634 – 12635.
[224] K. Critchley, B. P. Khanal, M. L. Gorzny, L. Vigderman, S. D. Evans, E. R. Zubarev, N. A. Kotov, *Adv. Mater.* **2010**, *22*, 2338 – 2342.
[225] J. U. Kim, S. H. Cha, K. Shin, J. Y. Jho, J. C. Lee, *Adv. Mater.* **2004**, *16*, 459 – 464.
[226] S. Nah, L. Li, R. Liu, J. Ha, S. B. Lee, J. T. Fourkas, *J. Phys. Chem. C* **2010**, *114*, 7774 – 7779.
[227] P. Kusar, C. Gruber, A. Hohenau, J. R. Krenn, *Nano Lett.* **2012**, *12*, 661 – 665.
[228] S. Lal, J. H. Hafner, N. J. Halas, S. Link, P. Norlander, *Acc. Chem. Res.* **2012**, *45*, 1887 – 1895.
[229] C. C. Mayorga-Martinez, M. Guix, R. E. Madrid, A. Merkoçi, *Chem. Commun.* **2012**, *48*, 1686 – 1688.
[230] A. K. Sra, T. D. Ewers, R. E. Schaak, *Chem. Mater.* **2005**, *17*, 758 – 766.
[231] Z. Jiang, Q. Zhang, C. Zong, B. J. Liu, B. Ren, Z. Xie, L. Zheng, *J. Mater. Chem.* **2012**, *22*, 18192 – 18197.
[232] L. Vigderman, E. R. Zubarev, *Langmuir* **2012**, *28*, 9034 – 9040.
[233] S. M. Yoo, T. Kang, H. Kang, H. Lee, M. Kang, S. Y. Lee, B. Kim, *Small* **2011**, *7*, 3371 – 3376.
[234] M. Wirtz, C. R. Martin, *Adv. Mater.* **2003**, *15*, 455 – 458.
[235] C. R. Bridges, P. M. DiCarmine, D. S. Seferos, *Chem. Mater.* **2012**, *24*, 963 – 965.

[236] F. Muench, U. Kunz, C. Neetzel, S. Lauterbach, H. J. Kleebe, W. Ensinger, *Langmuir* **2011**, *27*, 430 – 435.
[237] Y. Sun, B. Mayers, T. Herricks, Y. Xia, *Nano Lett.* **2003**, *3*, 955 – 960.
[238] N. R. Sieb, N. C. Wu, E. Majidi, R. Kukreja, N. R. Branda, B. D. Gates, *ACS Nano* **2009**, *3*, 1365 – 1372.
[239] Y. Yu, K. Kant, J. G. Shapter, J. Addai-Mensah, D. Losic, *Microporous Mesoporous Mater.* **2012**, *153*, 131 – 136.
[240] J. H. Ryu, S. Park, B. Kim, A. Klaikherd, T. O. Russell, S. Thayumanavan, *J. Am. Chem. Soc.* **2009**, *131*, 9870 – 9871.
[241] Z. Siwy, L. Trofin, P. Kohli, L. A. Baker, C. Trautmann, C. R. Martin, *J. Am. Chem. Soc.* **2005**, *127*, 5000 – 5001.
[242] M. Spuch-Calvar, J. Pacifico, J. Pérez-Juste, L. M. Liz-Marzan, *Langmuir* **2008**, *24*, 9675 – 9681.
[243] F. Tielens, J. Andrés, *J. Phys. Chem.* **2007**, *111*, 10342 – 10346.
[244] M. S. Bakshi, F. Possmayer, N. O. Petersen, *J. Phys. Chem. C* **2008**, *112*, 8259 – 8265.
[245] Y. Chen, S. Milenkovic, A. W. Hassel, *Nano Lett.* **2008**, *8*, 737 – 742.
[246] L. Li, Z. Wang, T. Huang, J. Xie, L. Qi, *Langmuir* **2010**, *26*, 12330 – 12335.
[247] L. J. E. Anderson, C. M. Payne, Y. R. Zhen, P. Nordlander, *Nano Lett.* **2011**, *11*, 5034 – 5037.
[248] Y. Kuroda, Y. Sakamoto, K. Kuroda, *J. Am. Chem. Soc.* **2012**, *134*, 8684 – 8692.
[249] S. Porel, S. Singh, T. P. Radhakrishnan, *Chem. Commun.* **2005**, 2387 – 2389.
[250] X. Sun, S. Dong, E. Wang, *Langmuir* **2005**, *21*, 4710 – 4712.
[251] B. Lim, P. H. C. Camargo, Y. Xia, *Langmuir* **2008**, *24*, 10437 – 10442.
[252] M. Yamamoto, Y. Kashiwagi, T. Sakata, H. Mori, M. Nakamoto, *Chem. Mater.* **2005**, *17*, 5391 – 5393.
[253] J. H. Lee, K. Kamada, N. Enomoto, J. Hojo, *Cryst. Growth Des.* **2008**, *8*, 2638 – 2645.
[254] X. Sun, S. Dong, E. Wang, *Angew. Chem.* **2004**, *116*, 6520 – 6523; *Angew. Chem. Int. Ed.* **2004**, *43*, 6360 – 6363.
[255] H. C. Chu, C. H. Kuo, M. H. Huang, *Inorg. Chem.* **2006**, *45*, 808 – 813.
[256] S. Hong, K. L. Shuford, S. Park, *Chem. Mater.* **2011**, *23*, 2011 – 2013.
[257] Y. Shao, Y. Jin, S. Dong, *Chem. Commun.* **2004**, 1104 – 1105.
[258] B. Liu, J. Xie, J. Y. Lee, Y. P. Ting, J. P. Chen, *J. Phys. Chem. B* **2005**, *109*, 15256 – 15263.
[259] Y. Zhang, G. Chang, S. Liu, W. Lu, J. Tian, X. Sun, *Biosens. Bioelectron.* **2011**, *28*, 344 – 348.
[260] J. Xie, J. Y. Lee, D. I. C. Wang, *J. Phys. Chem. C* **2007**, *111*, 10226 – 10232.
[261] L. Wang, X. Wu, X. Li, L. Wang, M. Pei, X. Tao, *Chem. Commun.* **2010**, *46*, 8422 – 8423.
[262] G. Lin, W. Lu, W. Cui, L. Jiang, *Cryst. Growth Des.* **2010**, *10*, 1118 – 1123.
[263] P. Pienpinijtham, X. X. Han, T. Suzuki, C. Thanmmacharoen, S. Ekgasit, Y. Ozaki, *Phys. Chem. Chem. Phys.* **2012**, *14*, 9636 – 9641.
[264] T. Deckert-Gaudig, V. Deckert, *Small* **2009**, *5*, 432 – 436.
[265] J. E. Millstone, S. J. Hurst, G. S. Métraux, J. I. Cutler, C. A. Mirkin, *Small* **2009**, *5*, 646 – 664.
[266] M. R. Jones, R. J. Macfarlane, A. E. Prigodich, P. C. Patel, C. A. Mirkin, *J. Am. Chem. Soc.* **2011**, *133*, 18865 – 18869.
[267] M. J. Banholzer, N. Harris, J. Millstone, G. C. Schatz, C. A. Mirkin, *J. Phys. Chem. C* **2010**, *114*, 7521 – 7526.
[268] J. Hu, Y. Zhang, B. Liu, J. Liu, H. Zhou, Y. Xu, Y. Jiang, Z. Yang, Z. Tian, *J. Am. Chem. Soc.* **2004**, *126*, 9470 – 9471.
[269] L. Huang, M. Wang, Y. Zhang, Z. Guo, J. Sun, N. Gu, *J. Phys. Chem. C* **2007**, *111*, 16154 – 16160.
[270] F. Li, T. Tian, H. Cui, *Luminescence* **2013**, *28*, 7 – 15.
[271] P. H. C. Camargo, Y. Xiong, L. Ji, J. M. Zuo, Y. Xia, *J. Am. Chem. Soc.* **2007**, *129*, 15452 – 15453.
[272] M. Grzelczak, A. Sanchez-Iglesias, H. H. Mezerji, S. Bals, J. Perez-Juste, L. M. Liz-Marzan, *Nano Lett.* **2012**, *12*, 4380 – 4384.
[273] M. Grzelczak, A. Sánchez-Iglesias, B. Rodríguez-González, R. Alvarez-Puebla, J. Pérez-Juste, L. Liz-Marzán, *Adv. Funct. Mater.* **2008**, *18*, 3780 – 3786.
[274] M. Fernanda Cardinal, B. Rodriguez-Gonzalez, R. A. Alvarez-Puebla, J. Perez-Juste, L. M. Liz-Marzan, *J. Phys. Chem. C* **2010**, *114*, 10417 – 10423.
[275] W. Xie, L. Su, P. Donfack, A. Shen, X. Zhou, M. Sackmann, A. Materny, J. Hu, *Chem. Commun.* **2009**, 5263 – 5265.
[276] E. Shaviv, U. Banin, *ACS Nano* **2010**, *4*, 1529 – 1538.
[277] G. Krylova, L. J. Giovanetti, F. G. Requejo, N. M. Dimitrijevic, A. Prakapenka, E. V. Shevchenko, *J. Am. Chem. Soc.* **2012**, *134*, 4384 – 4392.
[278] D. Y. Kim, T. Yu, E. C. Cho, Y. Ma, O. O. Park, Y. Xia, *Angew. Chem.* **2011**, *123*, 6452 – 6455; *Angew. Chem. Int. Ed.* **2011**, *50*, 6328 – 6331.
[279] L. Lu, K. Ai, Y. Ozaki, *Langmuir* **2008**, *24*, 1058 – 1063.
[280] S. K. Dondapati, T. K. Sau, C. Hrelescu, T. A. Klar, F. D. Stefani, J. Feldmann, *ACS Nano* **2010**, *4*, 6318 – 6322.
[281] H. Yuan, C. G. Khoury, H. Hwang, C. M. Wilson, G. A. Grant, T. Vo-Dinh, *Nanotechnology* **2012**, *23*, 075102.
[282] J. Xie, Q. Zhang, J. Y. Lee, D. I. C. Wang, *ACS Nano* **2008**, *2*, 2473 – 2480.
[283] B. Van de Broek, N. Devoogdt, A. D'Hollander, H. L. Gijs, K, Jan, L. Lagae, S. Muyldermans, G. Maes, G. Borghs, *ACS Nano* **2011**, *5*, 4319 – 4328.
[284] E. Hao, R. C. Bailey, G. C. Schatz, J. T. Hupp, S. Li, *Nano Lett.* **2004**, *4*, 327 – 330.
[285] Z. Li, W. Li, P. H. C. Camargo, Y. Xia, *Angew. Chem.* **2008**, *120*, 9799 – 9802; *Angew. Chem. Int. Ed.* **2008**, *47*, 9653 – 9656.
[286] H. L. Wu, C. H. Chen, M. H. Huang, *Chem. Mater.* **2009**, *21*, 110 – 114.
[287] S. Guo, L. Wang, E. Wang, *Chem. Commun.* **2007**, 3163 – 3165.
[288] S. Barbosa, A. Agrawal, L. Rodriguez-Lorenzo, I. Pastoriza-Santos, R. A. Alvarez-Puebla, A. Kornowski, H. Weller, L. M. Liz-Marzan, *Langmuir* **2010**, *26*, 14943 – 14950.
[289] C. L. Nehl, H. Liao, J. H. Hanfner, *Nano Lett.* **2006**, *6*, 683 – 688.
[290] F. Hao, C. L. Nehl, J. H. Hafner, P. Nordlander, *Nano Lett.* **2007**, *7*, 729 – 732.
[291] C. L. Nehl, J. H. Hafner, *J. Mater. Chem.* **2008**, *18*, 2415 – 2419.
[292] T. H. Lin, C. W. Lin, H. H. Liu, J. T. Sheu, W. H. Hung, *Chem. Commun.* **2011**, *47*, 2044 – 2046.
[293] T. Huang, F. Meng, L. Qi, *Langmuir* **2010**, *26*, 7582 – 7589.
[294] D. Huang, X. Bai, L. Zheng, *J. Phys. Chem. C* **2011**, *115*, 14641 – 14647.
[295] D. Huang, Y. Qi, X. Bai, L. Shi, G. Jia, D. Zhang, L. Zheng, *ACS Appl. Mater. Interfaces* **2012**, *4*, 4665 – 4671.
[296] L. R. Hirsch, A. M. Gobin, A. R. Lowery, F. Tam, R. A. Drezek, N. J. Halas, J. L. West, *Ann. Biomed. Eng.* **2006**, *34*, 15 – 22.
[297] C. Radloff, N. J. Halas, *Nano Lett.* **2004**, *4*, 1323 – 1327.
[298] S. J. Oldenburg, J. B. Jackson, S. L. Westcott, N. J. Halas, *Appl. Phys. Lett.* **1999**, *75*, 2897 – 2899.
[299] C. L. Nehl, N. K. Grady, G. P. Goodrich, F. Tam, N. J. Halas, J. H. Hafner, *Nano Lett.* **2004**, *4*, 2355 – 2359.
[300] F. Tam, G. P. Goodrich, B. R. Johnson, N. J. Halas, *Nano Lett.* **2007**, *7*, 496 – 501.
[301] R. Bardhan, N. K. Grady, J. R. Cole, A. Joshi, N. J. Halas, *ACS Nano* **2009**, *3*, 744 – 752.
[302] R. Bardhan, N. K. Grady, N. J. Halas, *Small* **2008**, *4*, 1716 – 1722.
[303] Y. Zhang, N. K. Grady, C. Ayala-Orozco, N. J. Halas, *Nano Lett.* **2011**, *11*, 5519 – 5523.

[304] C. Loo, A. Lowery, N. Halas, J. West, R. Drezek, *Nano Lett.* **2005**, *5*, 709 – 711.
[305] L. R. Hirsch, J. B. Jackson, A. Lee, N. J. Halas, J. L. West, *Anal. Chem.* **2003**, *75*, 2377 – 2381.
[306] A. M. Gobin, M. H. Lee, N. J. Halas, W. D. James, R. A. Drezek, J. L. West, *Nano Lett.* **2007**, *7*, 1929 – 1934.
[307] T. Zhou, B. Wu, D. Xing, *J. Mater. Chem.* **2012**, *22*, 470 – 477.
[308] D. Llamosa Pérez, A. Espinosa, L. Martínez, E. Román, C. Ballesteros, A. Mayoral, M. García-Hernández, Y. Huttel, *J. Phys. Chem. C* **2013**, *117*, 3101 – 3108.
[309] R. D. Averitt, D. Sarkar, N. J. Halas, *Phys. Rev. Lett.* **1997**, *78*, 4217 – 4220.
[310] R. D. Averitt, S. L. Westcott, N. J. Halas, *J. Opt. Soc. Am. B* **1999**, *16*, 1824 – 1832.
[311] E. Prodan, C. Radloff, N. J. Halas, P. Nordlander, *Science* **2003**, *302*, 419 – 422.
[312] S. J. Oldenburg, S. L. Westcott, R. D. Averitt, N. J. Halas, *J. Chem. Phys.* **1999**, *111*, 4729 – 4735.
[313] F. Caruso, M. Spasova, V. Salgueiriño-Maceira, L. M. Liz-Marzán, *Adv. Mater.* **2001**, *13*, 1090 – 1094.
[314] Z. Liang, A. Susha, F. Caruso, *Chem. Mater.* **2003**, *15*, 3176 – 3183.
[315] X. Feng, C. Mao, G. Yang, W. Hou, J. Zhu, *Langmuir* **2006**, *22*, 4384 – 4389.
[316] H. Liang, L. Wan, Chun. Bai, L. Jiang, *J. Phys. Chem. B* **2005**, *109*, 7795 – 7800.
[317] C. Song, G. Zhao, P. Zhang, N. L. Rosi, *J. Am. Chem. Soc.* **2010**, *132*, 14033 – 14035.
[318] C. L. Chen, P. J. Zhang, N. L. Rosi, *J. Am. Chem. Soc.* **2008**, *130*, 13555 – 13557.
[319] L. Hwang, G. Zhao, P. Zhang, N. L. Rosi, *Small* **2011**, *7*, 1939 – 1942.
[320] S. E. Skrabalak, J. Chen, Y. Sun, X. Lu, L. Au, C. M. Cobley, Y. Xia, *Acc. Chem. Res.* **2008**, *41*, 1587 – 1595.
[321] X. Lu, L. Au, J. McLellan, Z. Li, M. Marquez, Y. Xia, *Nano Lett.* **2007**, *7*, 1764 – 1769.
[322] M. A. Mahmoud, M. A. El-Sayed, *J. Am. Chem. Soc.* **2010**, *132*, 12704 – 12710.
[323] M. A. Mahmoud, M. A. El-Sayed, *Nano Lett.* **2011**, *11*, 946 – 953.
[324] S. A. Khan, R. Kanchanapally, Z. Fan, L. Beqa, A. K. Singh, D. Senapati, P. C. Ray, *Chem. Commun.* **2012**, *48*, 6711 – 6713.
[325] Y. Wang, X. Xie, X. Wang, G. Ku, K. L. Gill, D. P. O'Neal, G. Stocia, L. V. Wang, *Nano Lett.* **2004**, *4*, 1689 – 1692.
[326] C. M. Cobley, D. J. Campbell, Y. Xia, *Adv. Mater.* **2008**, *20*, 748 – 752.
[327] W. Wang, T. Yan, S. Cui, J. Wan, *Chem. Commun.* **2012**, *48*, 10228 – 10230.
[328] B. Khlebtsov, E. Panfilova, V. Khanadeev, O. Bibikova, G. Terentyuk, A. Lvanov, V. Rumyantseva, I. Shilov, A. Ryabova, V. Loshchenov, A. G. Khlebtsov, *ACS Nano* **2011**, *5*, 7077 – 7089.
[329] J. M. Liu, H. F. Wang, X. P. Yan, *Analyst* **2011**, *136*, 3904 – 3910.
[330] C. J. Murphy, A. M. Gole, S. E. Hunyadi, J. W. Stone, P. N. Sisco, A. Akilany, B. E. Kinard, P. Hankins, *Chem. Commun.* **2008**, 544 – 557.
[331] R. Wilson, *Chem. Soc. Rev.* **2008**, *37*, 2028 – 2045.
[332] L. Xu, H. Kuang, L. Wang, C. Xu, *J. Mater. Chem.* **2011**, *21*, 16759 – 16782.
[333] L. Rodríguez-Lorenzo, R. A. Álvarez-Puebla, F. J. García de Abajo, L. M. Liz-Marzán, *J. Phys. Chem. C* **2010**, *114*, 7336 – 7340.
[334] C. Hrelescu, T. K. Sau, A. L. Rogach, F. Jackel, J. Feldmann, *Appl. Phys. Lett.* **2009**, *94*, 153113.
[335] E. Nalbant Esenturk, W. Hight, *J. Raman Spectrosc.* **2009**, *40*, 86 – 91.
[336] H. Ko, S. Singamaneni, V. V. Tsukruk, *Small* **2008**, *4*, 1576 – 1599.
[337] X. H. Huang, I. H. El-Sayed, W. Qian, M. A. El-Sayed, *Nano Lett.* **2007**, *7*, 217 – 228.
[338] S. W. Bishnoi, C. J. Rozell, C. S. Levin, M. K. Gheith, B. R. Johnson, D. H. Johnson, N. J. Halas, *Nano Lett.* **2006**, *6*, 1687 – 1692.
[339] M. Haruta, N. Yamada, T. Kobayashi, S. Iijima, *J. Catal.* **1989**, *115*, 301 – 309.
[340] M. D. Hughes, Y. J. Xu, P. Jenkins, P. McMorn, P. Landon, D. I. Enache, A. F. Carley, G. A. Attard, G. J. Hutchings, F. King, E. H. Stitt, P. Johnston, K. Griffin, C. J. Kiely, *Nature* **2005**, *437*, 1132 – 1135.
[341] G. C. Bond, C. Louis, D. Thompson, *Catalysis by Gold*, Imperial Press, London, **2006**.
[342] *Nanoparticles and Catalysis* (Ed.: D. Astruc), Wiley-VCH, Weinheim, Chapters 12 – 15, **2008**.
[343] Y. Kuwauchi, H. Yoshida, T. Akita, M. Haruta, S. Takeda, *Angew. Chem.* **2012**, *124*, 7849 – 7853; *Angew. Chem. Int. Ed.* **2012**, *51*, 7729 – 7733.
[344] R. Narayanan, M. A. El-Sayed, *J. Phys. Chem. B* **2005**, *109*, 12663.
[345] M. H. Rashid, T. K. Mandal, *Adv. Funct. Mater.* **2008**, *18*, 2261 – 2271.
[346] M. A. Sanchez-Castillo, C. Couto, W. B. Kim, J. A. Dumesic, *Angew. Chem.* **2004**, *116*, 1160 – 1162; *Angew. Chem. Int. Ed.* **2004**, *43*, 1140 – 1142.
[347] W. An, Y. Pei, X. C. Zeng, *Nano Lett.* **2008**, *8*, 195 – 202.
[348] P. Li, Z. Wei, T. Wu, Q. Peng, Y. Li, *J. Am. Chem. Soc.* **2011**, *133*, 5660 – 5663.
[349] X. Cui, C. Zhang, F. Shi, Y. Deng, *Chem. Commun.* **2012**, *48*, 9391 – 9393.
[350] M. Stratakis, H. Garcia, *Chem. Rev.* **2012**, *112*, 4469 – 4506.
[351] N. Bi, Y. Chen, H. Qi, X. Zheng, Y. Chen, X. Liao, H. Zhang, Y. Tian, *Sens. Actuators B* **2012**, *166 – 167*, 766 – 771.
[352] F. M. Li, J. M. Liua, X. X. Wang, L. P. Lin, W. L. Cai, X. Lin, Y. N. Zeng, Z. M. Li, S. Q. Lin, *Sens. Actuators B* **2011**, *155*, 817 – 822.
[353] C. V. Durgadasa, V. Nair Lakshmib, C. P. Sharmaa, K. Sreenivasan, *Sens. Actuators B* **2011**, *156*, 791 – 797.
[354] G. Chen, Y. Jin, L. Wang, J. Deng, C. Zhang, *Chem. Commun.* **2011**, *47*, 12500 – 12502.
[355] E. C. Dreaden, M. A. El-Sayed, *Acc. Chem. Res.* **2012**, *45*, 1854 – 1865.
[356] L. Wu, Z. Wang, S. Zong, Z. Huang, P. Zhang, Y. Cui, *Biosens. Bioelectron.* **2012**, *38*, 94 – 99.
[357] M. J. Kwon, J. Lee, A. W. Wark, H. J. Lee, *Anal. Chem.* **2012**, *84*, 1702 – 1707.
[358] E. T. Castellana, R. C. Gamez, D. H. Russell, *J. Am. Chem. Soc.* **2011**, *133*, 4182 – 4185.
[359] Z. Li, Z. Zhu, W. Liu, Y. Zhou, B. Han, Y. Gao, Z. Tang, *J. Am. Chem. Soc.* **2012**, *134*, 3322 – 3325.
[360] P. Y. Chung, T. H. Lin, G. Schultz, C. Batich, P. Jiang, *Appl. Phys. Lett.* **2010**, *96*, 261108.
[361] A. Labande, J. Ruiz, D. Astruc, *J. Am. Chem. Soc.* **2002**, *124*, 1782 – 1789.
[362] M. C. Daniel, J. Ruiz, S. Nlate, J. C. Blais, D. Astruc, *J. Am. Chem. Soc.* **2003**, *125*, 2617 – 2628.
[363] Y. Zhu, H. Kuang, L. Xu, W. Ma, C. Peng, Y. Hua, L. Wang, C. Xu, *J. Mater. Chem.* **2012**, *22*, 2387 – 2391.
[364] M. H. Rashid, R. R. Bhattacharjee, T. K. Mandal, *J. Phys. Chem. C* **2007**, *111*, 9684 – 9693.
[365] Y. Bahari Mollamahalle, M. Ghorbani, A. Dolati, *Electrochim. Acta* **2012**, *75*, 157 – 163.
[366] J. You, R. Zhang, G. Zhang, M. Zhong, Y. Liu, C. S. Van Pelt, D. Liang, W. Wei, A. K. Sood, C. Li, *J. Controlled Release* **2012**, *158*, 319 – 328.

[367] X. Huang, I. H. El-Sayed, M. A. El-Sayed, *J. Am. Chem. Soc.* **2006**, *128*, 2115 – 2120.
[368] A. K. Oyelere, B. Chen, X. Huang, I. H. El-Sayed, M. A. El-Sayed, *Bioconjugate Chem.* **2007**, *18*, 1490 – 1497.
[369] A. L. Oldenburg, M. N. Hansen, D. A. Zweifel, A. Wei, S. A. Boppart, *Opt. Express* **2006**, *14*, 6724 – 6738.
[370] E. B. Dickerson, E. C. Dreaden, X. Huang, I. H. El-Sayed, H. Chu, S. Pushpanketh, J. F. McDonald, M. A. El-Sayed, *Cancer Lett.* **2008**, *269*, 57 – 66.
[371] E. C. Dreaden, A. M. Alkilany, X. Huang, C. J. Murphy, M. A. El-Sayed, *Chem. Soc. Rev.* **2012**, *41*, 2740 – 2779.
[372] C. Loo, L. Hirsch, M. H. Lee, E. Chang, J. West, N. J. Halas, R. Drezek, *Opt. Lett.* **2005**, *30*, 1012 – 1014.
[373] H. Ding, K. T. Yong, I. Roy, H. E. Pudavar, W. C. Law, E. J. Bergey, P. N. Prasad, *J. Phys. Chem. C* **2007**, *111*, 12552 – 12557.
[374] N. J. Durr, T. Larson, D. K. Smith, B. A. Korgel, K. Sokolov, A. Ben-Yakar, *Nano Lett.* **2007**, *7*, 941 – 945.
[375] J. L. Li, M. Gu, *Biomaterials* **2010**, *31*, 9492 – 9498.
[376] W. He, H. Wang, L. C. Hartmann, J. X. Cheng, P. S. Low, *Proc. Natl. Acad. Sci. USA* **2007**, *104*, 11760 – 11765.
[377] A. Agarwal, S. W. Huang, M. O'Donnell, K. C. Day, M. Day, N. Kotov, S. Ashkenazi, *J. Appl. Phys.* **2007**, *102*, 064701.
[378] P. C. Li, C. R. C. Wang, D. B. Shieh, C. W. Wei, C. K. Liao, C. Poe, S. Jhan, A. A. Ding, Y. N. Wu, *Opt. Express* **2008**, *16*, 18605 – 18615.
[379] X. Yang, S. E. Skrabalak, Z. Y. Li, Y. Xia, L. V. Wang, *Nano Lett.* **2007**, *7*, 3798 – 3802.
[380] J. Chen, D. Wang, J. Xi, L. Au, A. Siekkinen, A. Warsen, Z. Y. Li, H. Zhang, Y. Xia, X. Li, *Nano Lett.* **2007**, *7*, 1318 – 1322.
[381] See Ref. [324].
[382] X. C. Yang, B. Samanta, S. S. Agasti, Y. Jeong, Z. Zhu, S. Rana, O. R. Miranda, V. M. Rotello, *Angew. Chem.* **2011**, *123*, 497 – 501; *Angew. Chem. Int. Ed.* **2011**, *50*, 477 – 481.
[383] R. Mout, D. F. Moyano, S. Rana, V. M. Rotello, *Chem. Soc. Rev.* **2012**, *41*, 2539 – 2544.
[384] Y. C. Yeh, B. Creran, V. M. Rotello, *Nanoscale* **2012**, *4*, 1871 – 1880.
[385] Y. Horiguchi, T. Niidome, S. Yamada, N. Nakashima, Y. Niidome, *Chem. Lett.* **2007**, *36*, 952 – 953.
[386] D. A. Giljohann, D. S. Seferos, W. L. Daniel, M. D. Massich, P. C. Patel, C. A. Mirkin, *Angew. Chem.* **2010**, *122*, 3352 – 3366; *Angew. Chem. Int. Ed.* **2010**, *49*, 3280 – 3294.
[387] S. E. Lee, D. Y. Sasaki, T. D. Perroud, D. Yoo, K. D. Patel, L. P. Lee, *J. Am. Chem. Soc.* **2009**, *131*, 14066 – 14074.
[388] C. Loo, A. Lin, L. Hirsch, M. Lee, J. Barton, N. J. Halas, J. West, R. Drezek, *Technol. Cancer Res. Treat.* **2004**, *3*, 33 – 40.
[389] See Ref. [113].
[390] R. Bardhan, W. Chen, C. Perez-Torres, M. Bartels, R. M. Huschka, L. L. Zhao, E. Morosan, R. G. Pautler, A. Joshi, N. J. Halas, *Adv. Funct. Mater.* **2009**, *19*, 3901 – 3909; L. Dykman, N. Khlebtsov, *Chem. Soc. Rev.* **2012**, *41*, 2256 – 2282.
[391] A. Barhoumi, R. Huschka, R. Bardhan, M. W. Knight, N. J. Halas, *Chem. Phys. Lett.* **2009**, *482*, 171 – 179.
[392] R. Huschka, O. Neumann, A. Barhoumi, N. J. Halas, *Nano Lett.* **2010**, *10*, 4117 – 4122.
[393] W. Chen, R. Bardhan, M. Bartels, C. Perez-Torres, R. G. Pautler, N. J. Halas, A. Joshi, *Mol. Cancer Ther.* **2010**, *9*, 1028 – 1038.
[394] M. Choi, R. Bardhan, K. J. Stanton-Maxey, S. Badve, H. Nakshatri, K. M. Stantz, N. Cao, N. J. Halas, S. E. Clare, *Cancer Nano* **2012**, *3*, 47 – 54.
[395] W. Y. Li, X. Cai, C. Kim, G. Sun, Y. Zhang, R. Deng, M. X. Yang, J. Chen, S. Achilefu, L. V. Wang, Y. N. Xia, *Nanoscale* **2011**, *3*, 1724 – 1730.
[396] G. D. Moon, S. W. Choi, X. Cai, W. Y. Li, E. C. Cho, U. Jeong, L. V. Wang, Y. N. Xia, *J. Am. Chem. Soc.* **2011**, *133*, 4762 – 4765.
[397] See Ref. [327].
[398] E. Boisselier, D. Astruc, *Chem. Soc. Rev.* **2009**, *38*, 1759 – 1782.
[399] A. M. Alkilany, C. J. Murphy, *J. Nanopart. Res.* **2010**, *12*, 2313 – 2333.
[400] A. M. Alkilany, P. K. Nagaria, C. R. Hexel, T. J. Shaw, C. J. Murphy, M. D. Wyatt, *Small* **2009**, *5*, 701 – 708.
[401] K. Bilberg, M. B. Hovgaard, F. Besenbacher, E. Baatru, *J. Toxicol.* **2012**, *2012*, article ID 293784.
[402] D. Astruc, F. Lu, J. Ruiz, *Angew. Chem.* **2005**, *117*, 8062 – 8083; *Angew. Chem. Int. Ed.* **2005**, *44*, 7852 – 7872.
[403] W. Jiang, B. Y. S. Kim, J. T. Rutka, W. C. W. Chan, *Nat. Nanotechnol.* **2008**, *3*, 145 – 150.
[404] E. C. Cho, J. Xie, P. A. Wurm, Y. Xia, *Nano Lett.* **2009**, *9*, 1080 – 1084.
[405] E. C. Cho, Q. Zhang, Y. Xia, *Nanotechnology* **2011**, *6*, 385 – 391.
[406] Y. S. Chen, Y. C. Hung, I. Liau, G. S. Huang, *Nanoscale Res. Lett.* **2009**, *4*, 858 – 864.
[407] C. Lasagna-Reeves, D. Gonzalez-Romero, M. A. Barria, I. Olmedo, A. Clos, V. M. S. Ramanujam, A. Urayama, L. Vergara, M. J. Kogan, C. Soto, *Biochem. Biophys. Res. Commun.* **2010**, *393*, 649 – 655.
[408] W. H. De Jong, W. I. Hagens, P. Krystek, M. C. Burger, A. J. A. M. Sips, R. E. Geertsma, *Biomaterials* **2008**, *29*, 1912 – 1919.
[409] H. S. Choi, W. Liu, P. Misra, E. Tanaka, J. Zimmer, B. I. Ipe, M. G. Nawendi, J. V. Frangioni, *Nat. Biotechnol.* **2007**, *25*, 1165 – 1170.
[410] M. Semmler-Behnke, W. G. Kreyling, J. Lipka, S. Fertsch, A. Wenk, S. Takenaka, G. Schmid, W. Brandau, *Small* **2008**, *4*, 2108 – 2111.
[411] C. Zhou, M. Long, Y. Qin, X. Sun, J. Zheng, *Angew. Chem.* **2011**, *123*, 3226 – 3230; *Angew. Chem. Int. Ed.* **2011**, *50*, 3168 – 3172.
[412] J. L. Ferry, P. Craig, C. Hexel, P. Sisco, R. Frey, P. L. Pennington, M. H. Fulton, I. G. Scott, A. W. Decho, S. Kashiwada, C. J. Murphy, T. J. Shaw, *Nat. Nanotechnol.* **2009**, *4*, 441 – 444.
[413] Y. Xia, Y. Xiong, B. Lim, S. E. Skrabalak, *Angew. Chem.* **2009**, *121*, 62 – 108; *Angew. Chem. Int. Ed.* **2009**, *48*, 60 – 103.
[414] V. V. Pushkarev, Z. W. Zu, K. J. An, A. Hervier, G. A. Somorjai, *Top. Catal.* **2012**, *55*, 1257 – 1275.
[415] J. Ye, F. F. Wen, H. Sobhani, J. B. Lassiter, P. Van Dorpe, P. Nordlander, N. J. Halas, *Nano Lett.* **2012**, *12*, 1660 – 1667.
[416] **Note Added In Proof**: Major contributions to the field of anisotropic AuNPs have appeared in 2013 concerning syntheses,[417,418] mechanical properties,[419] polyelectrolytes,[420] DNA-directed self-assembly,[421] biomedicine,[422–424] catalysis,[425–429] and sensing.[429]
[417] G. J. Hutchings, C. J. Kiely, *Acc. Chem. Res.* **2013**, *46*, 1759 – 1772.
[418] D. Rodríguez-Fernández, T. Altantzis, H. Heidari, S. Bals, L. M. Liz-Marzán, *Chem. Commun.* **2014**, *50*, 79 – 81.
[419] C. Yan, I. Arfaoui, N. Goubet, M. – P. Pileni, *Adv. Funct. Mater.* **2013**, *23*, 2315 – 2321.
[420] S. T. Sivapalan, B. M. DeVetter, T. K. Yang, M. V. Schulmerich, R. Bhargava, C. J. Murphy, *J. Phys. Chem. C* **2013**, *117*, 10677 – 10682.
[421] S. J. Varrow, A. M. Funston, X. Wei, P. Mulvaney, *Nano Today* **2013**, *8*, 138 – 167.
[422] M. D. Blankschien, L. A. Pretzer, R. Huschka, N. J. Halas, R. Gonzalez, M. S. Wong, *ACS Nano* **2013**, *7*, 654 – 663.
[423] Y. Wang, K. C. L. Black, H. Luehmann, W. Li, Y. Zhang, X. Cai, D. Wan, S. – Y. Liu, M. Li, P. Kim, Z. – Y. Li, L. V. Wang, Y. Liu, Y. Xia, *ACS Nano* **2013**, *7*, 2068 – 2077.
[424] C. Leduc, S. Si, J. Gautier, M. Soto-Ribeiro, B. Wehrle-Haller, A. Gautreau, G. Giannone, L. Cognet, B. Lounis, *Nano Lett.* **2013**, *13*, 1489 – 1494.
[425] T. Akita, M. Kohyama, M. Haruta, *Acc. Chem. Res.* **2013**, *46*, 1773 – 1782.

[426] A. Corma, P. Concepción, M. Boronat, M. J. Sabater, J. Navas, M. J. Yacaman, E. Larios, A. Posadas, M. A. López-Quintela, D. Buceta, E. Mendoza, G. Guilera, A. Mayoral, *Nat. Chem.* **2013**, *5*, 775 – 781.
[427] M. A. Mahmoud, R. Narayanan, M. A. El-Sayed, *Acc. Chem. Res.* **2013**, *46*, 1795 – 1805.
[428] G. Liu, K. L. Young, X. Liao, M. L. Personick, C. A. Mirkin, *J. Am. Chem. Soc.* **2013**, *135*, 12196 – 12199.
[429] P. Zhao, N. Li, L. Salmon, N. Liu, J. Ruiz, D. Astruc, *Chem. Commun.* **2013**, *49*, 3218 – 3220.

